

**Chapter 14**  
**GEOTECHNICAL**  
**SEISMIC DESIGN**

**GEOTECHNICAL DESIGN MANUAL**

*January 2022*



## Table of Contents

<u>Section</u>	<u>Page</u>
14.1 Introduction.....	14-1
14.2 Geotechnical Seismic Design Approach .....	14-1
14.2.1 No Soil SSL Condition .....	14-2
14.2.2 Soil SSL Condition.....	14-2
14.3 Seismic Lateral Loadings.....	14-3
14.4 Seismic Active Soil Pressures.....	14-3
14.4.1 Mononobe-Okabe Method .....	14-4
14.4.2 Trial Wedge Method.....	14-6
14.4.3 Modification to MO Method to Consider Cohesion .....	14-7
14.4.4 LSR Method.....	14-8
14.4.5 GLE Method .....	14-17
14.4.6 Unyielding Structures.....	14-17
14.5 Seismic Passive Soil Pressures.....	14-18
14.6 Geotechnical Seismic Design of Bridges.....	14-27
14.6.1 ADRS Curves .....	14-28
14.6.2 Bridge Abutments .....	14-28
14.6.3 Bridge Approach Embankment .....	14-29
14.6.4 Bridge Foundations.....	14-29
14.7 Shallow Foundation Design .....	14-29
14.8 Deep Foundation Design .....	14-29
14.8.1 Axial Loads .....	14-30
14.8.2 Downdrag Loads.....	14-31
14.8.3 Lateral Soil Response of Liquefied Soils (p-y Curves).....	14-31
14.8.4 Soil Load Contribution on a Single Deep Foundation .....	14-33
14.8.5 Load Transfer Between Pile Group and Lateral Spreading Crust.....	14-34
14.8.6 Lateral Soil Loads Due to Seismic Hazard Displacements .....	14-36
14.8.7 Foundation Elements in Unstable Ground.....	14-39
14.9 Bridge Abutment Back Wall Passive Resistance.....	14-51
14.9.1 Development of Passive Resistance .....	14-51
14.9.2 Effective Width of Abutment Wall.....	14-59
14.10 Geotechnical Seismic Design of Embankments .....	14-62
14.11 Rigid Gravity Earth Retaining Structure Design.....	14-62
14.12 Flexible Gravity Earth Retaining Structure Design.....	14-69
14.13 Cantilever Earth Retaining System Design .....	14-75
14.13.1 Unanchored Cantilever ERSs .....	14-75
14.13.2 Anchored Cantilever ERSs .....	14-76
14.14 In-situ Reinforced Retaining System Design .....	14-77
14.15 Seismic Hazard Mitigation.....	14-77
14.15.1 Structural Mitigation .....	14-77
14.15.2 Geotechnical Mitigation.....	14-78
14.15.3 Selection of Mitigation Method .....	14-78
14.16 References .....	14-78

**List of Tables**

<b><u>Table</u></b>	<b><u>Page</u></b>
Table 14-1, Effective Pile Width Coefficient ( $\lambda$ ) .....	14-34
Table 14-2, Relative Movements Required to Reach Passive Earth Pressures .....	14-53
Table 14-3, Sand-Like Soil Parameters Used to Create Figure 14-53 .....	14-55
Table 14-4, Clay-Like Soil Parameters Used to Create Figure 14-54 .....	14-55
Table 14-5, $c$ - $\phi$ Soil Parameters Used to Create Figure 14-55 .....	14-55

### List of Figures

<u>Figure</u>	<u>Page</u>
Figure 14-1, Pseudo-Static Method – Inertial Forces and Seismic Loadings .....	14-4
Figure 14-2, Mononobe-Okabe Method .....	14-5
Figure 14-3, Trial Wedge Method.....	14-6
Figure 14-4, MO Active Seismic Wedge.....	14-8
Figure 14-5, LSR Active Seismic Wedge .....	14-9
Figure 14-6, Seismic Active Earth Pressure Coefficient ( $\delta = 0$ ; $C/\gamma H = 0.0$ ).....	14-10
Figure 14-7, Seismic Active Earth Pressure Coefficient ( $\delta = 0$ ; $C/\gamma H = 0.025$ ).....	14-10
Figure 14-8, Seismic Active Earth Pressure Coefficient ( $\delta = 0$ ; $C/\gamma H = 0.05$ ).....	14-11
Figure 14-9, Seismic Active Earth Pressure Coefficient ( $\delta = 0$ ; $C/\gamma H = 0.075$ ).....	14-11
Figure 14-10, Seismic Active Earth Pressure Coefficient ( $\delta = 0$ ; $C/\gamma H = 0.1$ ).....	14-12
Figure 14-11, Seismic Active Earth Pressure Coefficient ( $\delta = 1/2\phi$ ; $C/\gamma H = 0.0$ ).....	14-12
Figure 14-12, Seismic Active Earth Pressure Coefficient ( $\delta = 1/2\phi$ ; $C/\gamma H = 0.025$ ).....	14-13
Figure 14-13, Seismic Active Earth Pressure Coefficient ( $\delta = 1/2\phi$ ; $C/\gamma H = 0.05$ ).....	14-13
Figure 14-14, Seismic Active Earth Pressure Coefficient ( $\delta = 1/2\phi$ ; $C/\gamma H = 0.075$ ).....	14-14
Figure 14-15, Seismic Active Earth Pressure Coefficient ( $\delta = 1/2\phi$ ; $C/\gamma H = 0.1$ ).....	14-14
Figure 14-16, Seismic Active Earth Pressure Coefficient ( $\delta = 2/3\phi$ ; $C/\gamma H = 0.0$ ).....	14-15
Figure 14-17, Seismic Active Earth Pressure Coefficient ( $\delta = 2/3\phi$ ; $C/\gamma H = 0.025$ ).....	14-15
Figure 14-18, Seismic Active Earth Pressure Coefficient ( $\delta = 2/3\phi$ ; $C/\gamma H = 0.05$ ).....	14-16
Figure 14-19, Seismic Active Earth Pressure Coefficient ( $\delta = 2/3\phi$ ; $C/\gamma H = 0.075$ ).....	14-16
Figure 14-20, Seismic Active Earth Pressure Coefficient ( $\delta = 2/3\phi$ ; $C/\gamma H = 0.01$ ).....	14-17
Figure 14-21, LSR Passive Seismic Wedge.....	14-19
Figure 14-22, Seismic Passive Earth Pressure Coefficient ( $\delta = 0$ ; $C/\gamma H = 0.0$ ).....	14-20
Figure 14-23, Seismic Passive Earth Pressure Coefficient ( $\delta = 0$ ; $C/\gamma H = 0.025$ ).....	14-20
Figure 14-24, Seismic Passive Earth Pressure Coefficient ( $\delta = 0$ ; $C/\gamma H = 0.05$ ).....	14-21
Figure 14-25, Seismic Passive Earth Pressure Coefficient ( $\delta = 0$ ; $C/\gamma H = 0.075$ ).....	14-21
Figure 14-26, Seismic Passive Earth Pressure Coefficient ( $\delta = 0$ ; $C/\gamma H = 0.1$ ).....	14-22
Figure 14-27, Seismic Passive Earth Pressure Coefficient ( $\delta = 1/2\phi$ ; $C/\gamma H = 0.0$ ).....	14-22
Figure 14-28, Seismic Passive Earth Pressure Coefficient ( $\delta = 1/2\phi$ ; $C/\gamma H = 0.025$ ).....	14-23
Figure 14-29, Seismic Passive Earth Pressure Coefficient ( $\delta = 1/2\phi$ ; $C/\gamma H = 0.05$ ).....	14-23
Figure 14-30, Seismic Passive Earth Pressure Coefficient ( $\delta = 1/2\phi$ ; $C/\gamma H = 0.075$ ).....	14-24
Figure 14-31, Seismic Passive Earth Pressure Coefficient ( $\delta = 1/2\phi$ ; $C/\gamma H = 0.1$ ).....	14-24
Figure 14-32, Seismic Passive Earth Pressure Coefficient ( $\delta = 2/3\phi$ ; $C/\gamma H = 0.0$ ).....	14-25
Figure 14-33, Seismic Passive Earth Pressure Coefficient ( $\delta = 2/3\phi$ ; $C/\gamma H = 0.025$ ).....	14-25
Figure 14-34, Seismic Passive Earth Pressure Coefficient ( $\delta = 2/3\phi$ ; $C/\gamma H = 0.05$ ).....	14-26
Figure 14-35, Seismic Passive Earth Pressure Coefficient ( $\delta = 2/3\phi$ ; $C/\gamma H = 0.075$ ).....	14-26
Figure 14-36, Seismic Passive Earth Pressure Coefficient ( $\delta = 2/3\phi$ ; $C/\gamma H = 0.1$ ).....	14-27
Figure 14-37, Pile Damage Mechanisms in Liquefied Ground.....	14-30
Figure 14-38, P-Multipliers (mp) for Sand-Like Soils Subject to Cyclic Liquefaction .....	14-33
Figure 14-39, Load Transfer Between Pile Group and Lateral Spreading Crust.....	14-35
Figure 14-40, BNWF Methods for Evaluating Seismic Hazard Displacements .....	14-37
Figure 14-41, Methods for Imposing Kinematic Loads on Deep Foundations.....	14-38
Figure 14-42, Schematic of typical unstable soil problem.....	14-40
Figure 14-43, Rotational Stiffness Model (Caltrans (2017 B)).....	14-41
Figure 14-44, Modification to the profile of ultimate subgrade reaction, $p_u$ , .....	14-42
Figure 14-45, Pile Cap Idealized Force-Displacement Behavior.....	14-43
Figure 14-46, Pile Foundation Dimension Parameters .....	14-44
Figure 14-47, Design cases to determine soil crust ultimate passive load.....	14-44

Figure 14-48, Applied displacement profile for Winkles spring foundation model .....	14-48
Figure 14-49, Determination of the tributary width of an embankment.....	14-49
Figure 14-50, Determination of compatible displacements .....	14-50
Figure 14-51, End-Bent Schematic Plan View.....	14-51
Figure 14-52, Hyperbolic Force-Displacement Formulation.....	14-52
Figure 14-53, Bridge Abutment Wall Passive Pressure, Sand-Like Backfill Example .....	14-56
Figure 14-54, Bridge Abutment Wall Passive Pressure, Clay-Like Backfill Example .....	14-57
Figure 14-55, Bridge Abutment Wall Passive Pressure, c- $\phi$ Backfill Example .....	14-58
Figure 14-56, Skewed Bridge Abutment Wall Seismic Passive Resistance.....	14-61
Figure 14-57, Skewed Bridge Abutment Wall Seismic Sliding Resistance .....	14-62
Figure 14-58, Rigid Gravity ERS Seismic Force Diagram – Level Backfill.....	14-66
Figure 14-59, Rigid Gravity ERS Seismic Force Diagram – Sloping Backfill.....	14-66
Figure 14-60, Determination of Yield Acceleration (ky).....	14-68
Figure 14-61, Flexible Gravity ERS Seismic Force Diagram – Level Backfill.....	14-72
Figure 14-62, Flexible Gravity ERS Seismic Force Diagram – Sloping Backfill .....	14-72
Figure 14-63, Determination of Yield Acceleration (ky).....	14-75

# CHAPTER 14

## GEOTECHNICAL SEISMIC DESIGN

### 14.1 INTRODUCTION

This Chapter provides guidance for the geotechnical seismic design of bridges, embankments, ERSs, and miscellaneous structures. Geotechnical seismic design consists of evaluating the EE I limit state of transportation structures owned and maintained by the State of South Carolina for performance under seismic hazards (Chapter 13) and seismic lateral loadings (Chapter 14). Seismic lateral loadings (inertial accelerations) affect soil pressures by increasing static active soil pressures and decreasing static passive soil pressures. Methods for computing seismic active and passive soil pressures are included in this Chapter. The geotechnical seismic design will typically be evaluated using performance based design methodologies to evaluate if the structure's performance meets the geotechnical performance criteria established in Chapter 10. Force based design methodologies are included where appropriate for evaluating boundary conditions. If the performance limits are exceeded, seismic hazard mitigation methods will be discussed that can be used to meet the required performance limits.

The procedures for seismic geotechnical design are consistent with those procedures presented for static geotechnical design in this Manual. The seismic geotechnical design guidelines presented in this Manual may not be the only methods available particularly since geotechnical seismic design is constantly evolving and developing. The overall goal of this Chapter is to establish a state-of-practice that can and will evolve and be enhanced as methodologies improve and regional (CEUS) experience develops. Methods other than those indicated in this Manual may be brought to the attention of the PC/GDS or the PCS/GDS for consideration on a specific project or for consideration in future updates of this Manual, respectively.

### 14.2 GEOTECHNICAL SEISMIC DESIGN APPROACH

Geotechnical seismic design is typically performed using either a Force Based Design or Performance Based Design methodology. SCDOT LRFD geotechnical seismic design of transportation structures typically consists of using Performance Based Design methodologies. The EE I limit state performance criteria established in Chapter 10 should be used as a starting point with significant collaboration between the SEOR and the GEOR. The geotechnical seismic design approach will be consistent with design philosophy for structural design. It will be the responsibility of the design team to define the performance of bridges, roadway embankments, and ERSs within the frame work of SCDOT policy of maximizing the safety of the motoring public and minimizing the susceptibility of a bridge structure to collapse during strong earthquake shaking.

The design approach typically begins by designing the transportation structure for the Strength and Service limit states. The resulting structure is then evaluated for the EE I limit state.

For sites where bridges and bridge foundations are located within soils that are susceptible to SSL in accordance with Chapter 13 due to either cyclic liquefaction of Sand-Like soils or cyclic softening of Clay-Like soils, the design methodology shall include the evaluation of the following 2 conditions:

### 14.2.1 No Soil SSL Condition

The structure should first be analyzed and designed for the inertial forces induced by the EE I limit state without the soil SSL condition. This will allow the design team to understand the effect of just the inertial loading on the structures. The site response developed should not include any effects of the soil SSL.

### 14.2.2 Soil SSL Condition

The structure, as designed for the No Soil SSL condition, is reanalyzed assuming that the Sand-Like and Clay-Like soils have experienced soil SSL. The soils susceptible to SSL are assigned appropriate residual shear strengths in accordance with Chapter 13. The design spectrum for the No Soil SSL is used unless the period of the structure is greater than 1.0 second and the site response is susceptible to increase for the soil SSL condition in accordance with Chapter 12. The geotechnical seismic design is then performed using these soil and site response parameters.

If the structure meets the performance objectives (resistance factors and performance criteria) for the EE I limit state, the design is complete. Otherwise, measures to mitigate the effects of the seismic hazard are developed. The full horizontal acceleration ( $k_h = k_{avg}$ ) shall be used in design. However,  $k_y$  shall be determined and if the ratio of  $k_y$  to  $k_h$  is greater than or equal to 0.5 (i.e.,  $k_y/k_h \geq 0.5$ ) and displacement of approximately 2.0 inches can be tolerated then the design is complete. If 2.0 inches of displacement cannot be tolerated or if the ratio of  $k_y$  to  $k_h$  is less than 0.5 (i.e.,  $k_y/k_h < 0.5$ ), then the actual displacement shall be determined using the procedures described in Chapter 13. Displacements shall be computed in accordance with Chapter 13 when instability is determined. Mitigation can be accomplished by redesign of the structure to resist the seismic hazards (structural mitigation), reducing the effects of the seismic hazard by performing geotechnical mitigation measures, or by developing a mitigation approach that consists of both structural and geotechnical mitigation procedures.

The evaluation of the EE I limit state typically requires a geotechnical evaluation of the Geology and Seismicity (Chapter 11), and the Site Response (Chapter 12) and the evaluation of the effects of the Seismic Hazards (Chapter 13) on the transportation structures being designed. For transportation structures (bridges, ERSs, etc.) that require structural design of concrete or steel components, the GEOR typically provides the SEOR with site response analyses, soil-structure interaction modeling of foundations, seismic loadings (active and passive), and the effects of seismic hazards. When mitigation of seismic hazards is required, the GEOR provides geotechnical mitigation options and assists in the evaluation of structural mitigation options. When evaluating certain structural mitigation options, the GEOR may require input from the SEOR for the design of piles/shafts for providing slope stability of a roadway embankment or river/channel bank at a bridge crossing.

It should be noted that the procedures outlined in this Chapter are to be used with new construction. The seismic design or retrofit of existing structures is currently performed on a case-by-case basis. At the discretion of the Regional Production Engineer (RPE), the Regional Program Manager (PM), or the Regional Design Manager (DM), existing structures may be required to have seismic retrofit design performed.

### 14.3 SEISMIC LATERAL LOADINGS

Seismic lateral loadings are those seismic hazards that are induced by the acceleration of a soil mass or structure during earthquake shaking. The average seismic horizontal acceleration ( $k_{avg}$ ) that is generated by the earthquake is computed by using seismic acceleration coefficients as indicated in Chapter 13. The seismic lateral loadings are exhibited as either seismic active soil pressures or seismic passive soil pressures. Seismic active soil pressures are generated when seismic accelerations mobilize the active soil driving wedge behind an ERS or bridge abutments. Seismic passive soil pressures are generated when an earthquake load is applied from a structure to the soil. When passive soil pressures are generated as a result of seismic loadings, the earthquake's inertial acceleration forces also affect the passive soil wedge. The mechanism of this hazard is dependent on the type of structure being analyzed. Because a performance based design is used in the design of transportation structures, the effects of seismic lateral loadings must take into account the added force on the structure and any deformations caused by shearing of the soils. Examples of how this hazard can affect typical transportation structures are provided below:

- ERSs must not only resist static active soil pressure but also seismic active pressures as a result of the average earthquake accelerations acting on the active soil wedge. Additional lateral loads are generated as a result of the acceleration acting on the mass of the retaining structure and any soil that is contained in the structure.
- While a bridge abutment on one end of a bridge may experience the same seismic lateral loadings as ERSs, the abutment at the other end of the bridge may experience seismic induced lateral loads from the bridge and mass of the abutment that places a lateral seismic load on the soils behind the abutment, resulting in passive pressure resistance. Soils retained by bridge abutments will cycle between active and passive soil pressures throughout the earthquake shaking.
- Bridge approach and roadway embankments not only must resist static driving forces, but also seismic driving forces. Seismic driving forces result from peak ground accelerations acting on the soil mass contained within the bridge embankment failure surface.

### 14.4 SEISMIC ACTIVE SOIL PRESSURES

Earthquake-induced lateral loadings addressed in this Section are limited to those loadings (seismic active earth pressures) that are the result of soil-structure interaction between soils and ERSs. Seismic active soil pressures are generally analyzed using pseudo-static methods. The pseudo-static method is a force-equilibrium method that is used to analyze external forces and the effects (i.e., sliding, overturning, bearing capacity, etc.) on the structure being designed. The pseudo-static method used to analyze seismic active soil pressures uses the average horizontal acceleration coefficients that has been adjusted for wave scattering, ( $k_h = k_{avg}$ ), multiplied by the weight of the structural wedge (weight of the structure and any soil above the structure) and the weight of the active driving wedge,  $W_{DW}$ . The seismic active earth loadings in the pseudo-static method are illustrated in Figure 14-1.

The limit-equilibrium method is based on the following assumptions:

- The retaining wall yields sufficiently to produce active soil pressures during an earthquake.
- The backfill is a dry cohesionless soil (Mononobe-Okabe method).
- Active failure wedge behaves as a rigid body so that the accelerations are uniform throughout the soil mass.
- The soils behind the wall are not saturated and liquefaction does not occur.

The following methods can be used to evaluate the seismic active pressures:

1. Mononobe-Okabe (MO) Method
2. Trial Wedge Method
3. Modification to MO Method to Consider Cohesion
4. Log-Spiral-Rankine (LSR) Method – Shamsabadi, Xu, and Taciroglu (2013a and 2013b)
5. Generalized Limit Equilibrium (GLE) Method

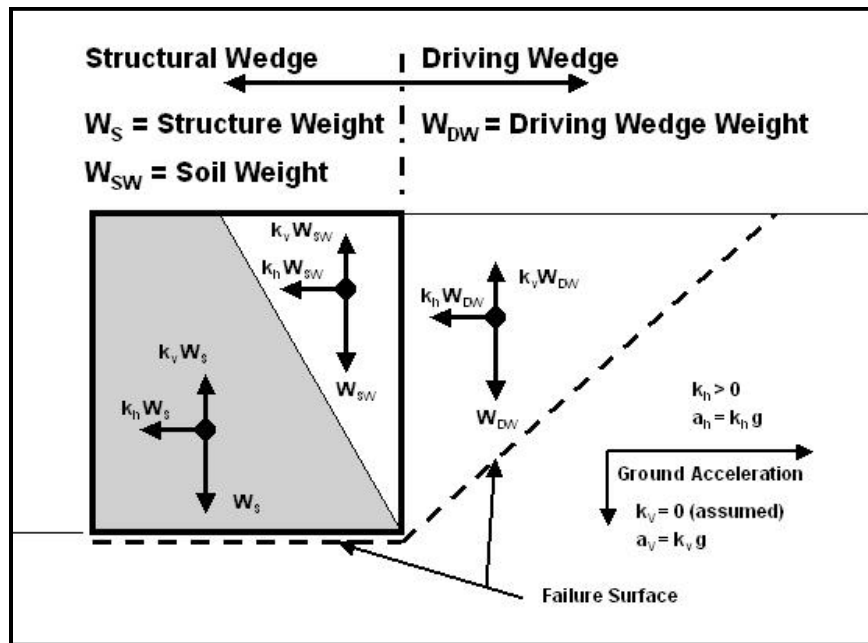


Figure 14-1, Pseudo-Static Method – Inertial Forces and Seismic Loadings (Modified Ebeling, et al. (2007))

#### 14.4.1 Mononobe-Okabe Method

One of the most frequent methods used to evaluate seismic active loadings is the Mononobe-Okabe (MO) method shown in Figure 14-2. The total dynamic active earth thrust,  $P_{ae}$ , is determined by the following equation:

$$P_{ae} = \frac{1}{2} * \gamma * H^2 * (1 - k_v) * K_{ae} \quad \text{Equation 14-1}$$

Where the seismic active earth pressure coefficient,  $K_{ae}$ , is determined as follows:

$$K_{ae} = \frac{\cos^2(\phi - \Psi - \theta)}{\cos \Psi * \cos^2 \theta * \cos(\Psi + \theta + \delta) * \left[ 1 + \sqrt{\frac{\sin(\phi + \delta) * \sin(\phi - \Psi - \beta)}{\cos(\delta + \Psi + \theta) * \cos(\beta - \theta)}} \right]^2} \quad \text{Equation 14-2}$$

Where,

- $\gamma$  = Unit weight of soil, pounds per cubic foot
- $H$  = Height of wall or effective height of wall ( $h_{eff}$ ), feet
- $\phi$  = Angle of internal friction of soil, degrees
- $\Psi$  =  $\tan^{-1}[k_h/(1-k_v)]$ , degrees
- $\delta$  = Angle of friction between soil and wall, degrees
- $k_h$  = Horizontal acceleration coefficient, g
- $k_v$  = Vertical acceleration coefficient, typically set to 0.0, g
- $\beta$  = Backfill slope angle, degrees
- $\theta$  = Angle of backface of the wall with the vertical, degrees

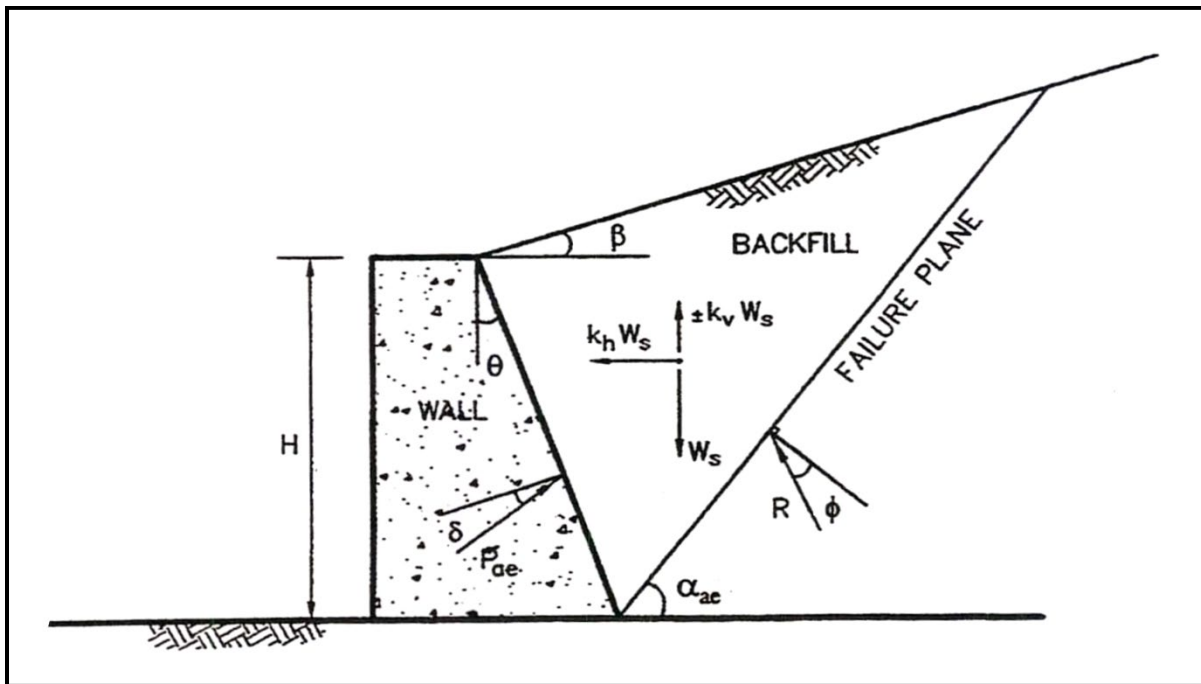


Figure 14-2, Mononobe-Okabe Method (Munfakh, et al. (1998))

Although the MO method is often used to compute seismic active soil pressures, this method has been found to produce very high pressures that tend to approach infinity when high accelerations and/or steep backslopes are analyzed. Richards and Elms (1979) indicates that when  $(\phi - \Psi - \beta)$  becomes negative no real solution to Equation 14-2 is possible. When this term is equal to 0, that maximum thrust is developed, thus establishing a limiting condition. Alternately, a limiting acceleration can be developed from Equation 14-4. This situation occurs when either of the following limiting conditions are met:

$$\beta \geq \phi - \Psi \quad \text{Equation 14-3}$$

$$k_h \leq (1 - k_v) * \tan(\phi - \beta) \quad \text{Equation 14-4}$$

Because the MO equation is limited to backfills consisting of dry cohesionless soils that may not typically be found at very large distances behind the wall, the MO method may not be the most appropriate analytical method.

Because of the various limitations associated with the MO method, the use of this method should be limited to the following criteria provided that the limiting conditions of Equations 14-3 and 14-4 are met:

- Backfill slopes,  $\beta \leq 18.4$  degrees (3H:1V or flatter)
- Limited to  $K_{ae} \leq 0.60$
- Free draining backfill materials (cohesionless soils) behind the wall should extend throughout the seismic active wedge.

#### 14.4.2 Trial Wedge Method

The Trial Wedge method can be used to determine critical earthquake-induced active forces when the MO method is not the appropriate method. The trial wedge method is more adaptable and can accommodate various types of soil behind the wall and relatively complex surface geometries. The Trial Wedge method is illustrated in Figure 14-3.

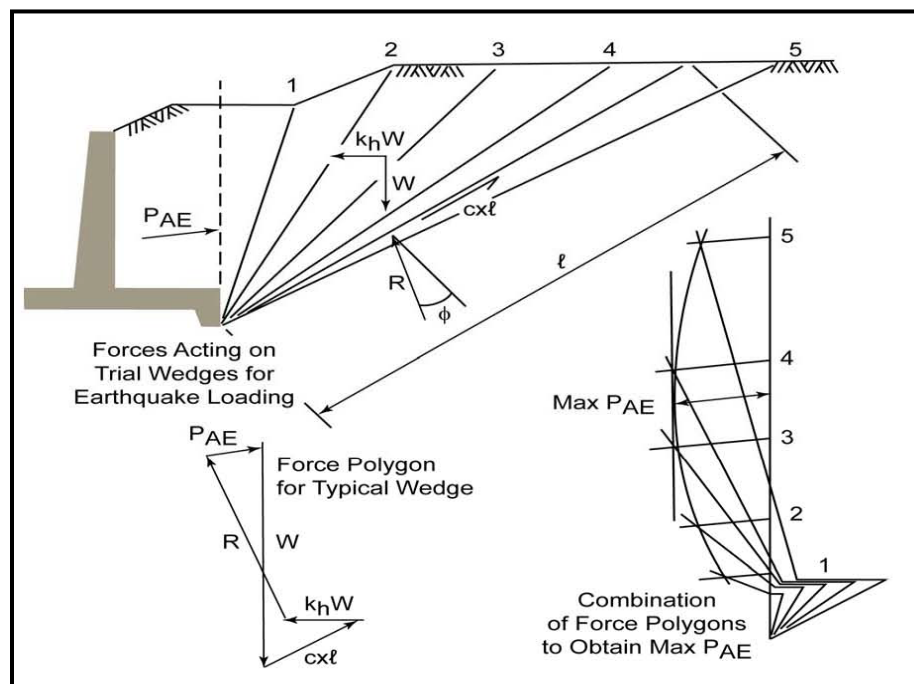


**Figure 14-3, Trial Wedge Method  
(Anderson, et al. (2008))**

Details on conducting the trial wedge method of analysis can be found in Ebeling, et al. (2007) and Bowles (1982). It should be noted that the seismic-induced inertial forces resulting from the structural wedge (retaining structure or soil mass contained within the structural wedge), as indicated in Figure 14-1, are not included in the MO method or the Trial Wedge method and that the structural wedge must also be included in the analysis.

When the horizontal acceleration,  $k_h$ , is equal to the peak horizontal ground acceleration (PGA), the seismic active loadings can become very large resulting in the design of the retaining structure becoming increasingly large and uneconomical. Designing for  $k_h = \text{PGA}$  will limit the deformations to 0.0. If deformations can be tolerated within the performance limits of the structure, then the horizontal acceleration,  $k_h$ , can be reduced. The method of reducing the horizontal acceleration,  $k_h$ , consists of allowing displacements to occur as provided in the Chapter 13.

### 14.4.3 Modification to MO Method to Consider Cohesion

Anderson, et al. (2008) has developed the following Coulomb-type wedge analysis that is based on the trial wedge method as shown in Figure 14-4. The following equation allows the input of cohesion into developing the seismic active earth pressure ( $P_{ae}$ ):

$$P_{nae} = \frac{W[(1 - k_v) \tan(\Xi) + k_h] - cL_n[\sin \alpha \tan(\Xi) + \cos \alpha] - c_a H[\tan(\Xi) \cos \omega + \sin \omega]}{[1 + \tan(\delta + \omega) \tan \Xi] * [\cos(\delta + \omega)]} \quad \text{Equation 14-5}$$

Where,

$P_{nae}$	=	Active earth pressure on each wedge (see Figure 14-4)
$\alpha$	=	Failure plane angle (Variable), degrees
$\phi$	=	Angle of internal friction of soil, degrees
$\Xi$	=	$\alpha - \phi$ , degrees
$k_h$	=	Average horizontal acceleration coefficient adjusted for wave scattering, g
$k_v$	=	Vertical acceleration coefficient, typically set to 0.0, g
$c$	=	Soil cohesion, pounds per square foot
$c_a$	=	Soil wall adhesion, pounds per square foot
$\delta$	=	Angle of friction between soil and wall ( $\delta = 0.67\phi$ ), degrees
$\omega$	=	Angle of backface of the wall with the vertical, degrees
$H$	=	Height of wall, feet
$L_n$	=	Length of failure surface AH located along failure plan angle ( $\alpha$ ), feet
$W_1$	=	Weight of wedge ABCDEF + $q_1$ + $f$ , pounds per foot of wall width
$W_n$	=	Weight of wedge ABCDEGH + $q_1$ + $q_2$ + $f$ , pounds per foot of wall width
$W_{n+1}$	=	Weight of wedge ABCDEGI + $q_1$ + $q_2$ + $f$ , pounds per foot of wall width
$q_1$	=	Uniform strip surcharge located between DE, pounds per foot per foot of wall width
$q_2$	=	Uniform strip surcharge located between GI, pounds per foot per foot of wall width
$f$	=	Line load located between BC, pounds per foot of wall width

The design parameters should be selected based on site conditions. The only parameter that must be determined on a trial basis is the failure plane angle ( $\alpha_n$ ). The failure plane angle ( $\alpha_n$ ) is determined by varying the failure plane angle ( $\alpha_n$ ) until the maximum  $P_{an} = P_{ae}$  is computed.





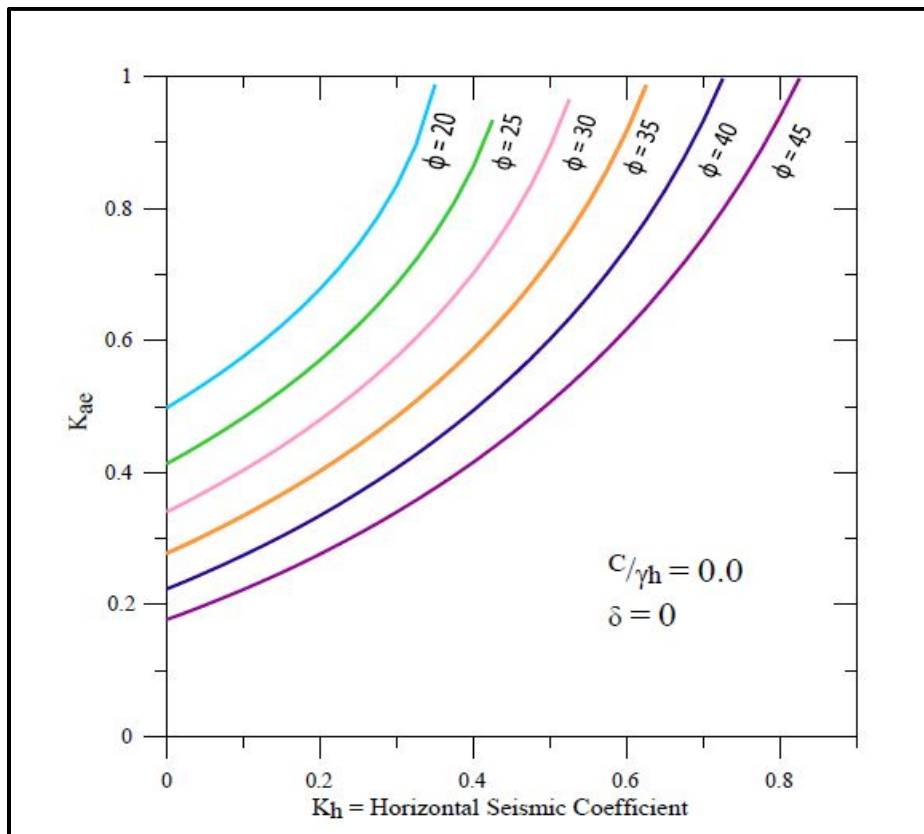


Figure 14-6, Seismic Active Earth Pressure Coefficient ( $\delta = 0$ ;  $C/\gamma_h = 0.0$ ) (modified Shamsabadi, et al. (2013b))

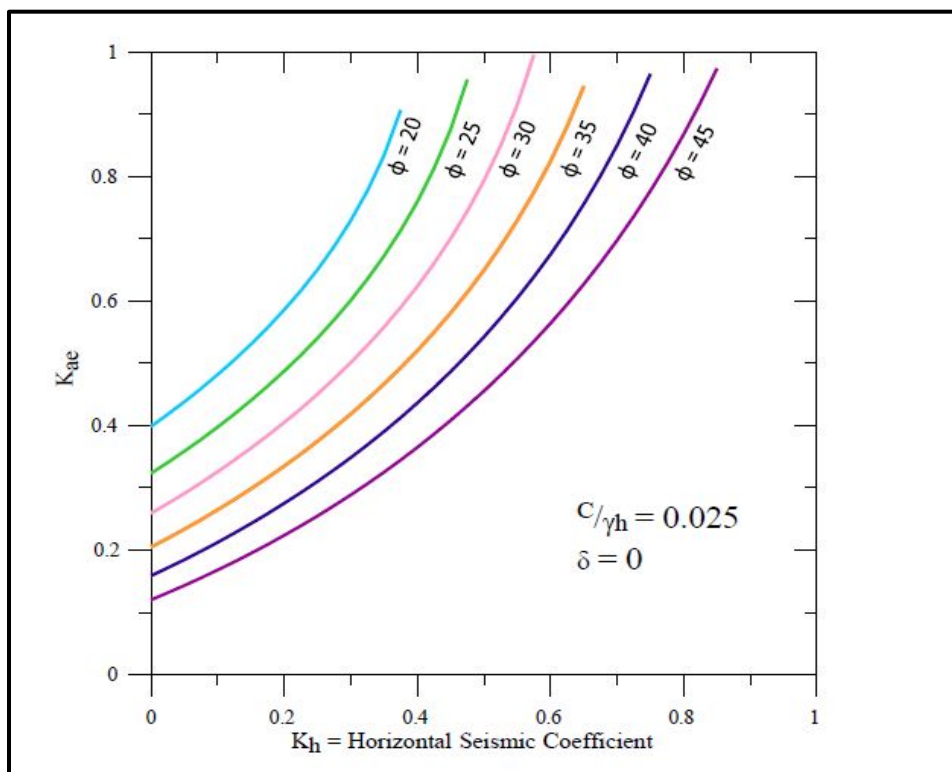


Figure 14-7, Seismic Active Earth Pressure Coefficient ( $\delta = 0$ ;  $C/\gamma_h = 0.025$ ) (modified Shamsabadi, et al. (2013b))

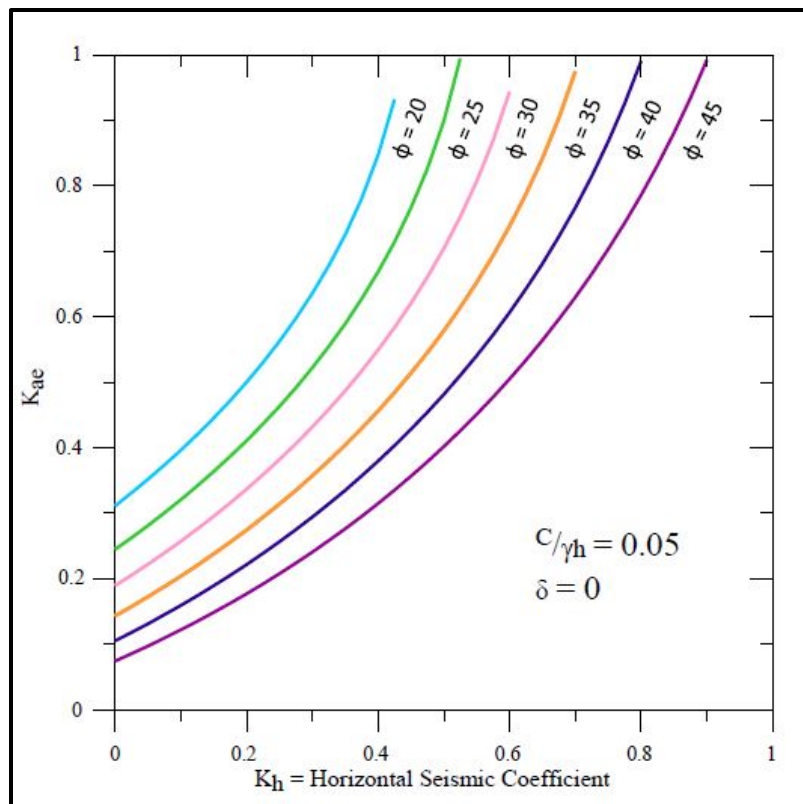


Figure 14-8, Seismic Active Earth Pressure Coefficient ( $\delta = 0$ ;  $C/\gamma_h = 0.05$ ) (modified Shamsabadi, et al. (2013b))

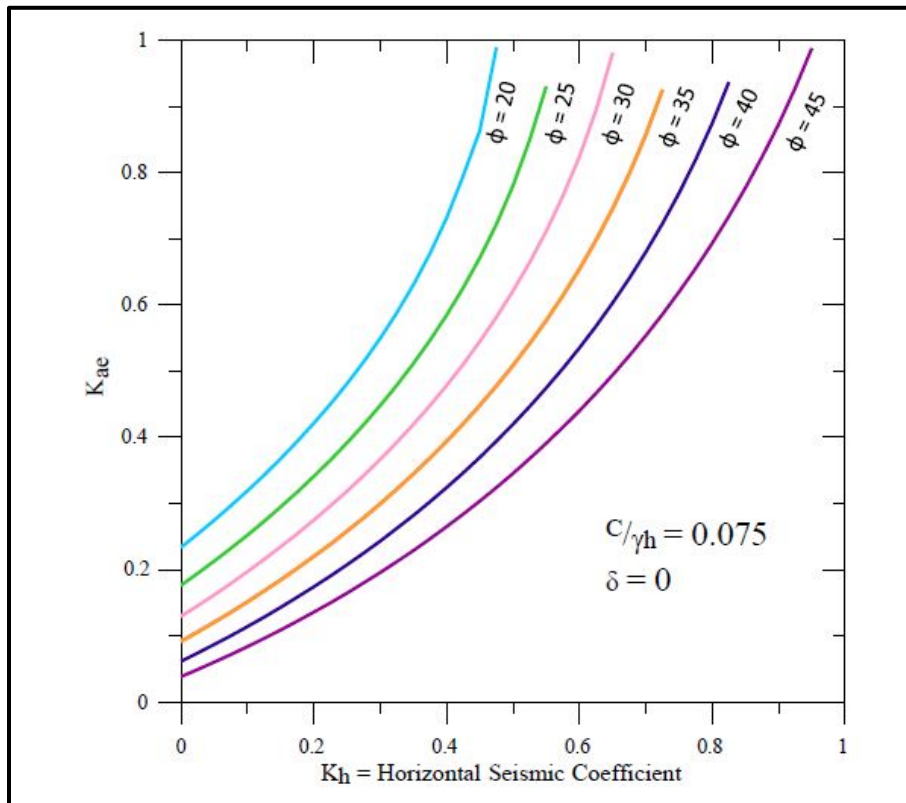


Figure 14-9, Seismic Active Earth Pressure Coefficient ( $\delta = 0$ ;  $C/\gamma_h = 0.075$ ) (modified Shamsabadi, et al. (2013b))

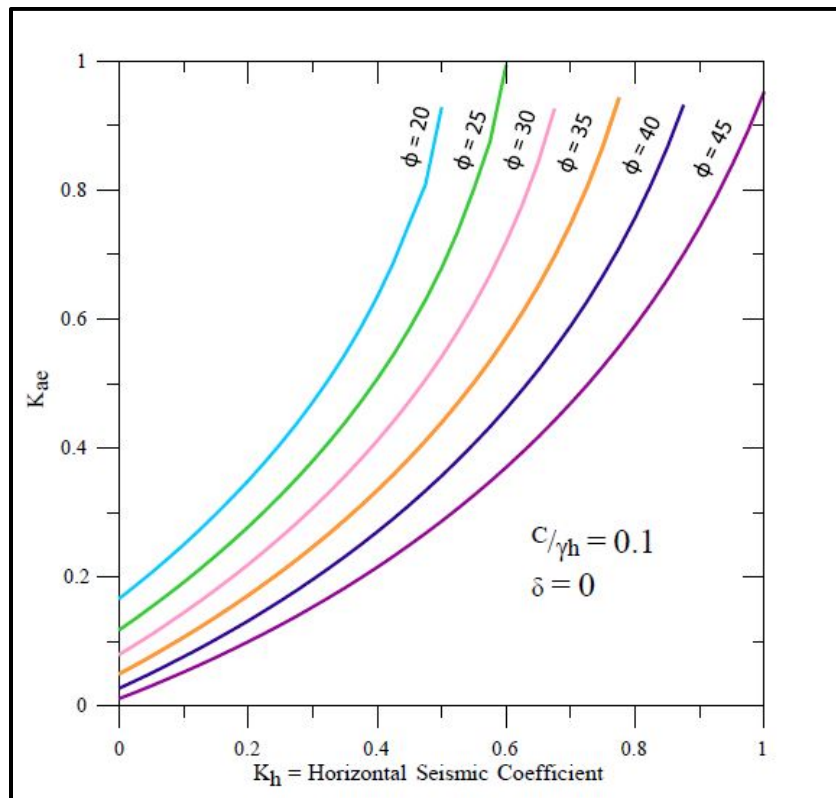


Figure 14-10, Seismic Active Earth Pressure Coefficient ( $\delta = 0$ ;  $C/\gamma_h = 0.1$ ) (modified Shamsabadi, et al. (2013b))

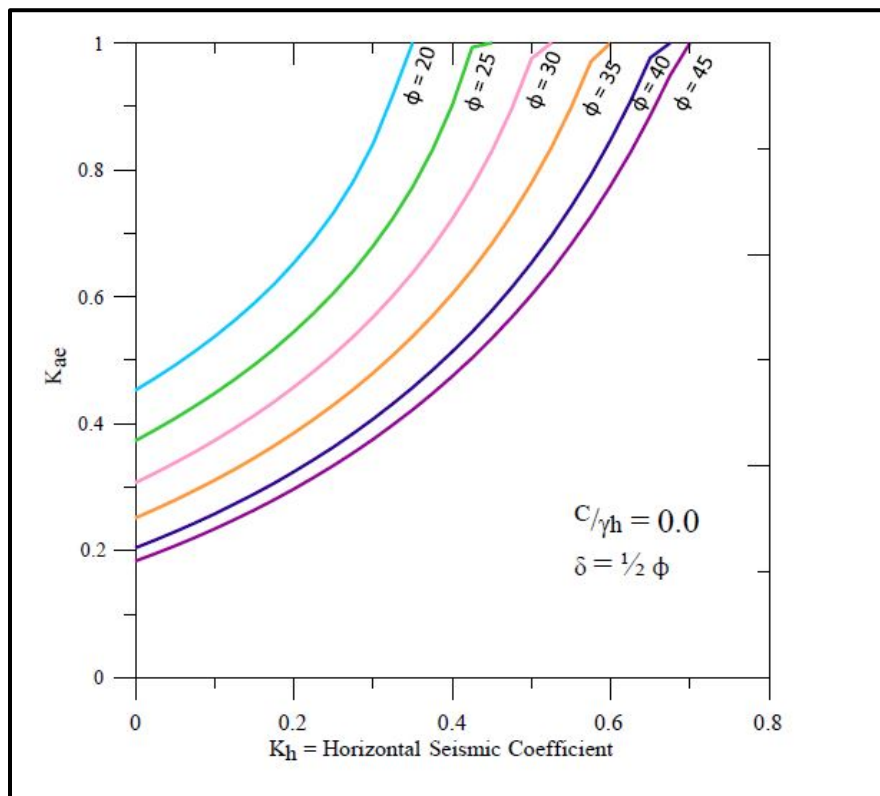


Figure 14-11, Seismic Active Earth Pressure Coefficient ( $\delta = 1/2\phi$ ;  $C/\gamma_h = 0.0$ ) (modified Shamsabadi, et al. (2013b))

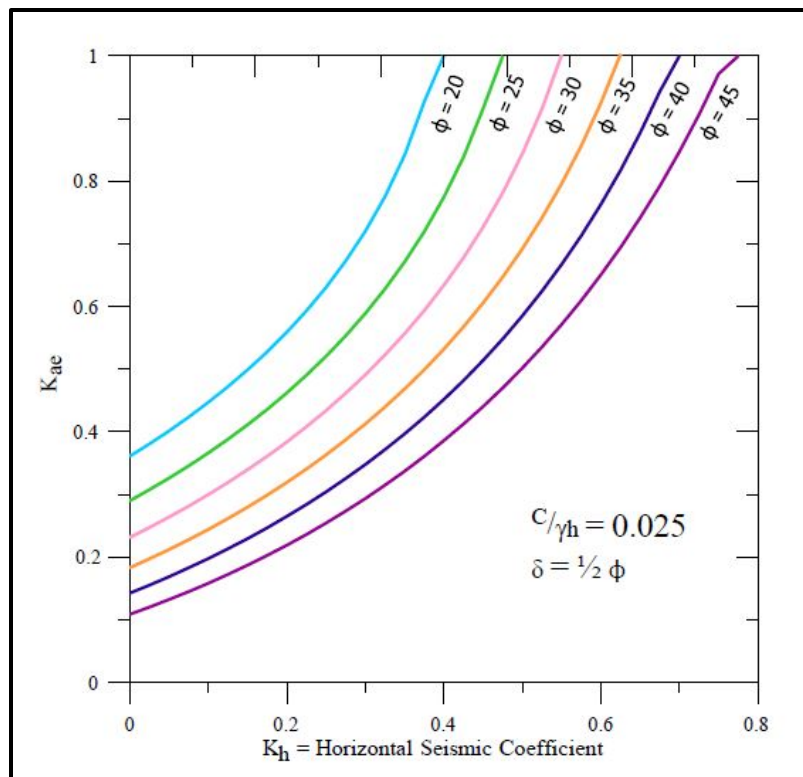


Figure 14-12, Seismic Active Earth Pressure Coefficient ( $\delta = 1/2\phi$ ;  $C/\gamma H = 0.025$ ) (modified Shamsabadi, et al. (2013b))

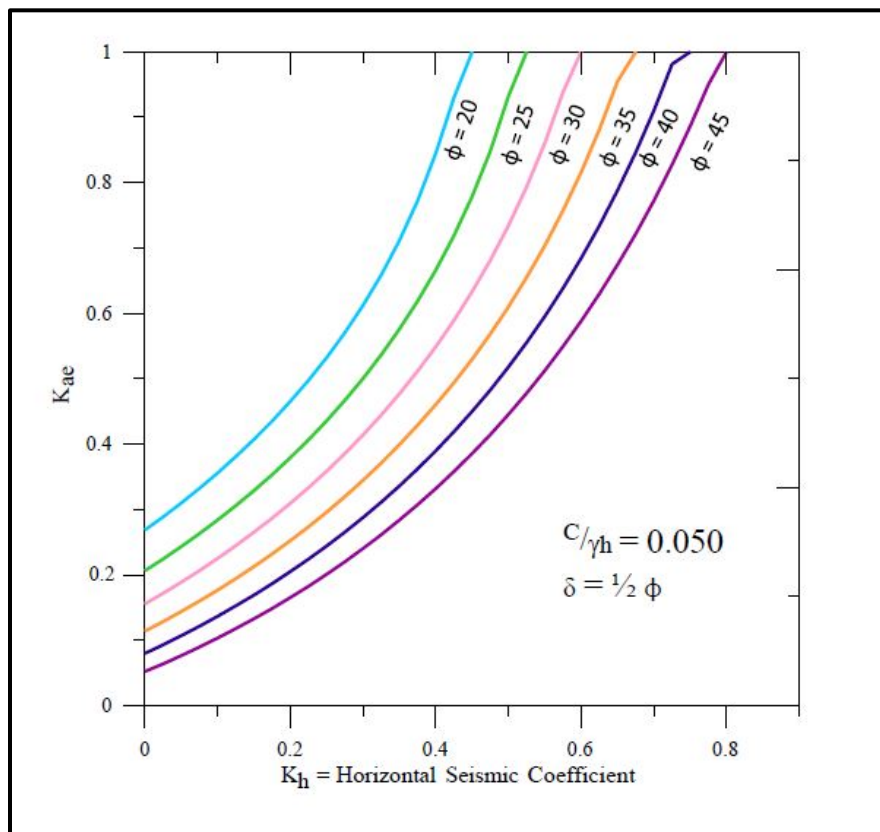


Figure 14-13, Seismic Active Earth Pressure Coefficient ( $\delta = 1/2\phi$ ;  $C/\gamma H = 0.05$ ) (modified Shamsabadi, et al. (2013b))

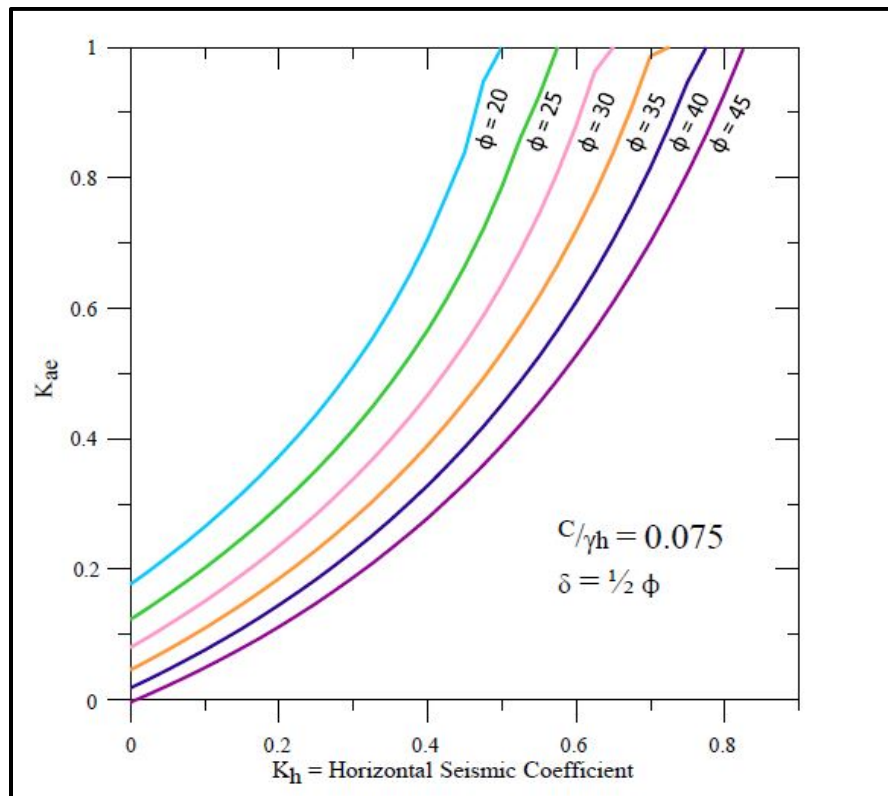


Figure 14-14, Seismic Active Earth Pressure Coefficient ( $\delta = 1/2\phi$ ;  $C/\gamma_h = 0.075$ ) (modified Shamsabadi, et al. (2013b))

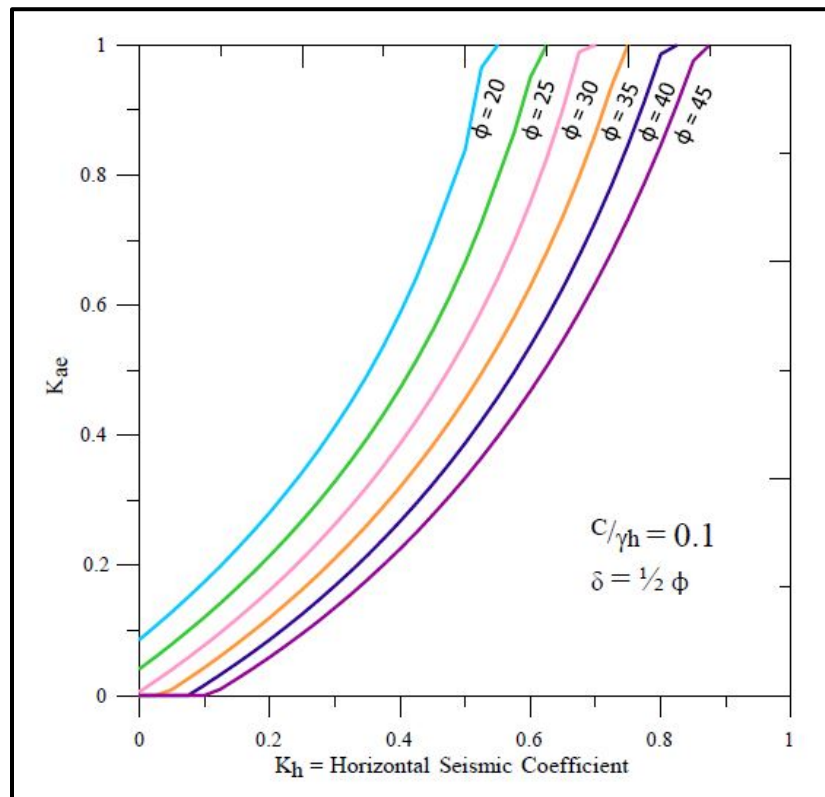


Figure 14-15, Seismic Active Earth Pressure Coefficient ( $\delta = 1/2\phi$ ;  $C/\gamma_h = 0.1$ ) (modified Shamsabadi, et al. (2013b))

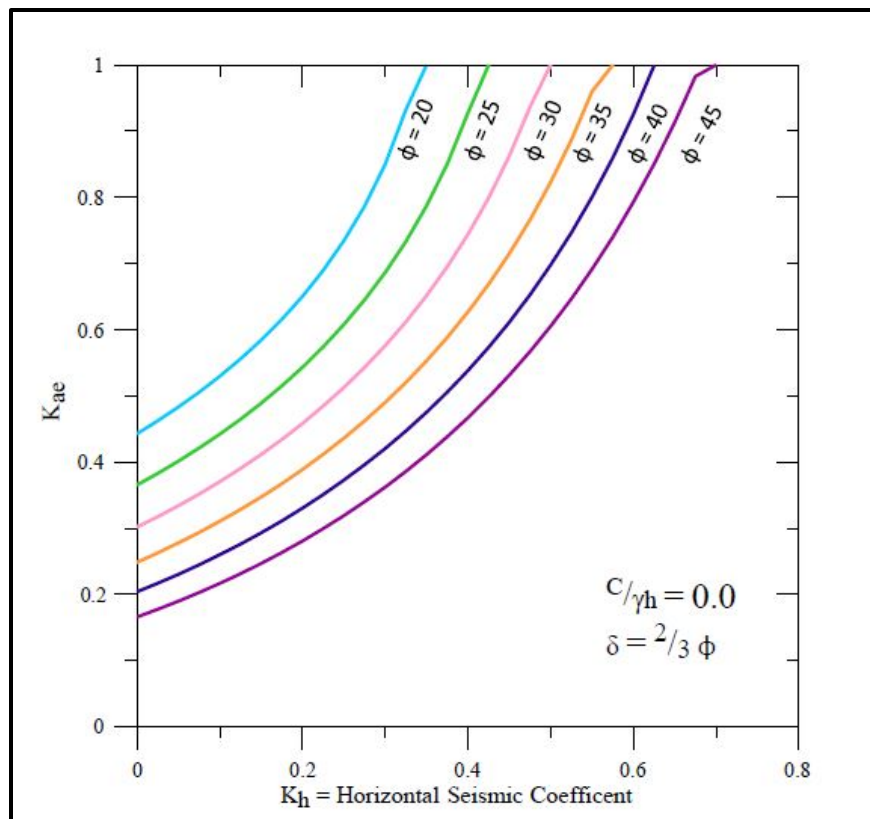


Figure 14-16, Seismic Active Earth Pressure Coefficient ( $\delta = 2/3\phi$ ;  $C/\gamma H = 0.0$ ) (modified Shamsabadi, et al. (2013b))

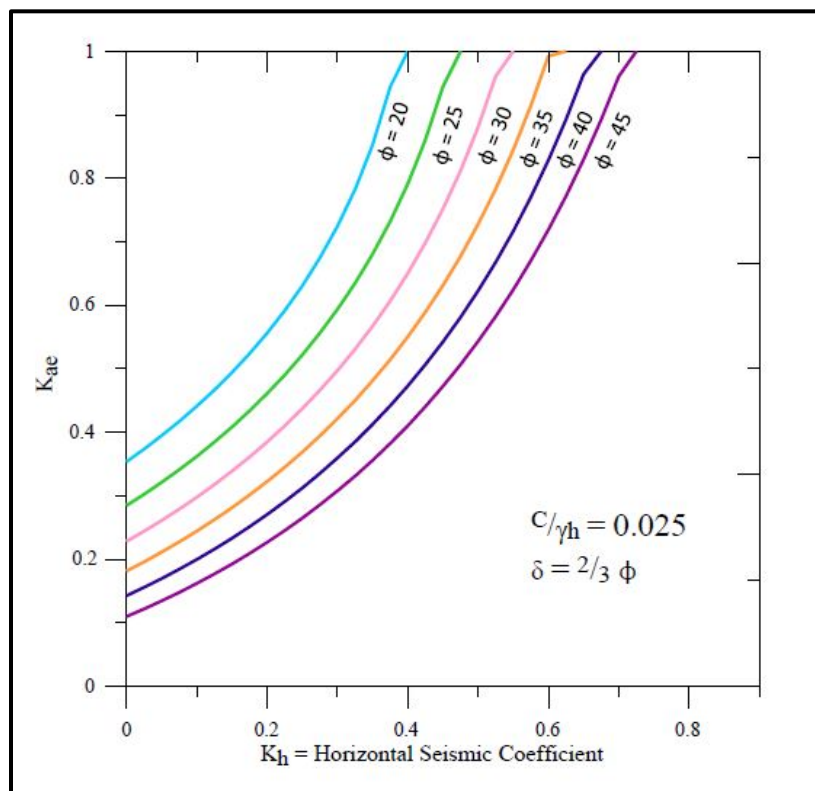


Figure 14-17, Seismic Active Earth Pressure Coefficient ( $\delta = 2/3\phi$ ;  $C/\gamma H = 0.025$ ) (modified Shamsabadi, et al. (2013b))

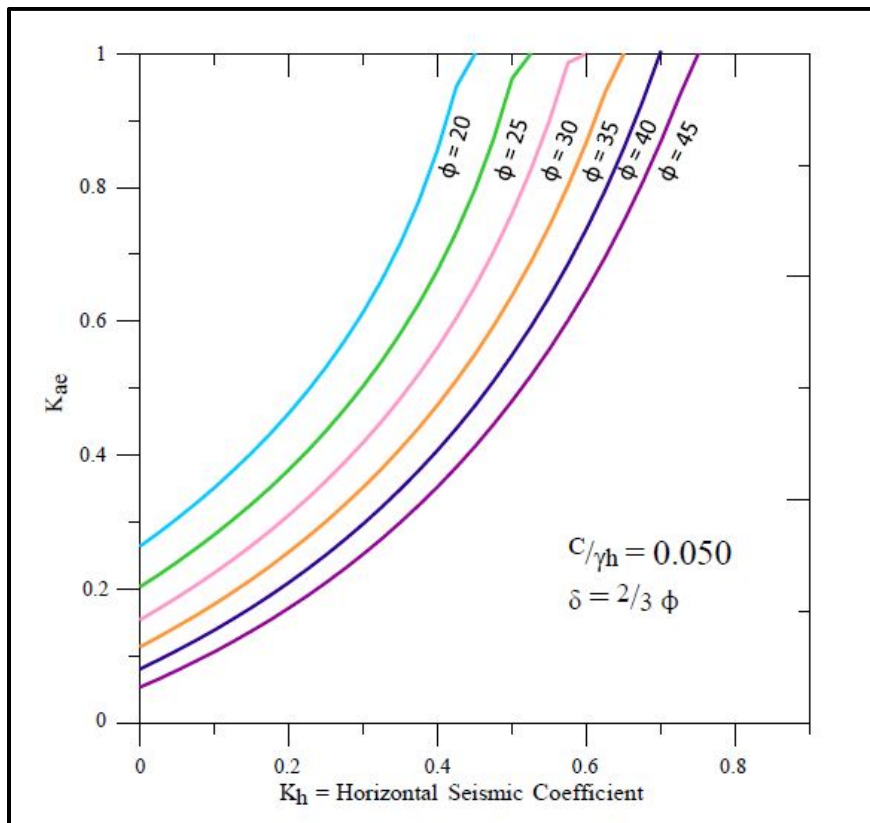


Figure 14-18, Seismic Active Earth Pressure Coefficient ( $\delta = 2/3\phi$ ;  $C/\gamma H = 0.05$ ) (modified Shamsabadi, et al. (2013b))

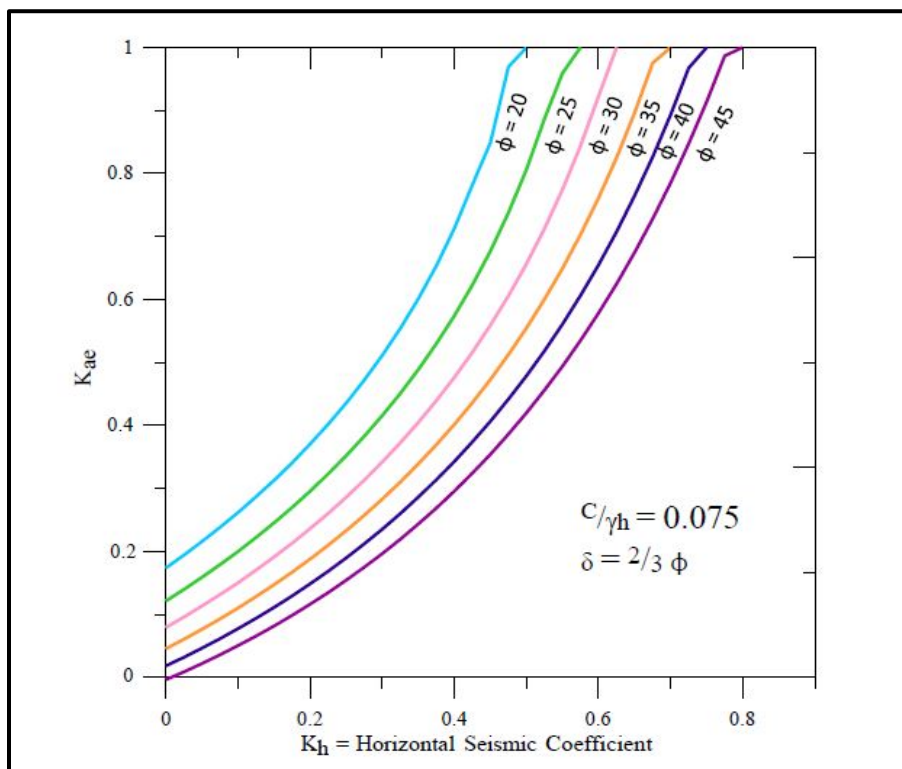


Figure 14-19, Seismic Active Earth Pressure Coefficient ( $\delta = 2/3\phi$ ;  $C/\gamma H = 0.075$ ) (modified Shamsabadi, et al. (2013b))

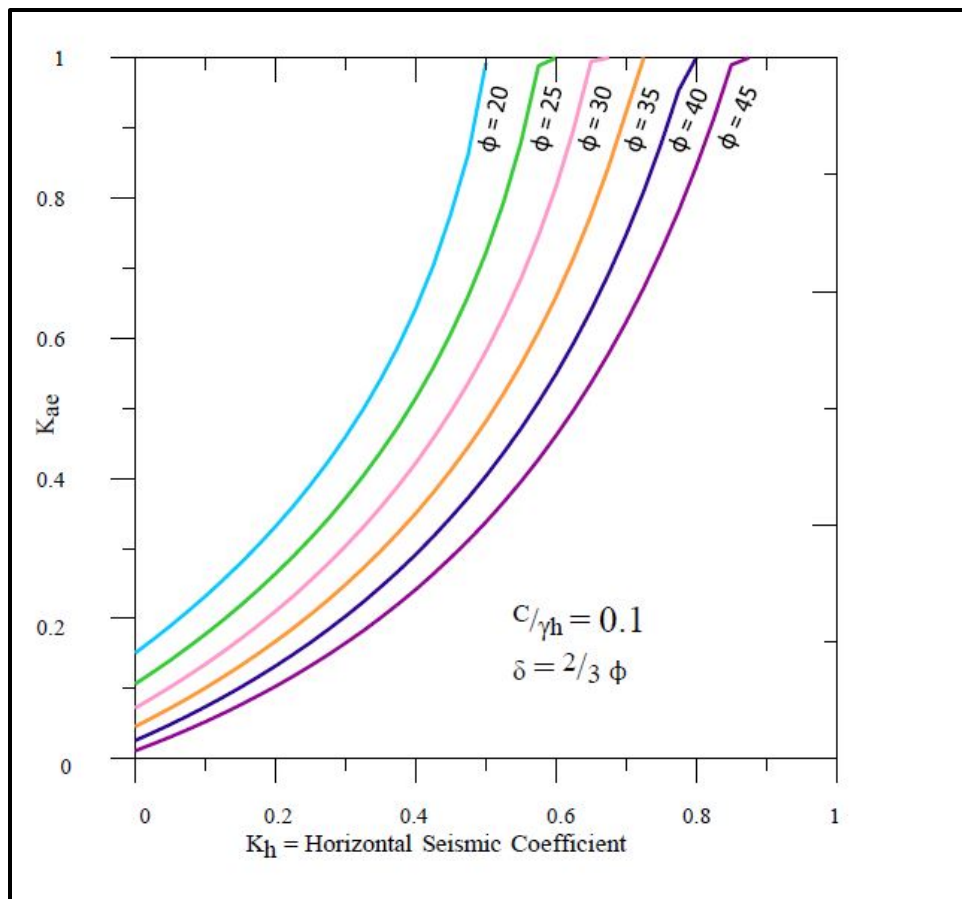


Figure 14-20, Seismic Active Earth Pressure Coefficient ( $\delta = 2/3\phi$ ;  $C/\gamma H = 0.01$ ) (modified Shamsabadi, et al. (2013b))

#### 14.4.5 GLE Method

The GLE method can also be used to evaluate critical seismically-induced active forces when the MO method is not the appropriate method. This method has been included in several conventional limit-equilibrium slope stability computer programs. This method is the most robust of the limit equilibrium methods because it can handle complex geometries, it incorporates various soil layers, and it allows the user to explore unlimited failure surfaces and soil combinations without sacrificing time or accuracy.

The slope stability method that shall be used in this analysis is Spencer's method because it satisfies the equilibrium of forces and moments. Circular, linear, multi-linear, or random failure surfaces should be investigated. Additional guidance on using this method can be obtained from NCHRP Report 611 by Anderson, et al. (2008) and Chugh (1995).

#### 14.4.6 Unyielding Structures

Seismic active soil pressures require that the wall yield sufficiently to mobilize minimum active soil pressures. Approximate values of relative movement required to reach active earth pressure conditions are provided in Chapter 18.

If the retaining structure is rigidly fixed or restrained from movement, the earthquake-induced forces will be much higher than those predicted by the seismic active pressures. Analytical methods to evaluate these types of loads on unyielding structures are not within the state of practice for this type of structure. AASHTO requires that walls and abutments that are rigidly fixed or restrained from movements be designed using horizontal acceleration coefficients that are 1.5 times the horizontal acceleration coefficient ( $k_h$ ). The average horizontal acceleration coefficient ( $k_h$ ) that has been adjusted for wave scattering should be used when computing seismic lateral loadings on unyielding structures. The vertical accelerations shall be set to 0.0.

## 14.5 SEISMIC PASSIVE SOIL PRESSURES

Seismically-induced lateral loadings can mobilize passive soil pressure resistance such as those that occur when an ERS resists sliding by either shear keys or when an abutment backwall is displaced into the backfill. The passive resistance versus displacement behind bridge abutment wall is provided in Section 14.9.

For retaining wall components subject to passive resistance that are less than 5 feet in height, the passive resisting forces shall be computed using static passive forces. Static passive forces for wall heights or foundation thicknesses less than 5 feet shall be used because it is anticipated that the inertial effects from earthquake loadings will be small (see Chapter 18). For retaining wall components subject to passive resistance that are 5 feet or greater in height, the passive resisting forces must take into account the inertial effects from the earthquake. The MO method of determining passive pressure coefficients shall not be used due to the various limitations of the method.

The Log-Spiral-Rankine (LSR) Method uses a both a log-spiral portion of the soil wedge behind the wall as well as a Rankine portion (see Figure 14-21). The LSR Method uses procedures that account for internal friction and cohesion as well as wall-soil interface friction and adhesion. The LSR Method can be used to determine the passive earth pressures and is more advantageous to passive earth pressures. The triangular (shaded) area in Figure 14-21 is a Rankine Zone, because the shear stress ( $\tau$ ) in this region is induced only by the horizontal seismic body forces without any contribution from friction or cohesion.

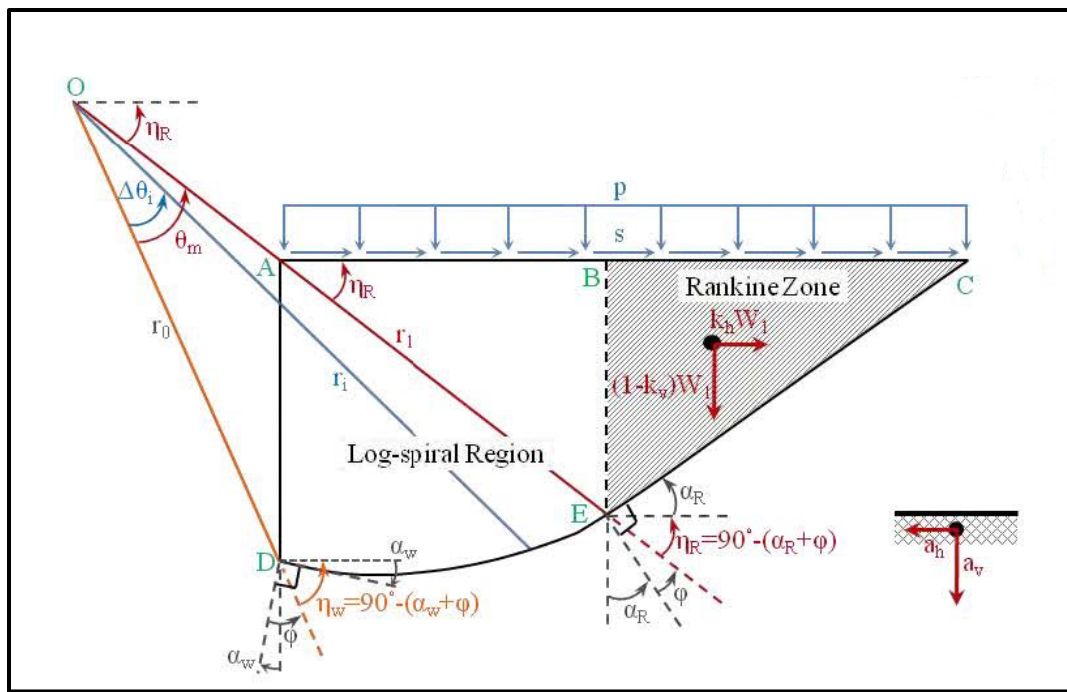


**Figure 14-21, LSR Passive Seismic Wedge (Shamsabadi, et al. (2013b))**

For a detailed explanation of the LSR Method please refer to Shamsabadi, Xu, and Taciroglu (2013a), Shamsabadi, Xu, and Taciroglu (2013b), and Xu, Shamsabadi and Taciroglu (2015). Because of the complexity of this method, design charts have been developed for the LSR Method based on the following site conditions:

1. Level ground behind the wall
2.  $k_v = 0g$
3. Wall friction angles of  $\delta = 0.0, 1/2(\phi), 2/3(\phi)$
4. Shear strength friction ratios of  $C/\gamma*H = 0.0, 0.025, 0.05, 0.075, \text{ and } 0.10$

Where:

- c = Cohesion, pounds per square foot
- $\gamma$  = Unit weight of soil, pounds per cubic foot
- H = Wall height, feet

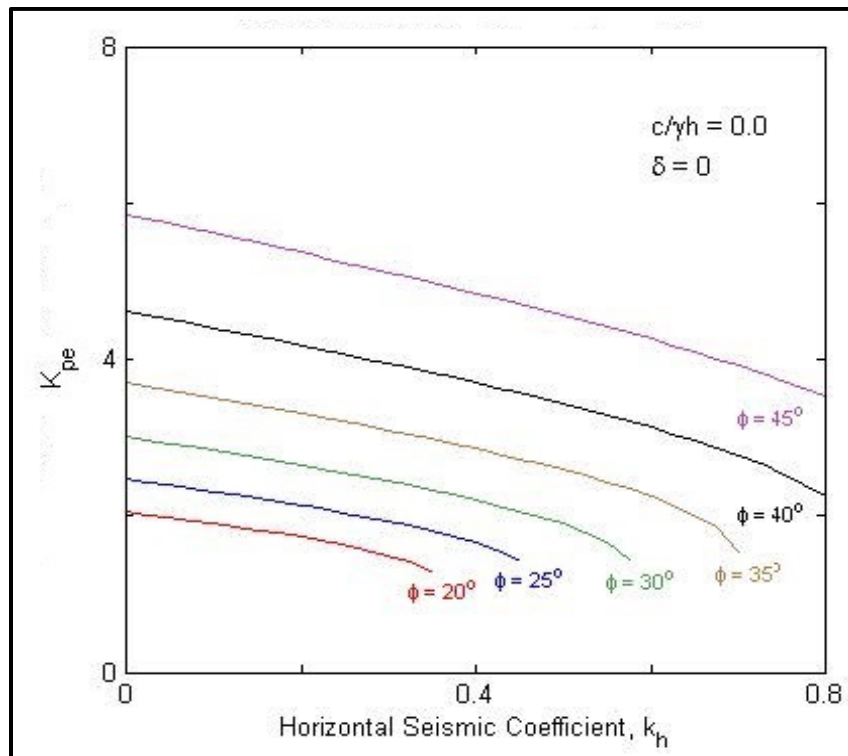


Figure 14-22, Seismic Passive Earth Pressure Coefficient ( $\delta = 0$ ;  $C/\gamma H = 0.0$ ) (modified Shamsabadi, et al. (2013b))

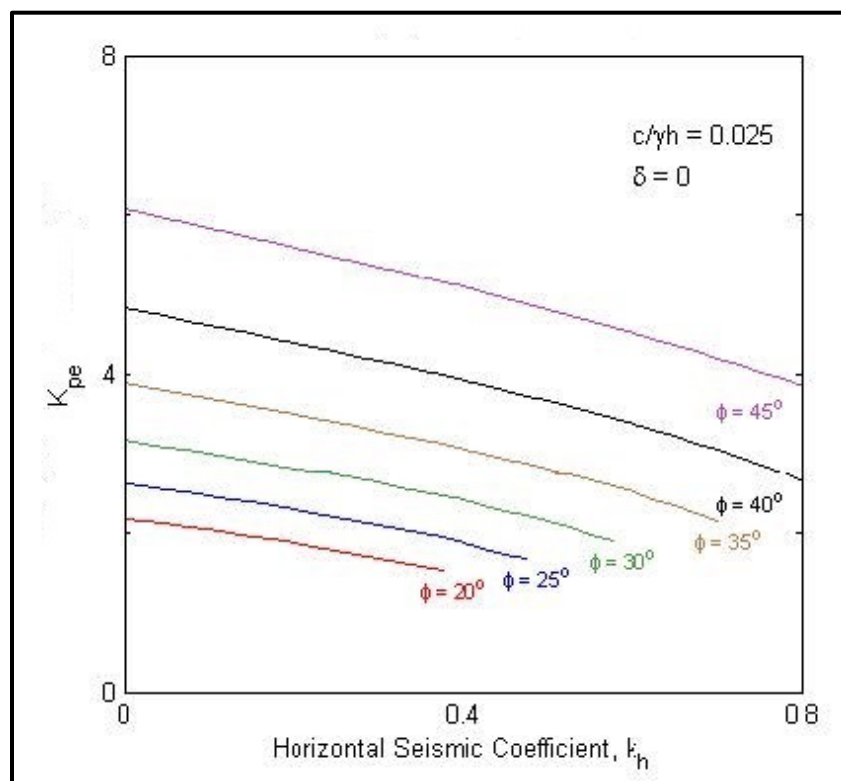


Figure 14-23, Seismic Passive Earth Pressure Coefficient ( $\delta = 0$ ;  $C/\gamma H = 0.025$ ) (modified Shamsabadi, et al. (2013b))

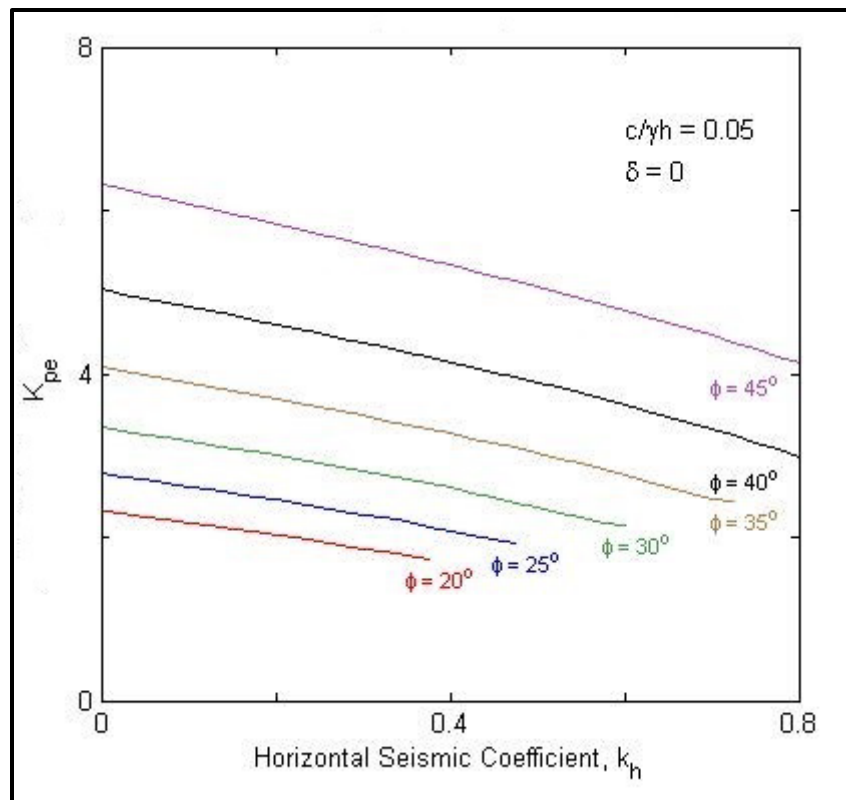


Figure 14-24, Seismic Passive Earth Pressure Coefficient ( $\delta = 0$ ;  $C/\gamma H = 0.05$ ) (modified Shamsabadi, et al. (2013b))

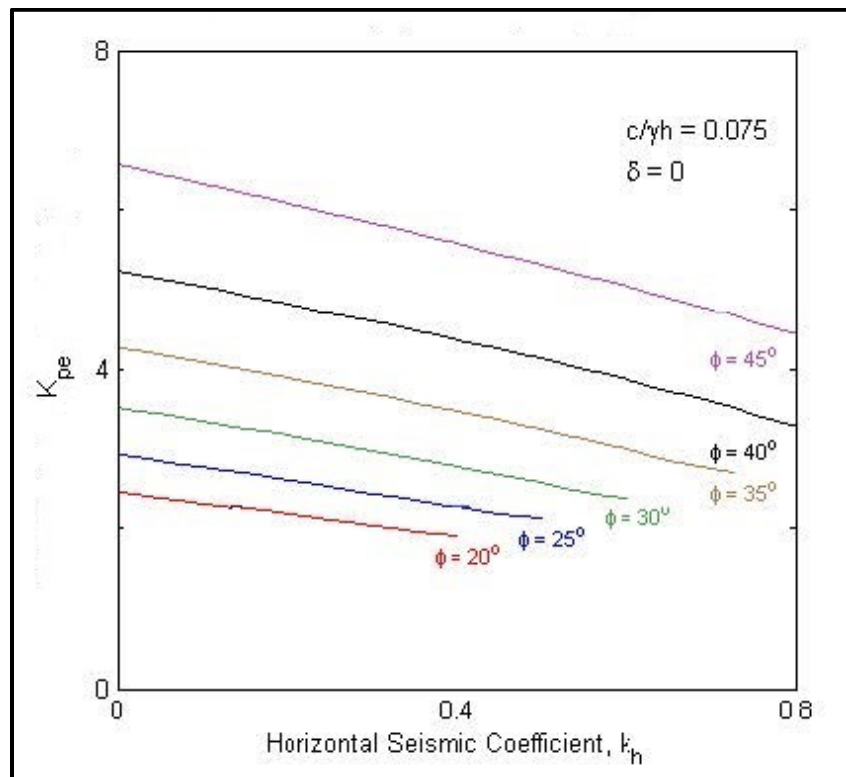


Figure 14-25, Seismic Passive Earth Pressure Coefficient ( $\delta = 0$ ;  $C/\gamma H = 0.075$ ) (modified Shamsabadi, et al. (2013b))

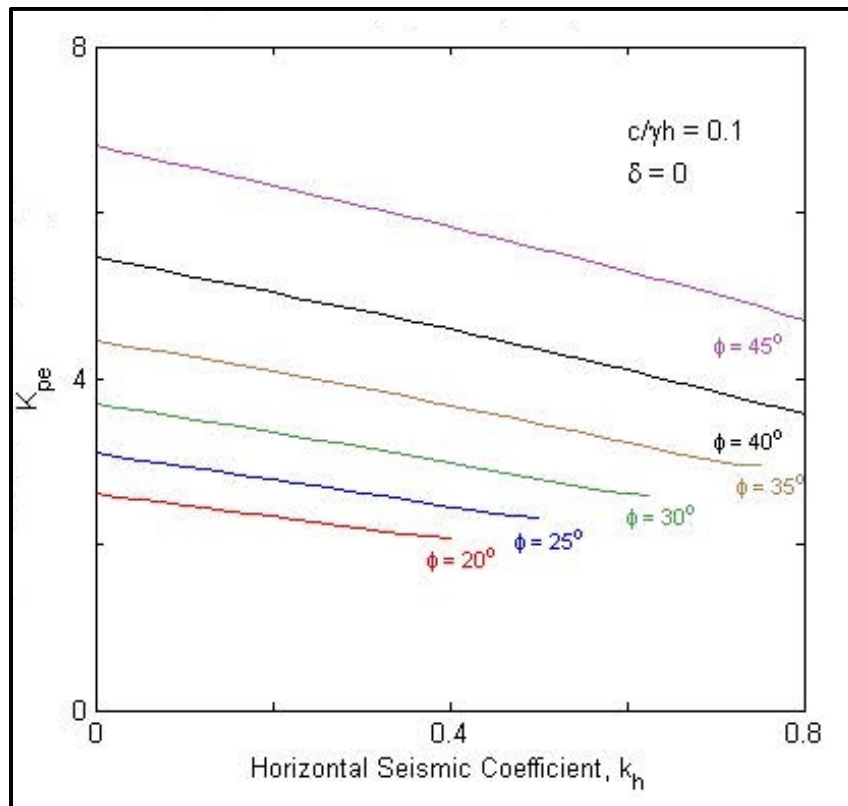


Figure 14-26, Seismic Passive Earth Pressure Coefficient ( $\delta = 0$ ;  $C/\gamma H = 0.1$ ) (modified Shamsabadi, et al. (2013b))

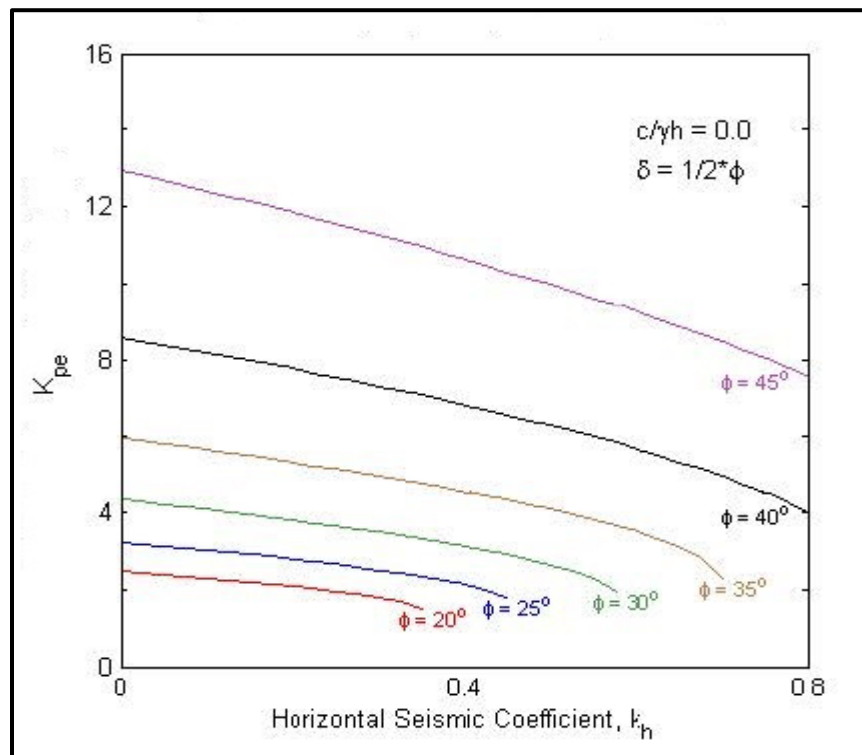
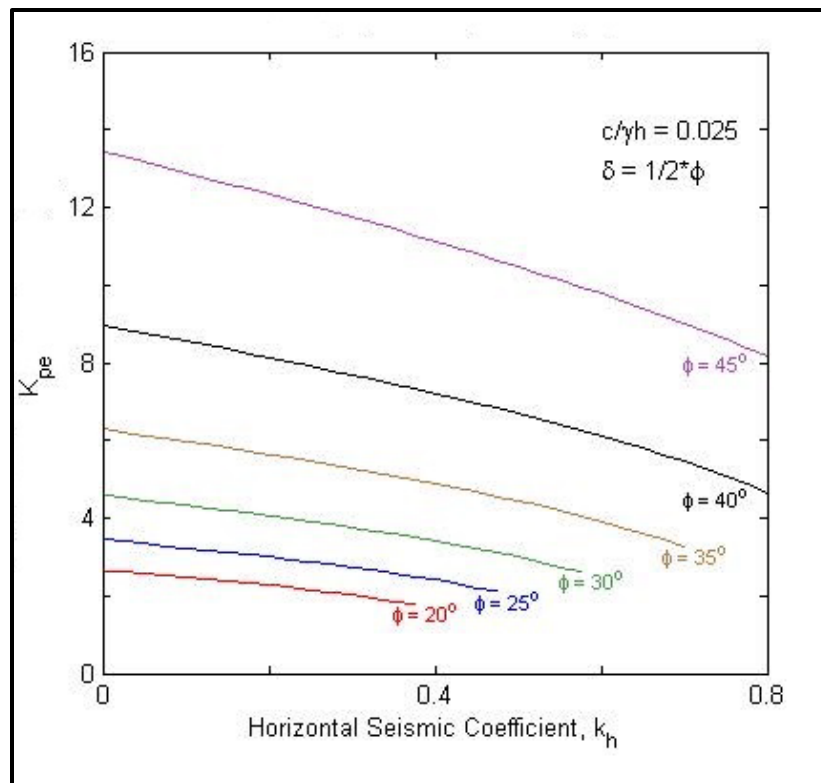
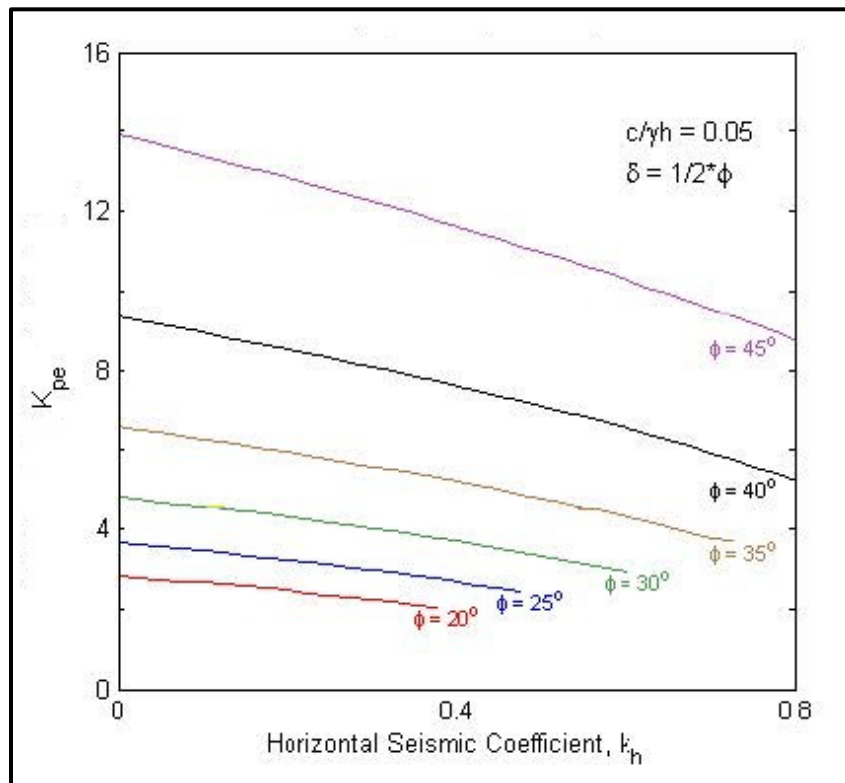


Figure 14-27, Seismic Passive Earth Pressure Coefficient ( $\delta = 1/2\phi$ ;  $C/\gamma H = 0.0$ ) (modified Shamsabadi, et al. (2013b))



**Figure 14-28, Seismic Passive Earth Pressure Coefficient ( $\delta = 1/2\phi$ ;  $C/\gamma H = 0.025$ ) (modified Shamsabadi, et al. (2013b))**



**Figure 14-29, Seismic Passive Earth Pressure Coefficient ( $\delta = 1/2\phi$ ;  $C/\gamma H = 0.05$ ) (modified Shamsabadi, et al. (2013b))**

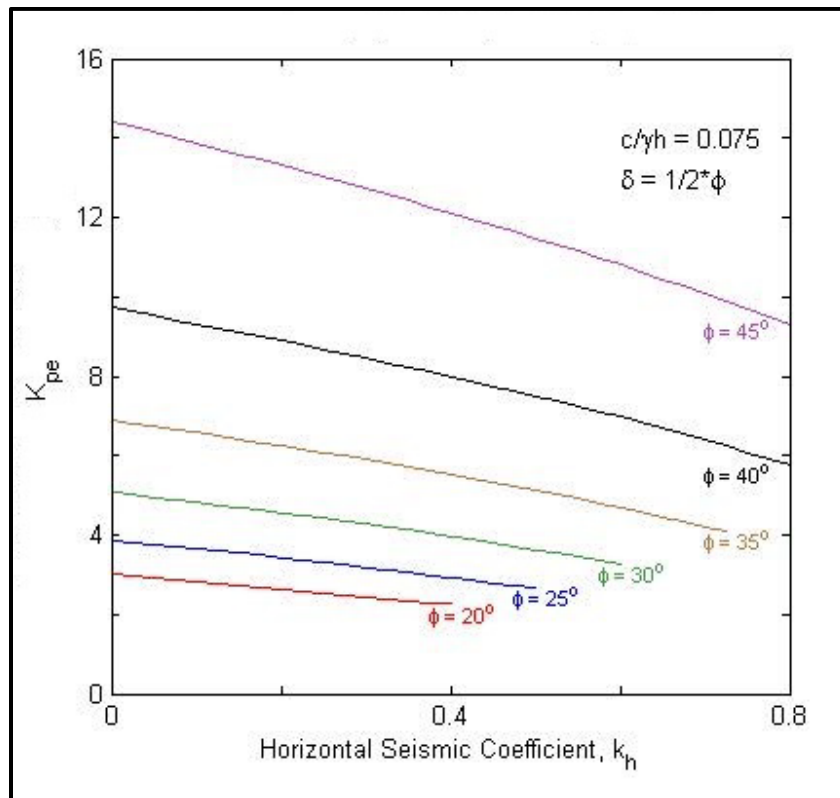


Figure 14-30, Seismic Passive Earth Pressure Coefficient ( $\delta = 1/2\phi$ ;  $C/\gamma H = 0.075$ ) (modified Shamsabadi, et al. (2013b))

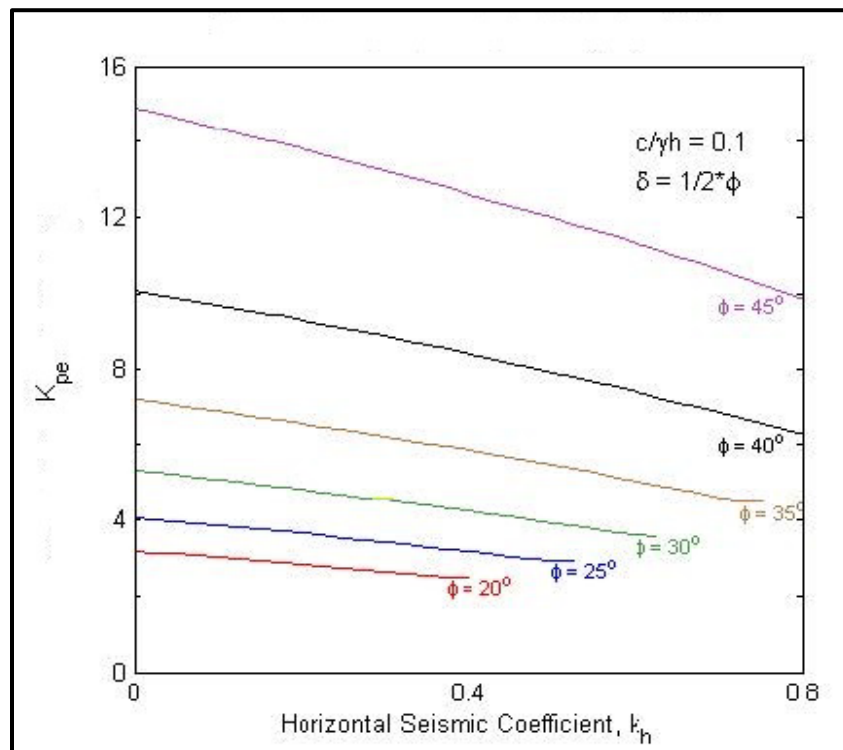


Figure 14-31, Seismic Passive Earth Pressure Coefficient ( $\delta = 1/2\phi$ ;  $C/\gamma H = 0.1$ ) (modified Shamsabadi, et al. (2013b))

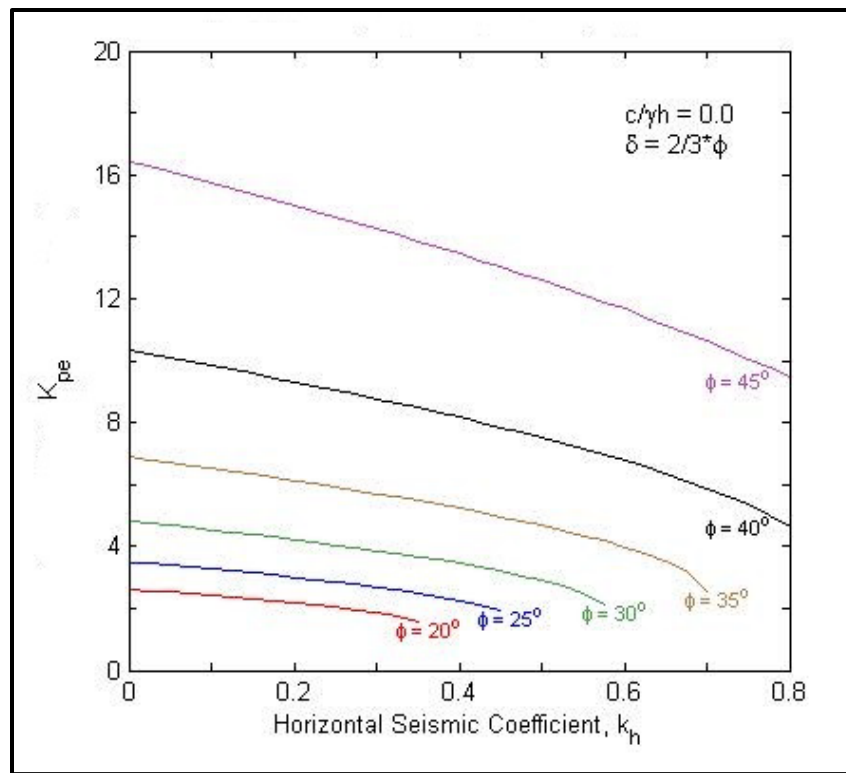


Figure 14-32, Seismic Passive Earth Pressure Coefficient ( $\delta = 2/3\phi$ ;  $C/\gamma H = 0.0$ ) (modified Shamsabadi, et al. (2013b))

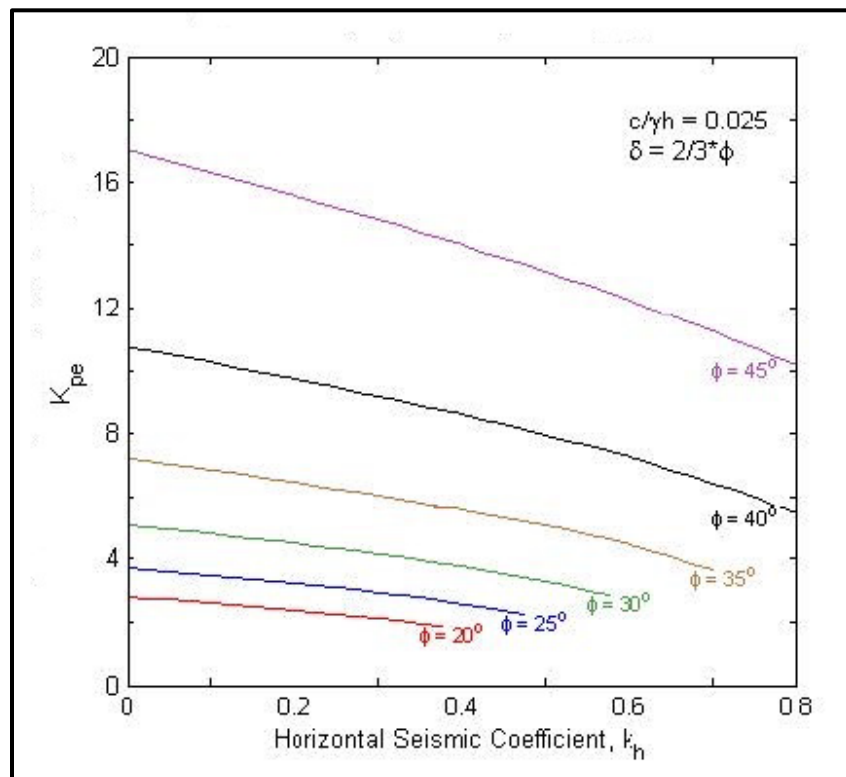


Figure 14-33, Seismic Passive Earth Pressure Coefficient ( $\delta = 2/3\phi$ ;  $C/\gamma H = 0.025$ ) (modified Shamsabadi, et al. (2013b))

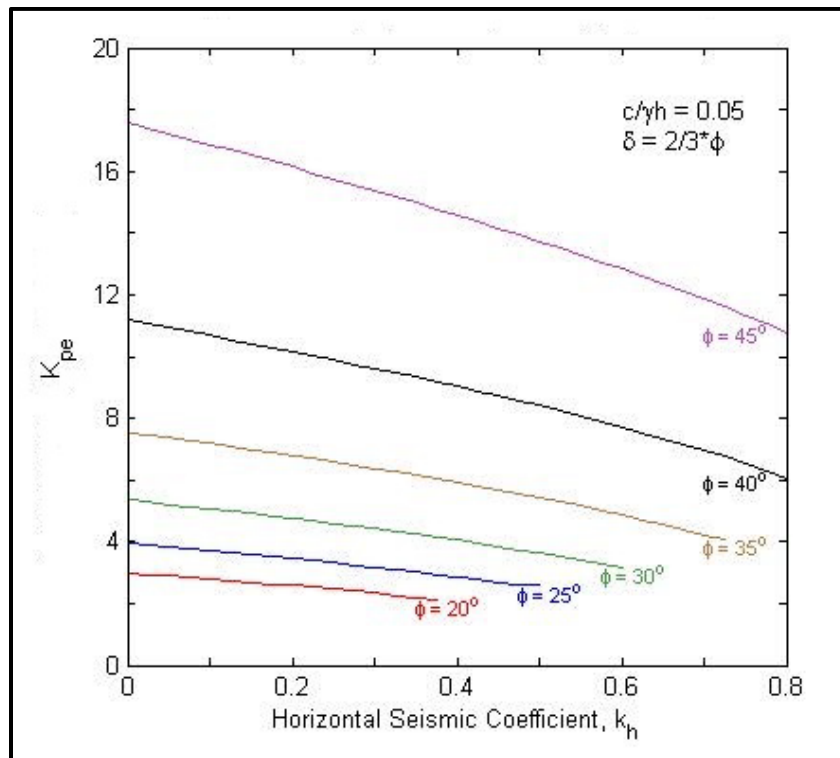


Figure 14-34, Seismic Passive Earth Pressure Coefficient ( $\delta = 2/3\phi$ ;  $C/\gamma H = 0.05$ ) (modified Shamsabadi, et al. (2013b))

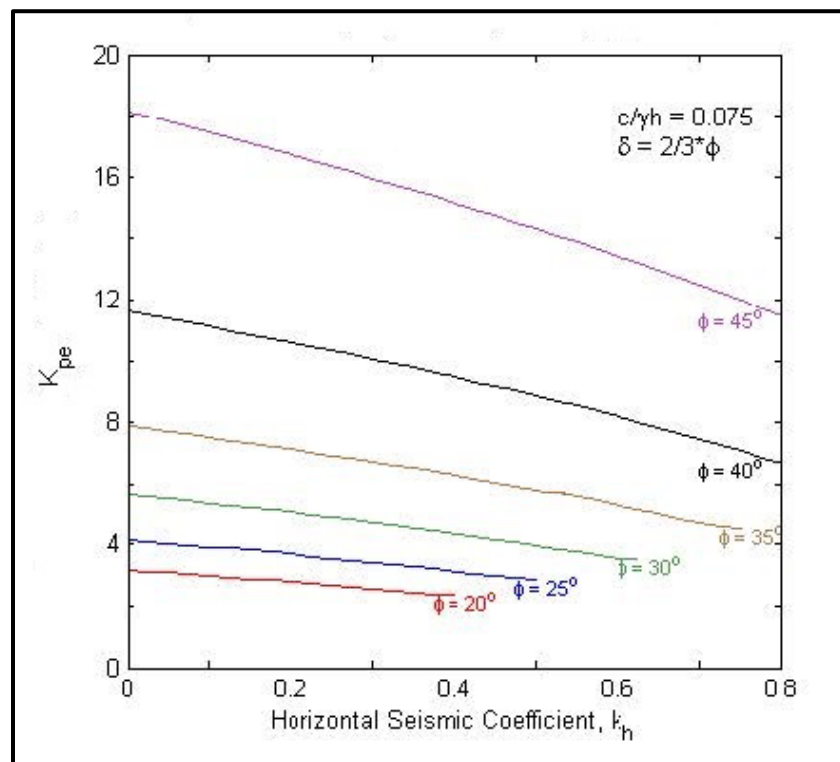
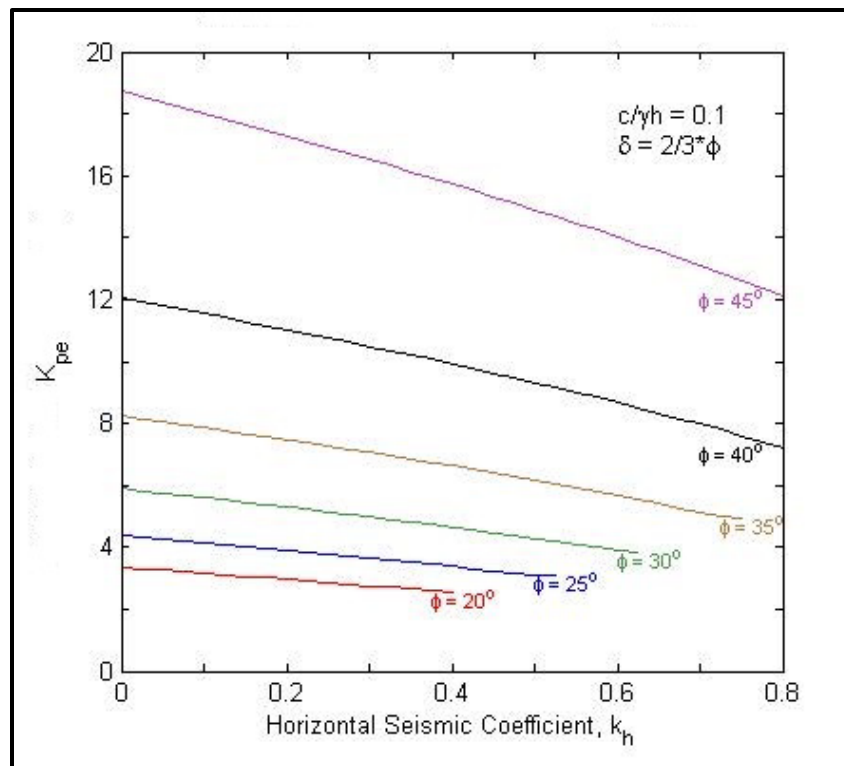


Figure 14-35, Seismic Passive Earth Pressure Coefficient ( $\delta = 2/3\phi$ ;  $C/\gamma H = 0.075$ ) (modified Shamsabadi, et al. (2013b))



**Figure 14-36, Seismic Passive Earth Pressure Coefficient ( $\delta = 2/3\phi$ ;  $C/\gamma H = 0.1$ ) (modified Shamsabadi, et al. (2013b))**

## 14.6 GEOTECHNICAL SEISMIC DESIGN OF BRIDGES

The geotechnical seismic design of bridges is a collaborative effort between the SEOR and the GEOR. In order to provide the appropriate geotechnical seismic design information, the GEOR will need to develop an understanding of the bridge design and behavior under seismic loading. The GEOR will need to become familiar with:

- Bridge Characteristics: structural fundamental period ( $T_0$ ), structure type, bridge damping (i.e., 5%), and bridge plans.
- Structural analysis method to be used by the SEOR to model the bridge foundations and abutments.
- Performance Criteria: Geotechnical seismic design for the EE I limit state design uses a Performance Based Design methodology. It is, therefore, necessary to establish performance criteria that are specific to the bridge being designed. The performance criteria provided in Chapter 10 should be used as a guide. Performance limits may need to be revised as the bridge design is modified to accommodate bridge movements.

The GEOR typically provides the SEOR the following:

- ADRS Curves
- Bridge Abutment Soil-Structure Interaction Boundaries
- Foundation Soil-Structure Interaction Boundaries
- Effects of Seismic Hazards on the Bridge

- Geotechnical mitigation options to eliminate or reduce the effects of seismic hazards

### **14.6.1 ADRS Curves**

The site response for the design earthquake (FEE or SEE) is represented by a horizontal ADRS curve that represents the pseudo-spectral accelerations for the uniform hazard at different frequencies or periods. The PC/GDS develops ADRS curves at either the ground surface or the depth-to-motion location of the bridge element being evaluated as presented in Chapter 12. The site response is evaluated by either using the 3-Point method or performing a Site-Specific Seismic Response Analysis.

Site-Specific Seismic Response Analysis shall be performed in accordance with Chapters 11 and 12. The Site-Specific Response Analysis is typically performed using 1-dimensional equivalent linear site response software (i.e., SHAKE2000). When the subsurface site conditions and earthquake motion input exceed the limitations of the 1-dimensional equivalent linear site response methodology as indicated in Chapter 12, a non-linear site response analysis using appropriate non-linear site response software (i.e., DMOD2000) must be used to develop the ADRS.

All earthquake input motions must be scaled to match the uniform hazard spectral accelerations. SCDOT typically provides the earthquake input motion by developing synthetic earthquake time histories. The software used to develop the synthetic earthquake input motions can vary the frequency content by using different seeds. The use of real strong motion earthquakes will follow the procedures developed in Chapters 11 and 12.

A bridge site can have multiple site response curves depending on the subsurface soils, depth-to-motion of the foundations (i.e., interior bents vs. bridge abutments), fundamental period of the bridge, and the number and locations of joints on the bridge (i.e., is the bridge jointless, regardless of length or does the bridge have a number of joints that have ability to absorb deflections). The development of a single ADRS curve for use in bridge seismic analyses will require input from the SEOR. The SEOR will provide input as to the site response curve that will have the largest effect on the behavior of the bridge during a seismic event. The SEOR is responsible for determining the Seismic Design Category (SDC) using  $S_{D1}$  and the requirements of the Seismic Specs. The GEOR's determination of the SDC does not relieve the SEOR of the responsibility for confirming that the correct SDC has been selected. For jointless bridges and those bridges without sufficient ability to absorb deflections, the site response curve generated at the bridge abutment typically has the largest impact on the seismic design of a bridge and may be used as the ADRS curve with concurrence from the SEOR. For bridges with sufficient ability to absorb deflections, it may be necessary to develop an ADRS curve that envelopes all of the site-response curves for the bridge site. This necessitates that the GEOR, PC/GDS and SEOR work together to evaluate the anticipated structure performance.

### **14.6.2 Bridge Abutments**

The GEOR needs to be familiar with the different types of bridge abutments that are currently being used by SCDOT and the effect of the seismic demand on the performance of the bridge abutment. See the BDM for a detailed explanation of each abutment type. Listed below are the 3 abutment types, typically used by SCDOT:

- Free-Standing End Bent
- Semi-Integral End Bent
- Integral End Bent

The GEOR will provide the soil component of the soil-structure design parameters for the bridge abutment to the SEOR. Soil-structure design parameters will be developed based on the SEOR's modeling requirements and anticipated abutment performance. Soil-structure parameters typically require either a single lateral linear spring to be used for the entire bridge abutment or a matrix of linear and rotational springs in all principal directions (i.e., x, y, and z). Because soil-structure interaction is typically non-linear, the secant modulus of linear springs must be provided to be compatible with the displacements. An analysis using the secant modulus typically requires several iterations on spring stiffness and displacement until the parameters converge.

### **14.6.3 Bridge Approach Embankment**

The bridge approach embankment (see Chapter 2 for definition) is designed to meet performance objectives of the bridge abutment by using performance limits that are based on the bridge OC. The bridge approach embankments are, therefore, designed for more stringent performance limits than are typically used for roadway embankments.

### **14.6.4 Bridge Foundations**

The performance of a bridge structure that is subjected to earthquake shaking is dependent on the superstructure and substructure (bridge foundations). Bridge foundations are typically driven piles or drilled shafts.

The GEOR is responsible for providing the soil component of the bridge foundation's soil-structure interaction model in order for the SEOR to be able to evaluate the performance of the bridge due to the seismic demand. Additional seismic design requirements are presented for shallow foundations in Section 14.7 and for deep foundations in Section 14.8.

## **14.7 SHALLOW FOUNDATION DESIGN**

Shallow foundations shall be designed for EE I loads using the procedures outlined in Chapter 15. Shallow foundations should not be considered when the subsurface soils are susceptible to SSL as defined in Chapter 13. If shallow foundations are to be considered at sites that are susceptible to SSL contact the PC/GDS for further guidance. In addition, shallow foundations shall not be used within any slope that becomes unstable during the EE I unless prior written approval is obtained from the PC/GDS. All of the limitations provided in Chapter 15 for shallow foundations shall apply to the use of shallow foundations during EE I. Any settlement induced by the EE I shall be determined in accordance with procedures indicated in Chapter 13.

## **14.8 DEEP FOUNDATION DESIGN**

The GEOR typically assists the SEOR in modeling the foundation performance. The performance of deep foundations is typically modeled by evaluating the soil-structure interaction between the deep foundation (i.e., driven piles, drilled shafts, etc.) and the subsurface soils. The soil-structure

interaction is dependent on maintaining compatibility between the response of the deep foundation and the response of the soil when evaluating axial and lateral loads.

Geotechnical seismic hazards (Chapter 13) can significantly impact deep foundations and consequently, the performance of the bridge. The failure mechanism of these geotechnical hazards needs to be thoroughly evaluated and understood in order to consider the effects of the geotechnical seismic hazard on deep foundations supporting a bridge. Deep foundation failure mechanisms are presented in Figure 14-37.

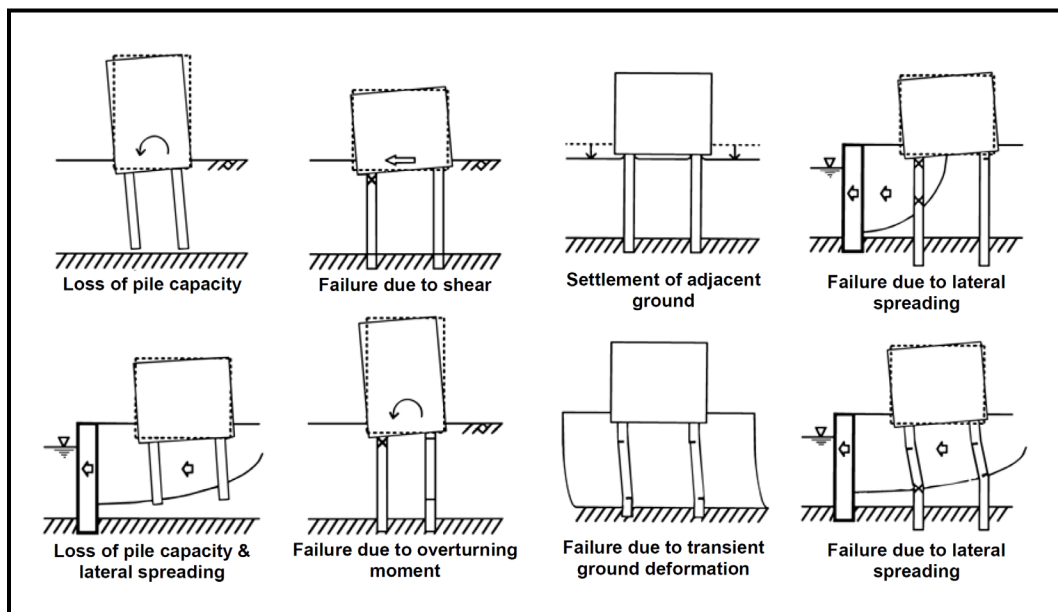


**Figure 14-37, Pile Damage Mechanisms in Liquefied Ground  
(Boulanger, et al. (2003))**

Geotechnical seismic hazards such as SSL and the resulting seismic settlement can reduce the axial bearing capacity of the deep foundation (Section 14.8.1) and the lateral soil resistance (Section 14.8.3). Deep foundation axial bearing capacity can be further reduced by downdrag loads (Section 14.8.2) induced during seismic settlement of the subsurface soils. Seismic hazard displacements due to flow slide failure and seismic global instability may impose lateral soil loads on the deep foundations (Section 14.8.4). The lateral soil loads on the deep foundations will increase the complexity of the soil-structure interaction. The effects of the lateral soil loads on soil-structure interaction between the substructure (i.e., footings, single deep foundations, deep foundation groups, etc.) are discussed in Section 14.8.5. The effects of geotechnical seismic hazards may significantly impact the performance of the bridge and may require mitigation as discussed in Section 14.15.

### 14.8.1 Axial Loads

When soil SSL is anticipated based on Chapter 13, the axial capacity of deep foundations for the EE I limit state shall be evaluated by adjusting the soil shear strength properties to residual soil shear strength in accordance with Chapter 13 and Section 14.8.2; and computing the axial capacity using the methods presented in Chapter 16. If the subsurface soils are susceptible to seismic settlement (Chapter 13), the axial capacity shall be evaluated using downdrag loads as indicated in Section 14.8.2.

### 14.8.2 Downdrag Loads

Geotechnical seismic hazards such as seismic soil settlement can induce downdrag loads on deep foundations similarly to downdrag loads that result from soil consolidation. Seismic soil settlements in unsaturated soils can occur as a result of densification or seismic compression. Seismic settlement of saturated soils is typically due to densification of Sand-Like soils that are subject to cyclic liquefaction.

Soils experiencing seismic settlement and those soils above the depth of seismic settlement will induce downdrag loads on deep foundations. Analytical methods for evaluating downdrag on deep foundations are provided in Chapter 16. Downdrag loads induced from unsaturated soils and soils not subject to seismic settlement should be based on soil-pile adhesion developed from total peak soil shear strengths. The shear strength of Sand-Like soils during cyclic liquefaction will initially be reduced to liquefied shear strength ( $\tau_{rl}$ ) as the soil reaches full liquefaction (excess pore pressure ratio  $R_u \approx 1.0$ ). As the pore pressure dissipates ( $R_u < 1.0$ ), seismic soil settlement occurs and at some point, the soil shear strength will begin to increase and the soils will be in a state of limited liquefaction. The soil-pile adhesion of Sand-Like soils during cyclic liquefaction is, therefore, greater than the liquefied shear strength ( $\tau_{rl}$ ), but considerably less than the undrained peak soil shear strengths ( $\tau_{Peak}$ ). Therefore, based on the relationship between the fully liquefied shear strength ( $\tau_{rl}$ ) and the peak undrained shear strength ( $\tau_{Peak}$ ), use a limited friction angle ( $\phi_{rl-lim}$ ) of  $20^\circ$  to determine the downdrag load induced by soils that have undergone liquefaction.

### 14.8.3 Lateral Soil Response of Liquefied Soils (p-y Curves)

Lateral resistance of deep foundations and cantilever retaining wall systems are typically modeled by “non-linear springs” that represent the lateral soil resistance and deflection response (P-y curves). The lateral response of liquefied soils consists of estimating the lateral resistance of the liquefied soils ( $P_{Liq}$ ) and the corresponding displacements ( $y$ ). These P-y curves of liquefied soils are used to model the non-linear soil response of applied load vs. displacement. Rollins, et al. (2005) has shown that P-y curves of liquefied soils have the following characteristics:

1. P-y curves of liquefied soils are characterized by a concave-up shape load-displacement curve. This shape appears to be due to dilative behavior of the soil during shearing.
2. P-y curves of liquefied sand transition from a concave-up shape to a concave-down shape as pore water pressure ( $u$ ) dissipates after full liquefaction ( $R_u = 1.0$ ).
3. P-y curves of liquefied sand stiffen with depth. Smaller displacements are required to develop significant resistance.
4. P-y curves of liquefied sand become progressively stiffer after liquefaction due to pore water pressure dissipation.
5. P-y curves of liquefied sand exhibit almost no lateral resistance (zone of no lateral resistance) followed by a stiffening response occurring after a certain relative displacement.
6. P-y curve zone of no lateral resistance is smaller for larger piles when compared to smaller piles.

The computer program, LPile Plus (Reese, et al. (2004)), is typically used to evaluate lateral loads on piles using P-y curves. The P-y curves for liquefied soils (Rollins, et al. (2005)) that are included in LPile Plus attempt to model the strain hardening behavior of liquefied soils, but tends to predict a response that is too soft. Since the Rollins, et al. (2005) model (Liquefied Sand in LPile Plus) has several limitations and response is very soft, it shall not be used to develop P-y curves of liquefied soils.

The P-y curves for Sand-Like soils subject to cyclic liquefaction should be estimated by either of the following two options:

1. The method recommended by Brandenberg, et al. (2007b) to develop P-y curves for fully liquefied Sand-Like soils (excess pore pressure ratio =  $R_u = u/\sigma'_v \approx 1.0$ ) consists of using static P-y curves for sands with a P-multiplier ( $m_p$ ). The  $m_p$  values developed by Brandenberg, et al. (2007b) are shown in Figure 14-38. The  $m_p$  should be selected using the thick red line shown in Figure 14-38 that is consistent with the range recommended by Brandenberg, et al. (2007b) of 0.05 for loose sand to 0.30 for dense sand. The  $m_p$  is selected based on corrected SPT blow counts ( $(N_1)_{60CS} = N_{1,60,CS}^*$  for Figure 14-38 only) which is consistent with the effects of relative density on undrained shear strength of sand. When limited liquefaction occurs ( $0.20 \leq R_u = u/\sigma'_v < 1.0$ ), the  $m'_p$  can be estimated by the following equation:

$$m'_p = 1 - [R_u * (1 - m_p)] \quad \text{Equation 14-6}$$

2. Alternatively, the static P-y curves for sands may be used to develop P-y curves for fully liquefied soils ( $R_u \approx 1.0$ ) by using the liquefaction shear strength ratio ( $\tau_{rl}/\sigma'_{vo}$ ) to compute a reduced soil friction angle ( $\phi_{rl}$ ). The liquefaction shear strength ratio ( $\tau_{rl}/\sigma'_{vo}$ ) can be estimated from Chapter 13. The reduced soil friction angle due to cyclic liquefaction ( $\phi_{rl}$ ) can be computed by the following equation:

$$\phi_{rl} = \tan^{-1} \frac{\tau_{rl}}{\sigma'_{vo}} \quad \text{Equation 14-7}$$

Use a reduced soil friction angle for limited liquefaction ( $\phi_{rl-lim}$ ) of  $20^\circ$  to develop the p-y curves.

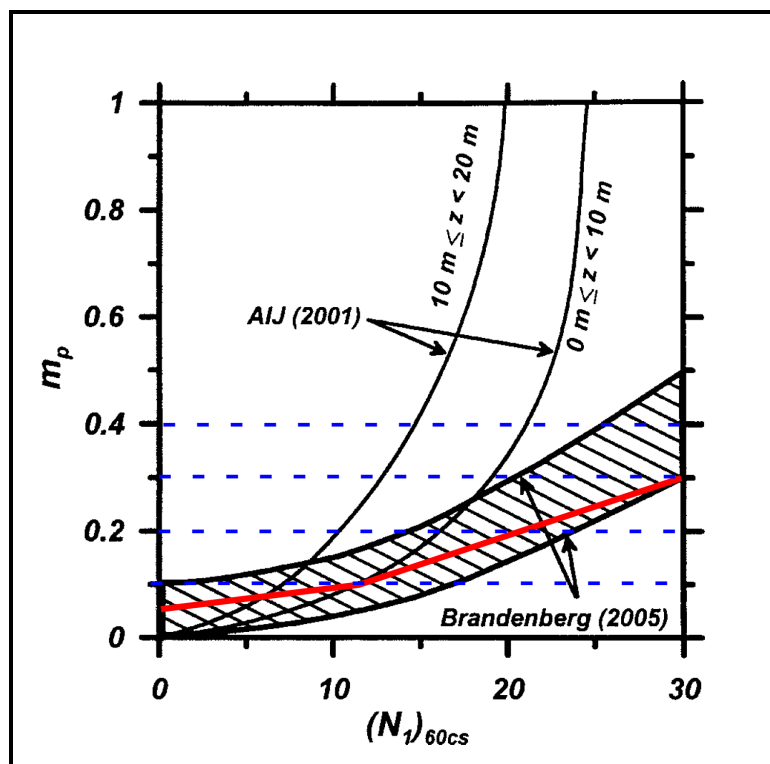


Figure 14-38, P-Multipliers ( $m_p$ ) for Sand-Like Soils Subject to Cyclic Liquefaction (Modified Brandenburg, et al. (2007b) with permission from ASCE)

Lateral loadings of pile groups that are in fully liquefied soils (excess pore pressure ratio =  $R_u = u/\sigma'_v > 1.0$ ) are not influenced by  $m_p$  when group effects are considered (even if closely spaced). During partial liquefaction ( $0.20 \leq R_u < 0.7$ ), prior to full liquefaction or after excess pore water pressures begin to dissipate, the group effects become increasingly apparent.

The preferred method to model lateral soil response is to use non-linear P-y curves. Because some structural software packages can only use linear springs to model lateral soil response, the secant modulus spring constant ( $K$ ) can be computed for the corresponding displacement of a non-linear soil response model. The use of linear springs makes it necessary to adjust the linear spring constant ( $K$ ) and it becomes an iterative process until displacements of the foundations match the displacement assumed in the development of the secant modulus spring constant.

#### 14.8.4 Soil Load Contribution on a Single Deep Foundation

The soil loading contribution from soil displacement on a single deep foundation (i.e., driven pile or drilled shaft) is very complex and generally depends on the soil shear strength, soil stiffness, spacing of piles, pile size (i.e., diameter or side dimension), arching effects, and construction method used to install the deep foundation. Although, there is no accepted method to evaluate the soil loading contribution, typical practice is that the contribution area of the soil loading or the effective pile width ( $B_{eff}$ ) can be estimated as some multiple ( $\lambda$ ) of pile size ( $B$ ) where the soil loading contribution would be defined as  $(\lambda B)$  for different soil shear strengths. It is accepted AASHTO LRFD practice that, if loading a single row of piles in the perpendicular direction and the pile spacing is less than  $5B$ , there should be a reduction in resistance of the soil when using Beam on Nonlinear Winkler Foundation (BNWF) methods (i.e., Com624, LPile). Conversely, it can be

estimated that the effective pile width ( $B_{eff} = \lambda B$ ) on a single pile will range somewhere between 1 pile diameter up to 5 pile diameters ( $B \leq \lambda B < 5B$ ). Until further research in this area becomes available, the effective pile width ( $B_{eff}$ ) to be used for loading contribution shall be determined using the following equation:

$$B_{eff} = \lambda * B \quad \text{Equation 14-8}$$

Where,

B	=	Pile size (i.e., diameter or side dimension), inches
$\lambda$	=	Effective pile width coefficient (Table 14-1)
$\phi$	=	Angle of internal friction of soil (backwall fill materials), degrees

The effective pile width coefficient is determined as follows:

**Table 14-1, Effective Pile Width Coefficient ( $\lambda$ )**  
(Adapted from Anderson, et al. (2008))

Pile Spacing	$\lambda$			
	Cohesive Soils		Cohesionless Soils	SSL of Sand-Like Soils
	$S_u < 1000$ psf & SSL of Clay-Like Soils	$S_u \geq 1000$ psf		
1B (side-by-side)	1	1	1	1
2B	1	2	$0.08\phi \leq 3$	1
3B	1	2	3	1
>3B	1	2	3	1

#### 14.8.5 Load Transfer Between Pile Group and Lateral Spreading Crust

Brandenberg, et al. (2007a) proposed the Structural Model and the Lateral Spreading Model to evaluate the load transfer between pile groups and laterally spreading crusts. In the Structural Model, the pile cap moves horizontally into a stationary soil mass. In the Lateral Spreading Model, the crust of non-liquefied soil moves laterally towards the stationary pile group. Brandenberg, et al. (2007a) suggests that the actual loading condition would likely include some combination of ground displacement and pile cap displacement. The 2 load transfer models suggested by Brandenberg, et al. (2007a) are to be used as an envelope of field loading behavior and do not capture the hysteretic dynamic behavior that actually occurs during shaking. A schematic to the pile group and block of stress influence in the non-liquefied crust is presented in Figure 14-39. A brief description of the Structural Model is presented in Section 14.8.5.1 and the Lateral Spreading Model discussed in Section 14.8.5.2. The GEOR is strongly encouraged to review and thoroughly understand the procedures presented in the Brandenberg, et al. (2007a) original publication.

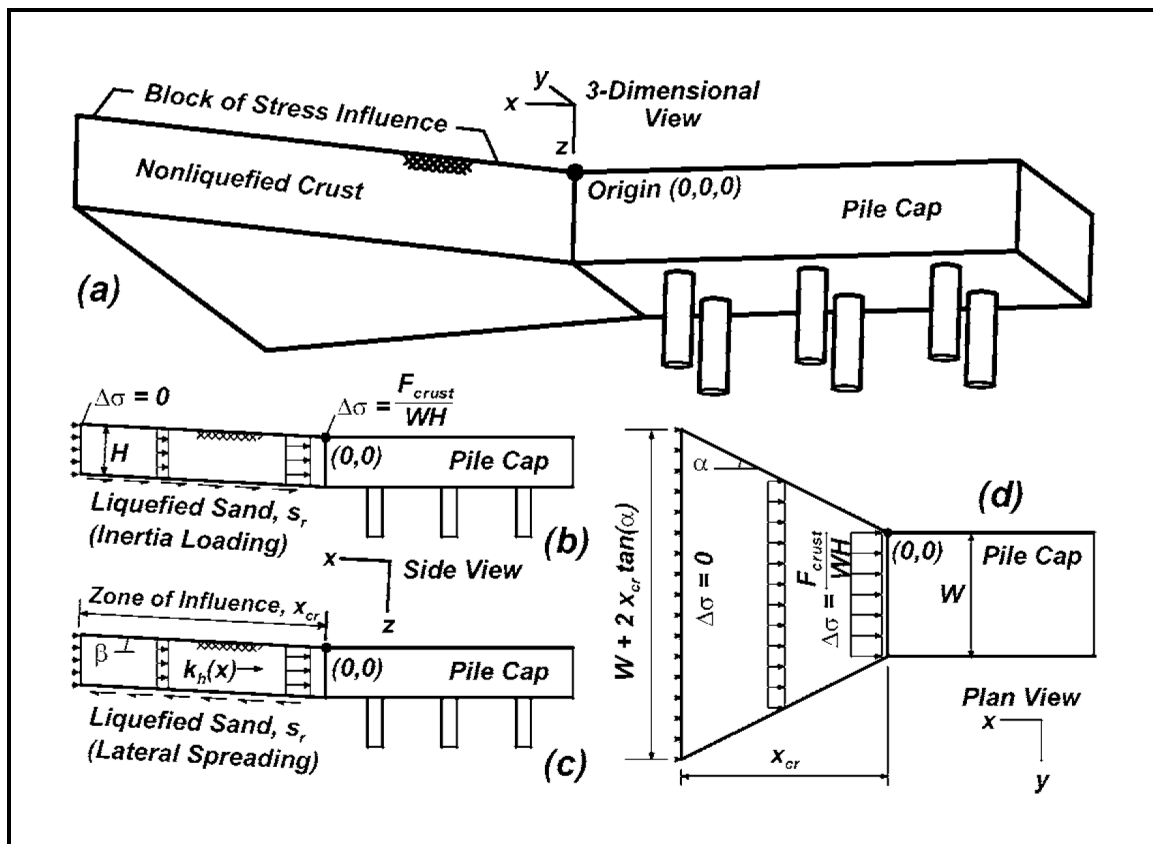


Figure 14-39, Load Transfer Between Pile Group and Lateral Spreading Crust (Brandenberg, et al. (2007a) with permission from ASCE)

#### 14.8.5.1 Structural Model

The pile cap moves horizontally into a stationary soil mass in the Structural Model. This model represents the superstructure and/or pile cap inertia loading cycle and transient ground displacements are small. The assumptions of the Structural model are as follows:

1. Inertia of non-liquefied crust is neglected since the ground is assumed stationary.
2. The residual strength of the liquefied sand is fully mobilized along the base of the non-liquefied crust and acts in the downslope direction against the force imposed by the pile group (Figure 14-39(b)).
3. Stresses attenuate within a 3D block of stress influence that geometrically extends at an angle  $\alpha$  from the backface of the pile cap in plan view (Figure 14-39(d)).

#### 14.8.5.2 Lateral Spreading Model

The crust of non-liquefied soil moves laterally towards the stationary pile group in the Lateral Spreading Model. This may occur when the lateral spreading soil fails in passive pressure mode and flows around a laterally stiff pile foundation that exhibits little cap displacement. The assumptions of the Lateral Spreading model are as follows:

1. Pile cap displacement is 0.0.

2. The residual strength of the liquefied sand is fully mobilized along the base of the non-liquefied crust and acts in the upslope direction to resist lateral spreading of the crust (Figure 14-39(c)).
3. Stresses attenuate within a block of stress influence that geometrically extends at an angle  $\alpha$  from the backface of the pile cap in plan view (Figure 14-39(d)).
4. Horizontal acceleration and downslope displacement at a given location in the nonliquefied crust layer must be compatible with the acceleration versus displacement relation obtained from sliding block solutions based on Newmark (1965) for a given ground motion.

#### **14.8.6 Lateral Soil Loads Due to Seismic Hazard Displacements**

Lateral loads on deep foundations resulting from seismic hazards can be evaluated by either displacement methods or force based methods. It may be necessary to use both methods to evaluate boundary conditions and reasonableness of the results.

Boulanger, et al. (2003) and Brandenberg, et al. (2007a and 2007b) have suggested modeling the effects of seismic hazard displacements using BNWF methods (i.e., Com624, LPile) that either use free-field soil displacement (Displacement Based Method: BNWF-SD) or limit pressures (Force Based Method: BNWF-LP) that are presented in Figures 14-40(a) and 14-40(b), respectively. The BNWF-SD method is a more general approach that consists of applying the Demand from seismic hazard free-field soil displacements (SD) on the free-end of the p-y soil springs. The BNWF-LP method consists of applying the limit pressures (LP) directly on the pile foundation and is therefore, a more restrictive approach, because it assumes that soil displacements are large enough to mobilize the ultimate loads from the spreading crust and liquefiable layer against the deep foundations. Application of the displacement boundary condition on the BNWF-SD method is typically more difficult than applying the force boundary condition on the BNWF-LP method. The BNWF-SD and the BNWF-LP methods are described in Sections 14.8.6.1 and 14.8.6.2, respectively. An alternate force based method that consists of using a limit equilibrium slope stability program is described in Section 14.8.6.3.

For either the displacement or force based method presented, the inertial forces should be included as static forces applied concurrently with the seismic hazard displacement demands.

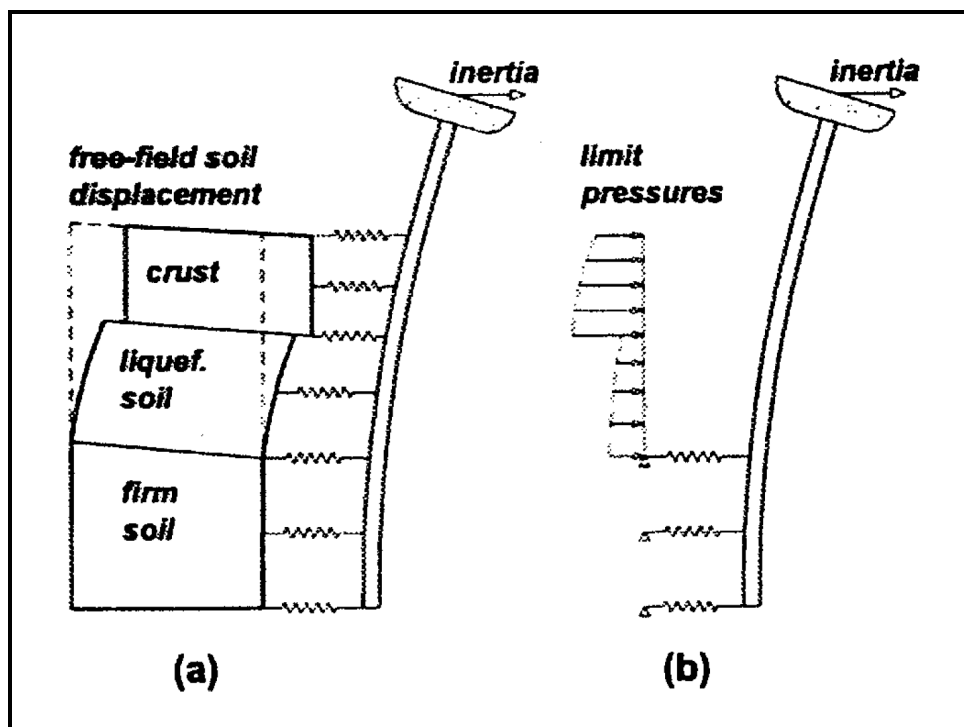


Figure 14-40, BNWF Methods for Evaluating Seismic Hazard Displacements (Brandenberg, et al. (2007b) with permission from ASCE)

#### 14.8.6.1 Displacement Based Methods (BNWF-SD)

The displacement based method for evaluating the effects of lateral loads on deep foundations is based on procedures developed by Boulanger, et al. (2003) and Brandenberg, et al. (2007a and 2007b). This method uses LPILE Plus or a similar computer program to perform the analysis. This performance based method is summarized below:

1. Estimate the free-field ground surface displacements of slope instability in accordance with Chapter 13.
2. Estimate the lateral displacements as a function of depth. The shear strain profile approach described in Zhang, et al. (2004) and illustrated by Idriss and Boulanger (2008) may be used. Another method would be to assume a constant displacement at the ground surface and crust; and then vary the displacements linearly with depth to the failure surface.
3. Model the free-field displacement and its displacement distribution with depth into LPILE Plus computer program to compute the mobilized soil reaction vs. depth.  $P_{Liq}$  is modeled in accordance with Section 14.8.3 and should be limited to:

$$P_{Liq} \leq 0.6 * \sigma'_{vo} * B \quad \text{Equation 14-9}$$

Where,

$\sigma'_{vo}$  = Effective overburden stress before seismic loading, pounds per square foot (psf)

B = Pile width, feet.

The lateral load analysis using LPILE Plus should consider the structural resistance of the foundation and the lateral resistance of the soil in front of the foundation as shown in Figure 14-41 (Imposed soil displacements).

4. Estimate the kinematic lateral loading effects on the deep foundation by using mobilized soil reaction vs. depth (Step 3) to evaluate deep foundation response using LPile Plus as shown in Figure 14-41 (Imposed pressure from spreading soil) to evaluate deflections, moments, shear, etc. Deep foundations should be evaluated for sufficient penetration below spreading soil to maintain lateral stability, location of plastic hinges, etc. If foundation resistance is greater than the applied pressures from the spreading soil, the soil will flow around the foundation. If the applied pressures from the spreading soil are greater than the deep foundation resistance, the foundation is likely to move along with the spreading soil. When pile caps are in contact with the spreading soil (or crust) passive pressures and side friction should be considered in the total loads applied to the foundation.

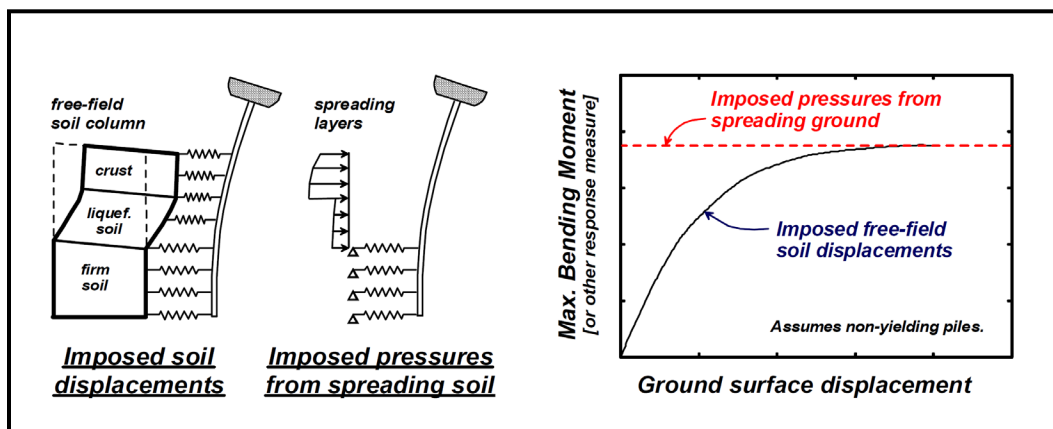


Figure 14-41, Methods for Imposing Kinematic Loads on Deep Foundations (Boulanger, et al. (2003))

#### 14.8.6.2 Force Based Methods (BNWF-LP)

This force based method for evaluating the effects of lateral loads on deep foundations is based on using limit pressures and BNWF modeling to evaluate lateral spreading induced loads on deep foundations. This method is based on back calculation from pile foundation failures caused by lateral spreading. Limit pressures assume that sufficient displacement occurs to fully mobilize lateral earth pressures. The LP for non-liquefied soils is computed based on full passive pressures acting on the foundation. For liquefied soils, the LP is computed as 30 percent of the total overburden pressure. The LP are then imposed on the deep foundation using LPILE Plus or a similar computer program to perform the analysis.

#### 14.8.6.3 Force Based Methods (Slope Stability-LP)

This force based method uses a limit equilibrium slope stability program to estimate the shear load the foundation must resist to achieve the target resistance factor,  $\phi$ , (Chapter 9). The shear loads are then distributed as a limit uniform pressure within the liquefiable zone on the deep foundation using LPILE Plus or similar computer program to perform the analysis.

## **14.8.7 Foundation Elements in Unstable Ground**

Seismic soil instability resulting from geotechnical seismic hazards can produce soil movements that may affect the performance of the bridge substructure (i.e., caps, single or group deep foundations, etc.). This Section describes the procedure to estimate the deformation demand and capacity of foundation elements and abutments due to SSL induced spreading ground. The spreading ground could be due to either lateral spreading or flow failure (see Chapter 2 for definitions). However, please note that lateral spread can transform into flow failure, making the determination of whether lateral spread occurs difficult based on visual observations. Be aware that this methodology is an approximation to solve a complex problem, but is the best available tool up to this date. This procedure is a structural mitigation strategy that requires coordination between the GEOR and SEOR. The analysis described is independent from the MSA/Pushover analysis. In order to use this approach, permission from OES/SDS is required.

Loads on the foundation elements due to the down slope movement of the soil crust often dominate over other loads. Excessive load or displacement demands caused by lateral spreading can be addressed using ground improvement (geotechnical mitigation) or structural enhancement of the bridge elements (structural mitigation). Due to the complexity of the foundation-soil-structure interaction, there must be a continuous communication between the GEOR and SEOR.

The approach applies an equivalent non-linear static analysis for foundation elements subjected to liquefaction-induced lateral spreading, based on the recommendations by Ashford, et al. (2010), and the procedures described by Caltrans (2017) and Arduino, et al. (2017). The procedure is applied to two different load cases (Figure 14-42): Case 1 is observed when the displacing soil crust is limited to the dimensions of the approach embankment, thus it is assumed that the abutment foundation is sufficiently stiff and strong to partially restrain the movement of the failure mass. In this case, the goal is to evaluate the load-displacement behavior of the foundation elements, determine the displacement of the sliding mass as a function of the foundation elements restraining force, and calculate the displacement where the foundation resistance is compatible with the sliding mass displacement. In Case 2, the displacing soil mass is large and its movement is unaffected by the presence of the foundation. If a broad transverse continuity is assumed for the site conditions, the lateral resistance of the interior bent in Figure 14-42 will be small compared with the sliding soil mass, thus the soil will displace the same amount regardless of the presence of the foundation. For Case 2, it is required to estimate the displacement of the crust and calculate the corresponding foundation loads and displacements due to the soil movement.

Generally, a global analysis of the bridge will predict more accurately the distribution of force and displacement demands throughout the bridge. However, this option does not always provide substantial refinement, thus a single bent model analysis might be sufficient. For the analysis, use software that are capable of lateral pile analysis and global slope stability analysis. The software for lateral pile analysis should have the ability to impose free field soil displacements against the pile by adjusting the location of the base of the soil springs.

### **14.8.7.1 Methodology of Analysis for Restrained Ground Displacements**

Case 1, assumes that the failure mass has a limited width and the lateral stiffness of the foundation elements will provide resistance to unstable soil movement. The procedure recommended is based on the pile pinning analysis concept. This case is representative of the

end bent foundation and the foundation elements stabilizing an embankment. Therefore, the width of the failing mass shall be limited to the width of the end bent.

The methodology accounts for pile pinning and 3-dimensional effects in a simplified manner, where a non-linear Winkler foundation model is combined with limit equilibrium slope stability analysis of the embankment. The displacement demand evaluation relies on an equivalent non-linear static analysis methodology. A pseudo-static slope stability analysis is used in conjunction with Newmark's sliding block case (initial fundamental period equal to zero) to estimate the horizontal displacement demand. A reduction in ground displacement, resulting from the restraining action of the foundation, is assessed by imposing a condition of displacement compatibility between the foundation and the soil crust. The methodology assumes that the failure surface is located in the middle of the liquefiable layer (Figure 14-42). The loading of the foundation by the unstable ground is assessed using a Winkler spring foundation model, where the base of the P-y springs is displaced an amount equal to the ground displacement.

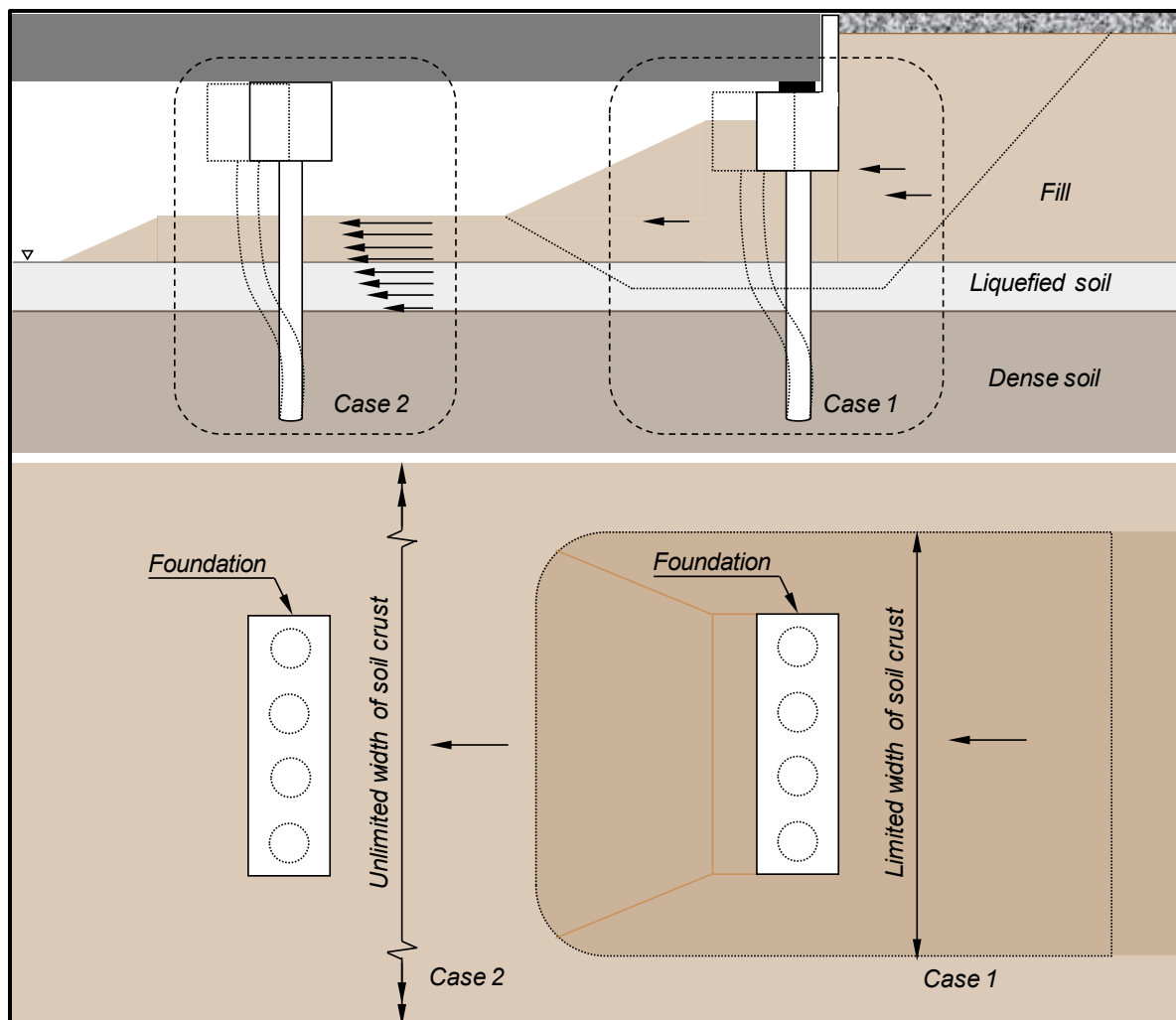


**Figure 14-42, Schematic of typical unstable soil problem**

The GEOR should assess the SSL potential and estimates the residual strength of the liquefied soil prior applying this methodology. To find the displacement demand on the foundation due to the crust displacement, and to evaluate the adequacy of the foundation elements, use the following procedure:

**Step 1:** SEOR defines the foundation model. For most bridges with uniform foundation elements, a single bent analysis is sufficient. In this case, a pile lateral analysis program is used and the properties of the bent foundation must be captured by an equivalent (single) “superpile.”

The interaction between the soil and foundation is modeled using non-linear soil springs (p-y curves). The equivalent beam used to model the foundation, piles and cap, may be defined assuming linear elastic or non-linear elastoplastic behavior. A non-linear elastic model is recommended (i.e. generate moment-curvature relationship). Note that the spatial arrangement of the piles is ignored and the equivalent beam is developed in a simplified manner. To create a non-linear “superpile” it is necessary to scale the moment-curvature by the number of piles in the group. If applicable, the rotational stiffness of the “superpile” must be determined. The rotational resistance of the pile group is dominated by the axial response of the piles about the corresponding axis of rotation. The pile head fixity, ranging from pinned to fixed, has little effect on the rotational stiffness of the pile group, then a pinned condition can be assumed (Norris, 1992). It is worth mentioning that the lateral stiffness will vary significantly depending on the assumed head fixity. The fixity could move from fully fixed to tending toward free as the lateral load increases. If the axial stiffness of a pile is similar in uplift and compression, the foundation will rotate about its center and the rotational stiffness can be simplified as shown in Equation 14-10 and Figure 14-43. If the axial stiffness of the pile is different in uplift and compression then the rotational stiffness of the pile group is best estimated using a pile group analysis program.

$$K_{\theta M} = 144K_{ax} \sum n_i X_i^2 \quad \text{Equation 14-10}$$

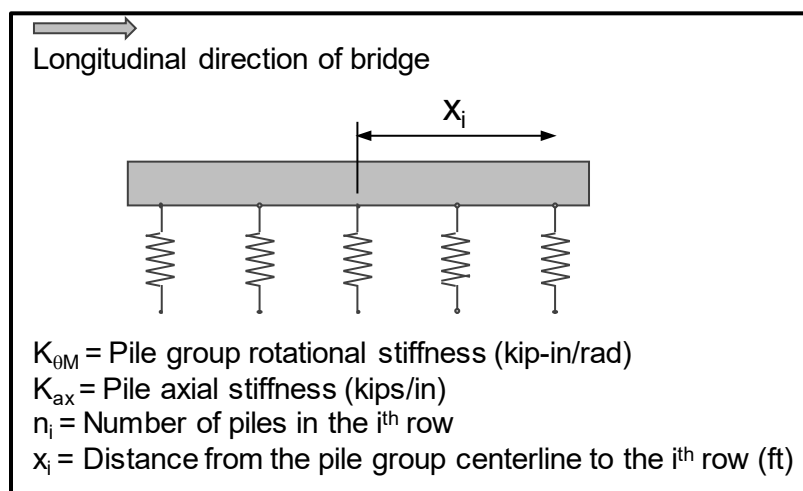


**Figure 14-43, Rotational Stiffness Model (Caltrans (2017 B))**

In addition, the corresponding “p” in the p-y curves for a single group pile must be scaled by a factor equal to the number of piles multiplied by a group efficiency factor. This efficiency factor is the average of the group reduction factors for each row in the pile group. For this methodology, the reduction factor for each row in the pile group is computed according with Chapter 16. For single row pile bents, which are the vast majority of the bridges in South Carolina, the group reduction factor is 1.0.

The p-y curves for soil-pile interaction are based on the work of Matlock (1970) for soft clay, Reese and Welch (1975) for stiff clay, and Reese, et al. (1974) for sand. Liquefied soil is modeled with a factored p-y curve using  $m_p$ -multipliers according with Chapter 14.8. The occurrence of liquefaction will affect the potential lateral resistance of nonliquefiable layers directly above and below the liquefied strata. Contrary, the overlying or underlying strong layers do not appreciably strengthen the p-y curve behavior in the liquefied sand. In order to avoid unrealistically large stiffness contrast between the liquefied layer and base layer, the “smeared” profile in Figure 14-44 can be used in the design of piles in approach embankments. The use of smeared profiles for large-diameter pile shafts requires further study, particularly because the distance  $S_b B$  can equal or exceed the thickness of a nonliquefied crust when B is large and the crust is relatively thin.

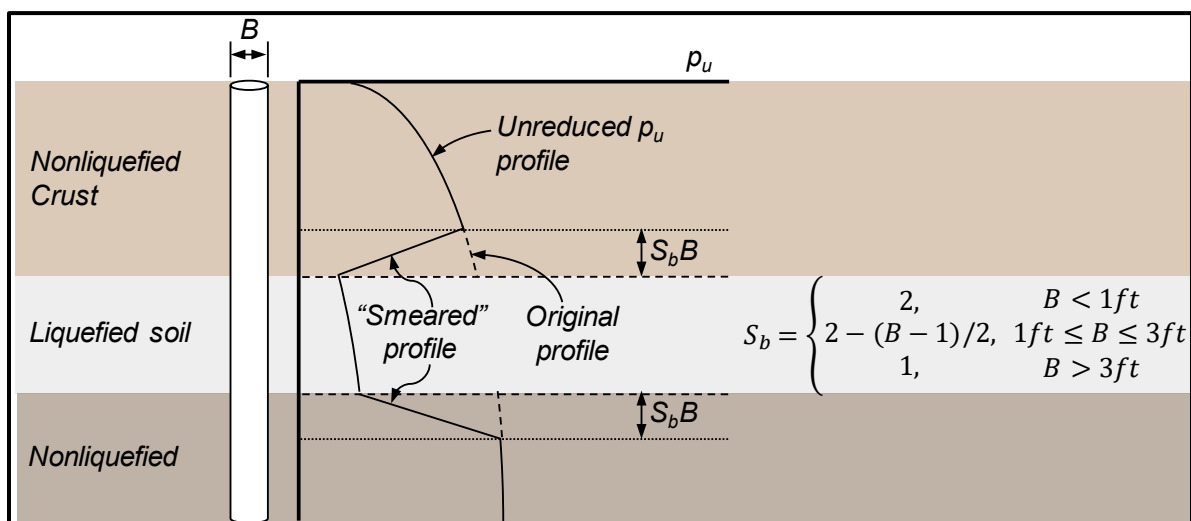


**Figure 14-44, Modification to the profile of ultimate subgrade reaction,  $p_u$ , (Ashford, 2010)**

The p-y curve for the cap/abutment-soil interaction is defined by a trilinear curve (Figure 14-45) based on the ultimate crust load on the foundation elements,  $F_{ULT}$ , and the relative displacement required to achieve  $F_{ULT}$ ,  $\Delta_{MAX}$ . Figure 14-46 shows the dimensions necessary to create the cap/abutment-soil interaction model. The trilinear curve is used for this methodology to simplify the input in the single pile analysis software.

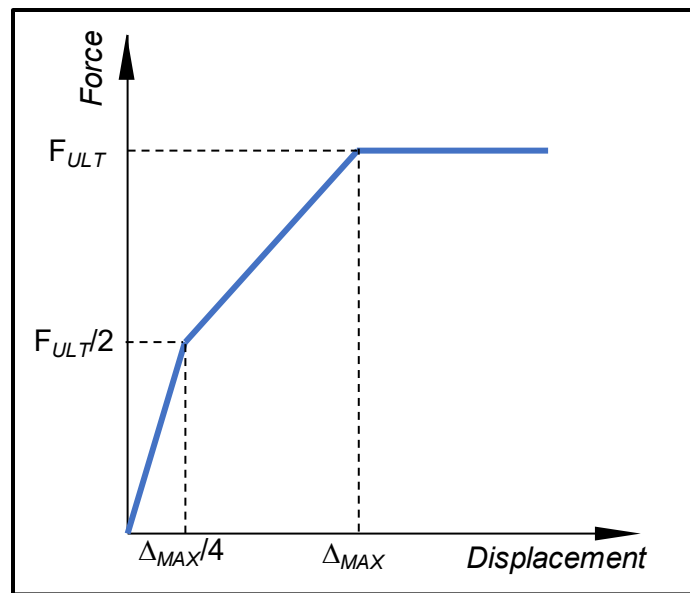


Figure 14-45, Pile Cap Idealized Force-Displacement Behavior

$$F_{ULT} = F_{PASSIVE} + F_{SIDES} \quad \text{Equation 14-11}$$

Where,

$F_{PASSIVE}$  = Passive force resulting from the compression of soil on the up slope face of the foundation

$F_{SIDES}$  = Friction or adhesion of the soil moving along the side of the foundation (do not include wing walls)

Forces, such as the friction force below the pile cap caused by the soil flowing between the piles, are neglected because they are small in comparison with the passive force and difficult to calculate.

Two failure cases could be considered to determine  $F_{ULT}$ . The cases are log-spiral based passive pressure (Case A) and Rankine passive pressure (Case B) (Figure 14-47). The case that results in smaller foundation loads is selected. Typically, Rankine's formulation results in smaller loads and it is used for cases where the pile cap or composite cap-pile-soil block extends to the top of the liquefiable layer. Presented below is a procedure for the estimation of  $F_{ULT}$  for Case A (log-spiral) and Case B (Rankine).

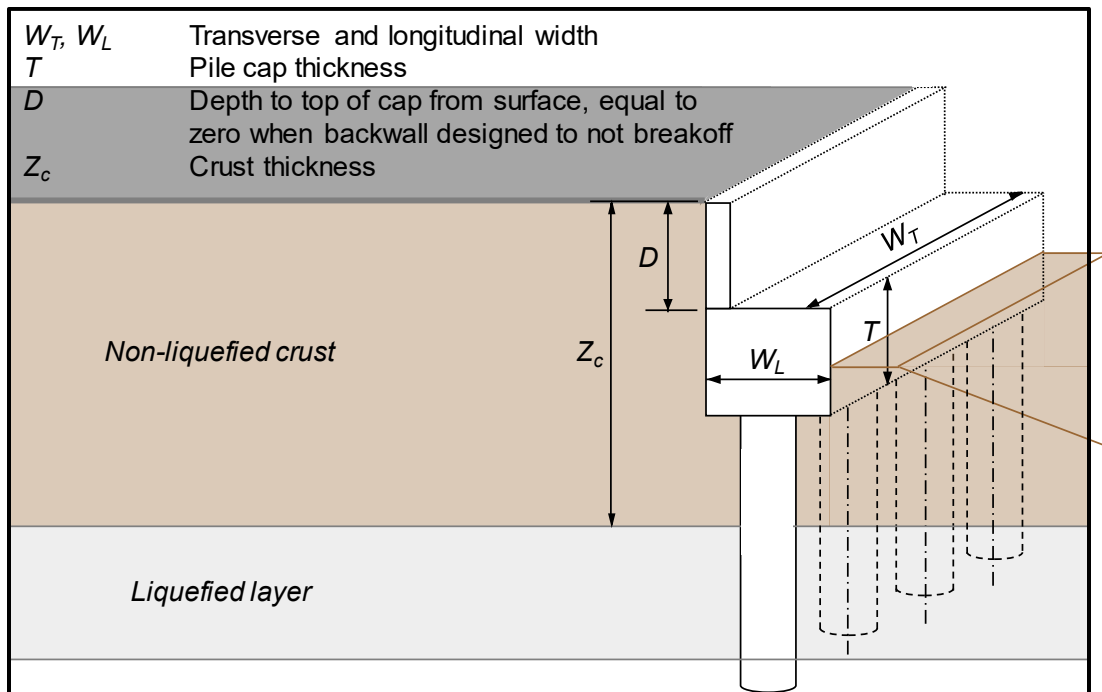


Figure 14-46, Pile Foundation Dimension Parameters

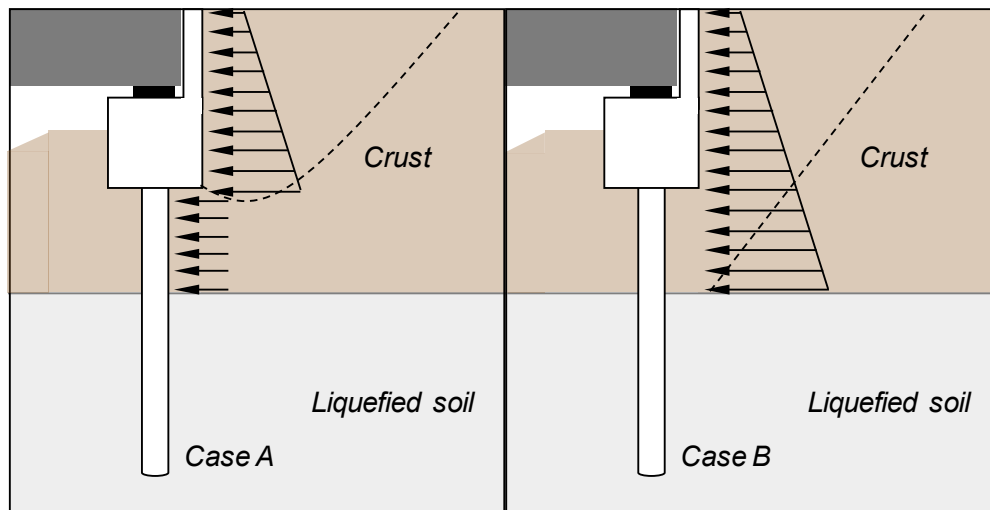


Figure 14-47, Design cases to determine soil crust ultimate passive load

Case A:

This case considers the combined loading of a log-spiral passive wedge acting on the pile cap and the ultimate resistance provided by the portion of individual pile length above the liquefied zone.

$$F_{ULT-A} \approx F_{PASSIVE-A} + F_{PILES-A} + F_{SIDES-A} \quad \text{Equation 14-12}$$

$$F_{PILES-A} \approx n GRF P_{ULT} L_c \quad \text{Equation 14-13}$$

Where,

- n = Number of piles
- GRF = Group reduction factor
- $L_c$  = Length of the pile extending through the crust
- $P_{ULT}$  = Ultimate lateral resisting force per unit length of pile (it is called resisting force because it is resisting the movement of the crust, not related with capacity of the pile)

For Sand-Like,

$$P_{ULT} = (C_1 \bar{H} + C_2 B) \gamma \bar{H} \quad \text{Equation 14-14}$$

$$C_1 = 3.42 - 0.295\phi + 0.00819\phi^2 \quad \text{Equation 14-15}$$

$$C_2 = 0.99 - 0.0294\phi + 0.00289\phi^2 \quad \text{Equation 14-16}$$

For Clay-Like,

$$P_{ULT} = 9cB \quad \text{Equation 14-17}$$

Where,

- $\bar{H}$  = Average pile depth in the crust
- B = Pile diameter
- $\gamma$  = Effective unit weight of the crust
- c = Undrained shear strength
- $\phi$  = Friction angle of crust,  $20^\circ < \phi < 40^\circ$

Case B:

This case considers the loading of a Rankine passive wedge acting on a composite soil block above the liquefaction zone and assumes that the pile cap, soil crust beneath the pile cap, and the piles within the crust act as a composite block and it is loaded by the Rankine passive pressure.

$$F_{ULT-B} \approx F_{PASSIVE-B} + F_{SIDES-B} \quad \text{Equation 14-18}$$

$F_{PASSIVE}$ :

For soils with a frictional component (i.e., Sand-Like or  $c - \phi$  soils), the passive force is given by the following equation, the passive pressure coefficient depends on the Case (A or B) used:

$$F_{PASSIVE} = (\bar{\sigma}_v K_p + 2c' \sqrt{K_p}) T W_T k_w \quad \text{Equation 14-19}$$

Where,

- $\bar{\sigma}_v$  = Mean vertical effective stress along the pile cap face
- $W_T$  = Transverse pile cap width
- T = Cap thickness
- $c'$  = Cohesion intercept

$k_w$  = Adjustment factor for a wedge shaped failure surface.  
Calculated with equation developed by Ovesen (1964)

**Equation 14-20**

$$k_w = 1 + (K_p + K_a)^{2/3} \left\{ 1.1 \left( 1 - \frac{T}{D+T} \right)^4 + \frac{1.6}{1 + \frac{5W_T}{T}} + \frac{0.4(K_p + K_a) \left( 1 - \frac{T}{D+T} \right)^3}{1 + \frac{0.05W_T}{T}} \right\}$$

Where,

- $D$  = Depth from ground surface to top of pile cap, equal to zero if back wall designed to not break off.
- $K_p$  = Passive earth pressure coefficient of the crust materials and depends on if Case A or B is used
- $K_a$  = Active earth pressure coefficient of the crust materials as determined in Chapter 18

Case A is based on log-spiral failure surface. If  $\phi > 0$  (i.e., Sand-Like or  $c - \phi$  soils), with  $\phi$  ranging from  $20^\circ$  to  $45^\circ$  and  $\delta \leq \phi$ , the approximation given by Equation 14-21 for  $K_{p, \log\text{-spiral}}$  may be used. The contribution of cohesion is ignored for  $c - \phi$  soils (i.e., if  $\phi = 0$ ,  $K_{p, \log\text{-spiral}}$  is equal to 1).

**Equation 14-21**

$$K_{p, \log\text{-spiral}} = \text{Tan}^2 \left( 45 + \frac{\phi}{2} \right) \left[ 1 + (0.8152 - 0.0545\phi + 0.001771\phi^2) \frac{\delta}{\phi} - 0.15 \left( \frac{\delta}{\phi} \right)^2 \right]$$

Where,

- $\phi$  = Peak friction angle of the crust
- $\delta$  = Pile cap-soil crust interface friction angle (use  $\delta = \phi/3$  when soils undergo SSL (i.e., liquefaction))

For Case B where the pile cap or composite cap-pile-soil block extends to the top of the liquefiable layer,  $K_p$  should be calculated using Rankine's formulation instead of a log-spiral solution since the presence of the liquefiable layer impedes the development of the deeper log-spiral failure surface.

$$K_{p, Rankine} = \text{Tan}^2 \left( 45 + \frac{\phi}{2} \right) \quad \text{Equation 14-22}$$

For cases where the crust is Clay-Like (i.e.,  $\phi = 0$ ) the passive force should be estimated using the equation by Mokwa et al. 2000:

$$F_{PASSIVE} = \left( 4 + \frac{\alpha(D+T)}{c} + \frac{D+T}{4W_T} + 2\gamma \right) cW_T \frac{(D+T)}{2} \quad \text{Equation 14-23}$$

Where,

$\alpha$  = Adhesion factor and can be assumed to be 0.5

$F_{SIDES}$ :

The force on the sides for both cases, is calculated using one of the following equations:

Sand-Like or c -  $\phi$  soils

$$F_{SIDES} = 2(\overline{\sigma'_v} \tan(\delta) + \alpha c') W_L T \quad \text{Equation 14-24}$$

Clay-Like soils

$$F_{SIDES} = 2\alpha c W_L T \quad \text{Equation 14-25}$$

Where,

$W_L$  = Longitudinal pile cap width

For case B, the cap thickness, T, is replaced by the thickness of the composite block (Crust thickness,  $Z_c$  minus depth to top of cap, D)

**Determination of  $\Delta_{MAX}$ :**

For the case of a crust overlying a liquefied layer to mobilize the passive force fully, a relatively large displacement, more than the typical 5% of the wall height, is required. The effect of the crust thickness with respect to the pile cap thickness and width is accounted for with the factors  $f_{depth}$  and  $f_{width}$  in the equation to estimate  $\Delta_{MAX}$ .

$$\Delta_{MAX} = T(0.05 + 0.45f_{depth}f_{width}) \quad \text{Equation 14-26}$$

$$f_{depth} = e^{-3\left(\frac{Z_c - D}{T} - 1\right)} \quad \text{Equation 14-27}$$

$$f_{width} = \frac{1}{\left(\frac{10}{\frac{W_T}{T} + 4}\right)^4 + 1} \quad \text{Equation 14-28}$$

**Step 2:** SEOR determines if the bridge deck can be expected to provide longitudinal resistance to abutment movement. The restraining force from the bridge superstructure depends on the structural configuration, the characteristics of the embankment soils, as well as the capacity of the opposite abutment. The restraining force that develops at the abutment must be transferred to the intermediate bents and the opposite abutment. If superstructure restraint is considered in the lateral spreading analysis, it is recommended that a global structural model is used. However, if it is possible to assume that the interior bents and opposite abutment are stiff enough to transfer load through the bridge deck, the restraining force is limited by the ultimate passive resistance of the soil behind the abutment back wall. In order for the bridge deck to be used, the backwall cannot be designed to break off. The SEOR calculates the passive force expected from full mobilization of this resistance.

**Step 3:** SEOR performs a displacement analysis of the foundation model. SEOR imposes a series of increasing soil displacement profiles on the foundation (Figure 14-48) and records the shear resistance offered by the foundation. For each displacement increment, determine the shear force on the pile at the center of the liquefied layer (R). As the failure mass begins to slide, the foundation mass is not constant. Thus, to ensure displacement compatibility between sliding mass and the foundation resisting its movement, the running average foundation shear force for each displacement increment must be used. The imposed displacement is applied until the displacement measured at the bottom of the failure surface of the liquefied layer reaches 24 inches. The imposed displacement and the running average of the shear force are recorded and plotted.

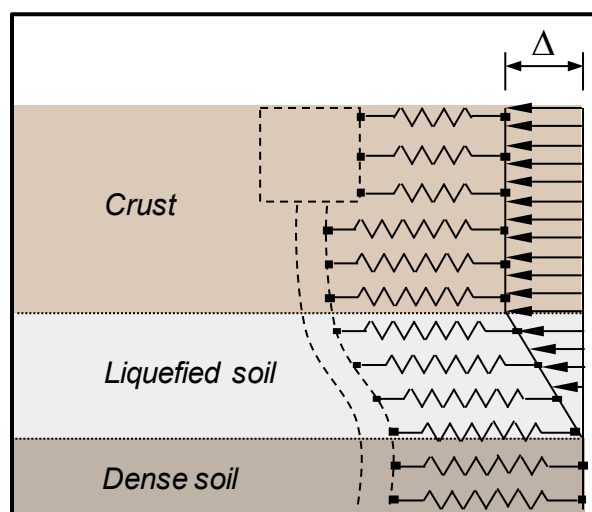


**Figure 14-48, Applied displacement profile for Winkles spring foundation model**

**Step 4:** GEOR performs a slope stability and deformation analysis of the bridge embankment. The slope stability model is used to determine the foundation resisting forces at the center of the liquefied layer for a series of horizontal accelerations applied to the model as a constant initial force. Constraints must be imposed on the critical failure surface used to determine the yield coefficient,  $k_c$ , to avoid an unrealistic proportion of the critical failure surface. Record the resisting force when

the slope achieves a resistance factor of 1.0. In these analyses, the restraining forces are applied on the lower edge of the failure surface, and the failure surface is constrained to the center of the liquefied layer. Newmark's rigid sliding block case is used to compute the slope displacement corresponding to the applied horizontal acceleration. The corresponding displacement for each yield coefficient can be calculated using Bray and Travararou (2007).

Equation 14-29

$$d = \text{Exp} \left[ -0.22 - 2.83 \ln(k_c) - 0.333 (\ln(k_c))^2 + 0.566 \ln(k_c) \ln(PGA) + 3.04 \ln(PGA) - 0.244 (\ln(PGA))^2 + 0.278 (M_w - 7) \right]$$

Where,

d	=	Displacement, cm
$k_c$	=	Yield coefficient
PGA	=	Peak ground acceleration, g
$M_w$	=	Magnitude of seismic event

Since this force is recorded by unit width, it needs to be multiplied by the width of the sliding mass. Adjustments need to be made for non-rectangular embankment shapes (Figure 14-49).

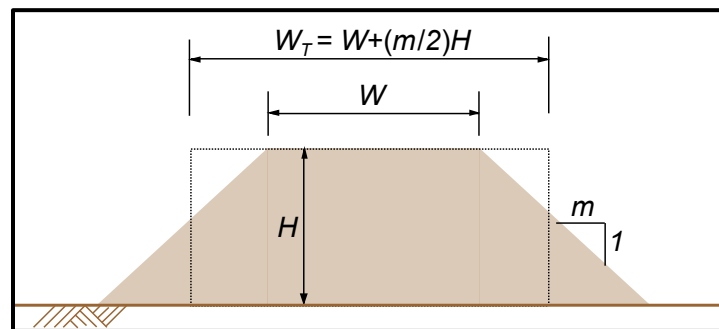


Figure 14-49, Determination of the tributary width of an embankment

**Step 5:** SEOR / GEOR, combine the results from Step 3 and Step 4. The former reflects the foundation resistive force corresponding to a given crustal displacement. In Step 4, the results correspond to the expected crustal displacement given a constant resistive force. The displacement corresponding to the intersection of these two curves represents the expected displacement demand on the foundation (Figure 14-50).

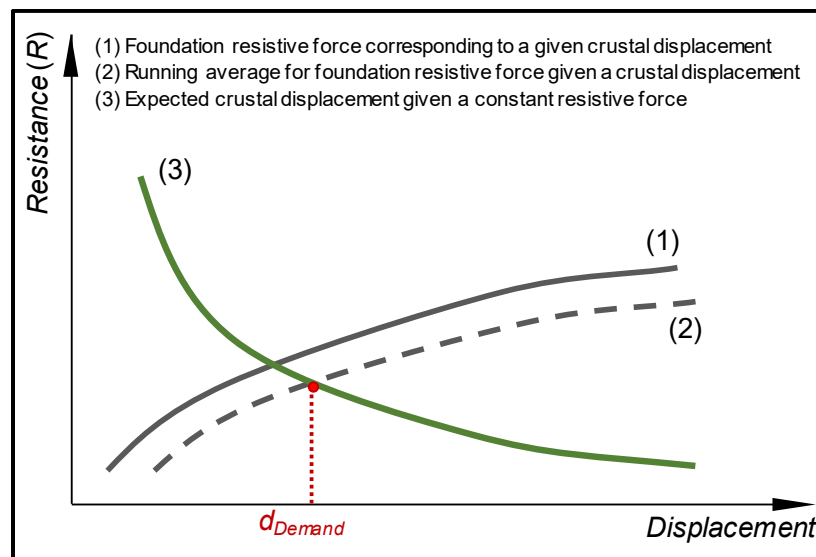


Figure 14-50, Determination of compatible displacements

**Step 6:** SEOR evaluates the performance of the foundation, comparing the displacement demand, calculated in the previous step, with the allowable displacement of the foundation. Pile moment and shear at this displacement demand are also checked. The methodology assumes that the unstable soil will occur during strong shaking and the inertial loading of the foundation must be considered in tandem with kinematic loading.

100% kinematic  $\pm$  50% inertial  $\rightarrow$  (peak pile cap displacement)

100% kinematic  $\pm$  50% inertial  $\rightarrow$  (peak pile moment or shear)

In some instances peak pile demands occur when the direction of the inertial load is opposite to the kinematic load.

#### 14.8.7.2 Methodology of Analysis for Unrestrained Ground Displacements

The following methodology is applicable to Case 2, where the failure mass is large and it is assumed that soil movement will be unaffected by the presence of the foundation. Since the foundation is affected by the sliding mass at a local level, it is recommended to check adequacy of the foundation elements by estimating the crust displacement and evaluating the corresponding foundation loads and displacements. Once the SSL potential is assessed and the residual strength of the liquefied soil is estimated, use the following procedure to perform the foundation assessment:

**Step 1:** GEOR evaluates the slope factor of safety (FS). If  $FS \leq 1.05$ , a flow type failure with corresponding large displacement should be assumed. Typically, an assumption of approximately 5 feet is sufficient. If  $FS > 1.05$ , determine the crustal displacement using Equation 14-29.

**Step 2:** SEOR develops a foundation model using an equivalent superpile, the pile cap p-y curves using the idealized Force-Displacement Behavior (Figure 14-45), and liquefied p-y curves. If applicable, calculate the pile rotational stiffness.

- Step 3:** SEOR imposes on the foundation model a soil displacement profile that represents the lateral displacement of the soil mass in conjunction with inertial loads from the superstructure and Step 1, above. Apply inertial loads in combination with displacement profile.
- Step 4:** SEOR Evaluates foundation adequacy by comparing calculated demands with the allowable demands.

## 14.9 BRIDGE ABUTMENT BACK WALL PASSIVE RESISTANCE

Earthquake-induced lateral loadings addressed in this Section are limited to the loads that are a result of soil-structure interaction between soils and abutment walls. The abutment walls are used to provide seismic passive resistance (Capacity) to earthquake-induced lateral loadings (Demand). Abutment walls discussed in this Section include the bridge back or end, wing, and shear walls, see Figure 14-51. The term “abutment wall” is used generically for this Section; however, the designer (both GEOR and SEOR) is required to know the specific location of the wall that is being analyzed. The bridge back wall and/or end wall are defined in the BDM. Shear walls are placed perpendicular to the abutment to resist transverse seismic loads. Wing walls are placed to retain sloping fills and can be used as shear walls. However, only the passive resistance developed by a fully embedded wing wall shall be used (i.e., no passive resistance will be allowed to be developed on the exterior face of the wing wall). In addition, only the passive resistance developed by the wing and/or shear walls in the transverse direction shall be used. When multiple shear walls are used, the walls shall be placed with sufficient spacing to avoid overlap of the passive resistance wedges. The development of the seismic passive resistance is discussed in detail in the following Sections. Limitations on the development of full seismic passive pressures due to wall skews are also discussed.

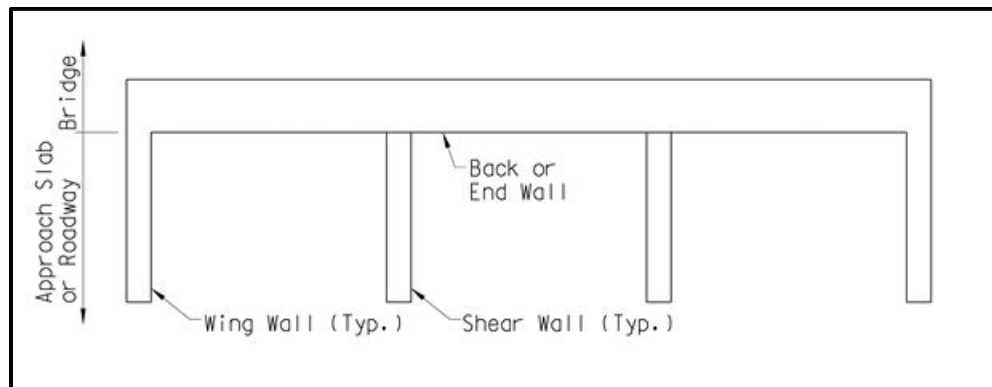
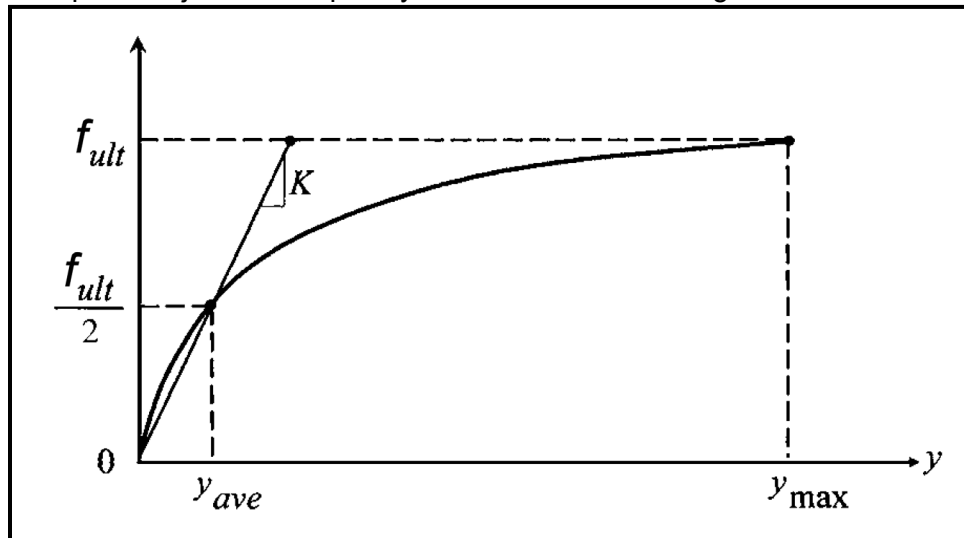


Figure 14-51, End-Bent Schematic Plan View

### 14.9.1 Development of Passive Resistance

Seismic lateral loadings can mobilize seismic passive soil pressures (resistances) such as those that occur at bridge abutments (in both the longitudinal and transverse directions) during a seismic event. Because the design methodologies presented in this Manual are performance-based, a nonlinear soil-abutment-bridge structure interaction model is used to compute the mobilized passive resistance as a function of displacement. The method to develop this model is based on the work by Shamsabadi (2006) and Shamsabadi, et al. (2007 and 2010). The basic framework of the

model is a logarithmic spiral passive failure wedge coupled with a modified hyperbolic abutment-backfill stress-strain behavior (LSH). A hyperbolic force-displacement (HFD) curve is calculated by using the LSH relationship. The HFD curve is defined as shown in Figure 14-52. The HFD model is based on the assumption that the bridge superstructure is in direct contact with the back wall (i.e., the expansion joint is completely closed for free-standing end bents).



**Figure 14-52, Hyperbolic Force-Displacement Formulation (Modified Shamsabadi, et al. (2007) with permission from ASCE)**

The total maximum abutment passive resistance for the entire wall,  $F_{ult}$ , is developed at the maximum deflection ( $y_{max}$ ) considering the effective width of the wall.  $F_{ult}$  is determined as indicated below:

$$F_{ult} = f_{ult} * b_{wall} \quad \text{Equation 14-30}$$

The maximum abutment passive resistance per unit width of wall is computed as follows:

$$f_{ult} = p_{wall} * h_{wall} \quad \text{Equation 14-31}$$

Where,

- $f_{ult}$  = Maximum abutment passive resistance developed at a maximum displacement ( $y_{max}$ ), kips per foot of wall width
- $y_{max}$  = Maximum displacement where the maximum abutment passive resistance per unit width ( $f_{ult}$ ) is developed, inches
- $b_{wall}$  = Width of abutment wall or the effective width of the abutment depending on the skew angle, feet
- $p_{wall}$  = Maximum average uniform wall pressure developed at a maximum displacement ( $y_{max}$ ), kips per square foot
- $h_{wall}$  = Height of abutment wall, feet

The maximum abutment passive resistance ( $f_{ult}$ ) is estimated to occur when the ratio of the wall movement ( $y_{max}$ ) to wall height ( $h_{wall}$ ) is equal to the values in Table 14-2. This ratio ( $y_{max}/h_{wall}$ ) is also dependent on the type of backfill (Sand-Like or Clay-Like soils). These values are recommended by Shamsabadi, et al. (2007) and Shamsabadi, et al. (2010). These values are in

general agreement with those  $y_{max}/h_{wall}$  values observed by Clough and Duncan (1991) for passive earth pressures.

**Table 14-2, Relative Movements Required to Reach Passive Earth Pressures  
(Modified Clough and Duncan (1991))**

Type of Backfill		$y_{max}^{(1)}$
<b>Sand-Like (Cohesionless)</b>	Dense Sand	$0.05 * h_{wall}^{(2)}$
	Medium Dense Sand	
	Loose Sand	
	Compacted Silt	
<b>Clay-Like (Cohesive - c-φ Soils)</b>	Compacted Lean Clay	$0.10 * H_{WALL}^{(2)}$
	Compacted Fat Clay	

<sup>(1)</sup> $y_{max}$  = maximum movement at top of wall (feet)

<sup>(2)</sup> $h_{wall}$  = height of wall (feet)

Shamsabadi, et al. (2010) indicates a maximum uniform wall passive resistance ( $p_{wall}$ ) of 1.0 ksf for a 5-1/2-foot high wall as a result of full-scale tests that were primarily conducted in California using select backfill properties that are not representative of the backfill materials that are typically used on SCDOT projects. Therefore, the maximum uniform wall passive resistance ( $p_{wall}$ ) shall be computed as indicated in Equation 14-32. The method presented to compute the maximum uniform wall passive resistance ( $p_{wall}$ ) allows for the variation in abutment wall height, backfill type and soil properties, and the effect of the seismic inertial forces on the passive wedge.

$$p_{wall} = 2 * c * \sqrt{K_{pe}} + 0.5 * \gamma_{backfill} * h_{wall} * K_{PE} \quad \text{Equation 14-32}$$

Where,

- c = Soil cohesion (total stress condition), pounds per square foot
- $K_{pe}$  = Seismic passive earth pressure coefficient determined in accordance with Section 14.5.
- $\gamma_{backfill}$  = Backfill unit weight, pounds per cubic foot
- $h_{wall}$  = Height of abutment wall, feet

Seismic passive resistance shall be computed using total stress soil parameters since the rate of loading in a seismic event is not sufficient to allow dissipation of pore pressures. The actual shear strength parameters used to design the embankments shall be used unless the designer can provide a technical explanation for using different shear strength parameters.

The height of the abutment wall ( $h_{wall}$ ) depends on the type of bridge abutment (see BDM for abutment types) used and how the abutment is expected to perform. For example in an integral abutment the back wall and pile cap are typically rigidly connected so that abutment and pile cap act as a single unit. Therefore,  $h_{wall}$  is the sum of back wall plus the pile cap. However, in a free-standing abutment (seat-type), the back wall may be designed to “break off”. Therefore,  $h_{wall}$  is the height of the back wall of the abutment that “breaks off”. The GEOR is required to fully understand the anticipated abutment type and how the abutment is expected to perform. In addition,  $h_{wall}$  affects the length,  $\overline{AC}$ , (see Figure 14-21) of the passive wedge. The passive wedge distance  $\overline{AC}$  is determined using the following equation, which is based on Shamsabadi, et al. (2010):

$$\overline{AC} = 3.25 * h_{wall} \quad \text{Equation 14-33}$$

The average soil stiffness,  $K_{avg}$ , of the HFD curve shall be assumed to be  $K_{avg}=50\text{k/in/ft}$  and  $K_{avg}=25\text{k/in/ft}$  as default values for Sand-Like and Clay-Like and/or  $c-\phi$  soils, respectively, unless site-specific soil information is available. The stiffness of the aggregate drain shall not be included in the average soil stiffness. The average soil stiffness,  $K_{avg}$  (slope  $K$  in Figure 14-52), is defined as indicated below:

$$K_{avg} = \frac{0.5 * f_{ult}}{y_{avg}} \quad \text{Equation 14-34}$$

Where,

- $f_{ult}$  = Maximum abutment passive resistance developed at a maximum displacement ( $y_{max}$ ), kips per foot of wall width
- $y_{avg}$  = Average displacement where the abutment passive resistance is equal to half of the abutment passive resistance ( $0.5f_{ult}$ ) [ $y_{ave}$  in Figure 14-52], inches

The development of the HFD curve is based on the following three boundary conditions:

- Condition I:  $f=0$  at  $y_i=0$
- Condition II:  $f=0.5f_{ult}$  at  $y_i=y_{ave}=y_{avg}$
- Condition III:  $f=f_{ult}$  at  $y_i=y_{max}$

The force-relationship is a function of displacement ( $f\{y_i\}$ ) in the general hyperbolic form as defined by the following equation:

$$f\{y_i\} = \frac{C * y_i}{1 + D * y_i} \quad \text{Equation 14-35}$$

Where,

- $y_i$  = Displacement, inches
- $C$  and  $D$  = Constants as defined below:

$$C = \left( 2 * K_{avg} - \frac{f_{ult}}{y_{max}} \right) \quad \text{Equation 14-36}$$

$$D = 2 * \left( \frac{K_{avg}}{f_{ult}} - \frac{1}{y_{max}} \right) \quad \text{Equation 14-37}$$

Where,

- $f_{ult}$  = Maximum abutment passive resistance developed at a maximum displacement ( $y_{max}$ ) (see Equation 14-31), kips per foot of wall width
- $y_{max}$  = Maximum displacement where the maximum abutment passive resistance per unit width ( $f_{ult}$ ) is developed (see Table 14-2), inches
- $K_{avg}$  = Average soil stiffness, either 50 k/in/ft for Sand-Like soils or 25 k/in/ft for Clay-Like and/or  $c-\phi$  soils

The GEOR shall provide the SEOR the appropriate HFD curves ( $f$  vs.  $y$ ) and wall secant modulus stiffness-displacement curves ( $K$  vs.  $y$ ) similar to those shown in Figure 14-53 for Sand-Like Soils,

Figure 14-54 for Clay-Like Soils, and Figure 14-55 for  $c$ - $\phi$  soils. The soil parameters indicated in Tables 14-3, 14-4, and 14-5 were used to develop the examples depicted in Figures 14-53, 14-54, and 14-55, respectively. However for bridges that have a SDC of "A", the determination of the seismic passive pressure is not required.

**Table 14-3, Sand-Like Soil Parameters Used to Create Figure 14-53**

Wall Type:	Free-standing abutment back wall				
$h_{wall} =$	5.5 ft	$b_{wall} =$	50 ft	$\alpha =$	$0^\circ$
Earthquake:	SEE	$S_{D1} =$	0.20	$k_{max} =$	0.30
$\beta =$	0.67	$\alpha_w =$	1.0	$k_h$	0.30
Soil Type:	Sand-Like	$\phi =$	$30^\circ$	$c =$	0 psf
$\gamma =$	120 pcf	$c/\gamma^*H$	0	$K_{PE} =$	3.9
$\overline{AE}$	17.9 ft	$p_{wall} =$	1.29 ksf	$f_{ult} =$	7.08 k/ft
$y_{max}/h_{wall}$	0.05	$y_{max} =$	3.3 in.	$K_{avg} =$	50 k/in/ft
$y_{avg} =$	0.07 in.	$C =$	97.86	$D =$	13.52

**Table 14-4, Clay-Like Soil Parameters Used to Create Figure 14-54**

Wall Type:	Free-standing abutment back wall				
$h_{wall} =$	5.5 ft	$b_{wall} =$	50 ft	$\alpha =$	$0^\circ$
Earthquake:	SEE	$S_{D1} =$	0.20	$k_{Max} =$	0.30
$\beta =$	0.67	$\alpha_w =$	1.0	$k_h$	0.30
Soil Type:	Clay-Like	$\phi =$	$0^\circ$	$c =$	2,500 psf
$\gamma =$	115 pcf	$c/\gamma^*H$	3.95	$K_{PE} =$	1.0
$\overline{AE}$	17.9 ft	$p_{wall} =$	5.32 ksf	$f_{ult} =$	29.24 k/ft
$y_{max}/h_{wall}$	0.10	$y_{max} =$	6.6 in.	$K_{avg} =$	25 k/in/ft
$y_{avg} =$	0.58 in.	$C =$	45.57	$D =$	1.41

**Table 14-5,  $c$ - $\phi$  Soil Parameters Used to Create Figure 14-55**

Wall Type:	Free-standing abutment back wall				
$h_{wall} =$	5.5 ft	$b_{wall} =$	50 ft	$\alpha =$	$0^\circ$
Earthquake:	SEE	$S_{D1} =$	0.20	$k_{Max} =$	0.30
$\beta =$	0.67	$\alpha_w =$	1.0	$k_h$	0.30
Soil Type:	$c$ - $\phi$	$\phi =$	$20^\circ$	$c =$	150 psf
$\gamma =$	110 pcf	$c/\gamma^*H$	0.25	$K_{PE} =$	4.0
$\overline{AE}$	17.9 ft	$p_{wall} =$	1.81 ksf	$f_{ult} =$	9.96 k/ft
$y_{max}/h_{wall}$	0.10	$y_{max} =$	6.6 in.	$K_{avg} =$	25 /in/ft
$y_{avg} =$	0.20 in.	$C =$	58.49	$D =$	5.72

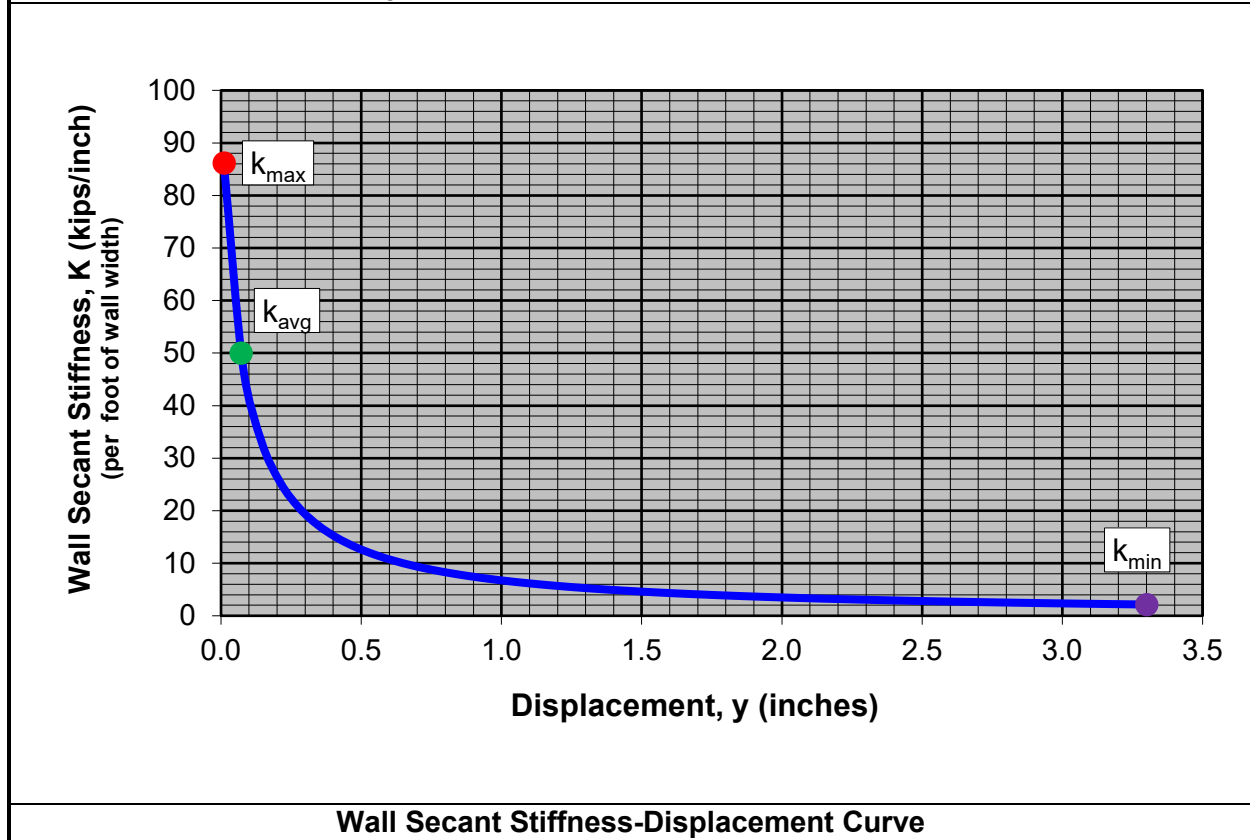
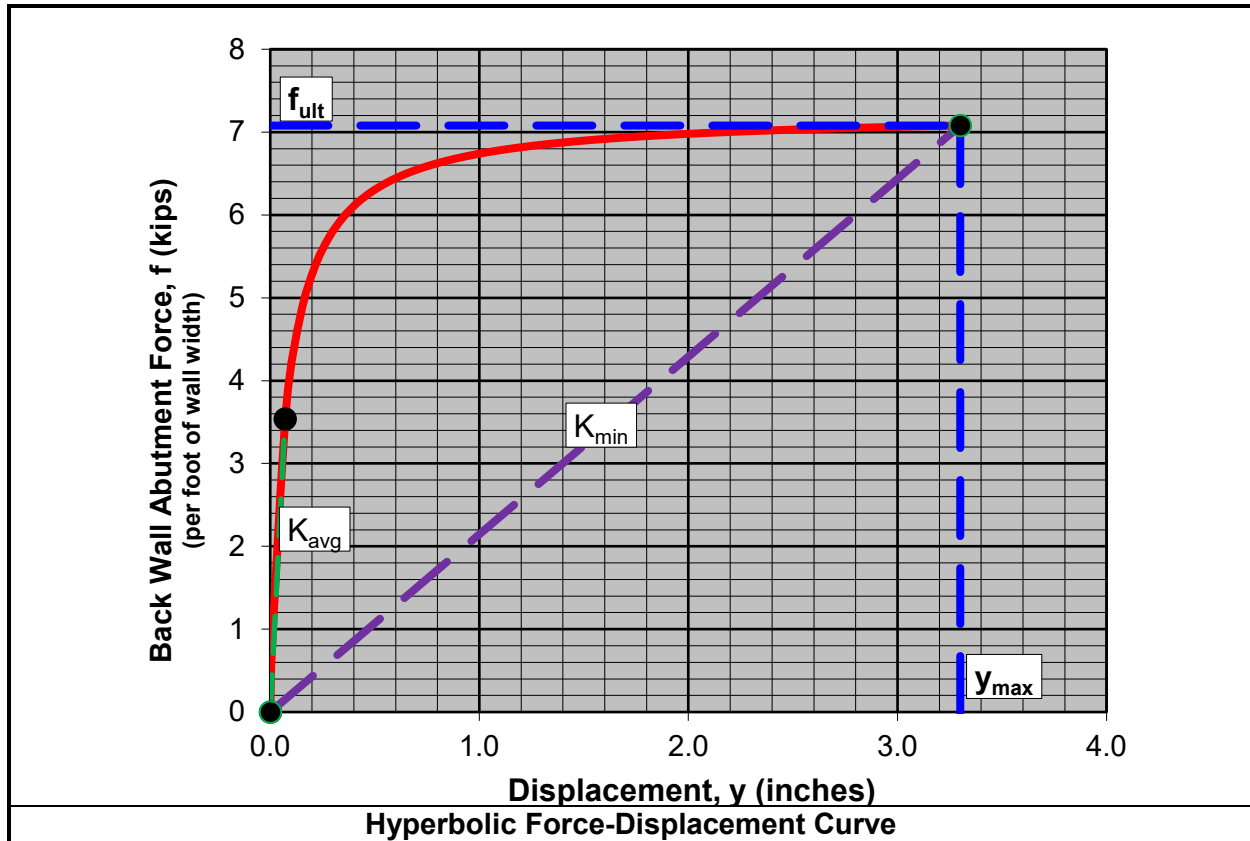
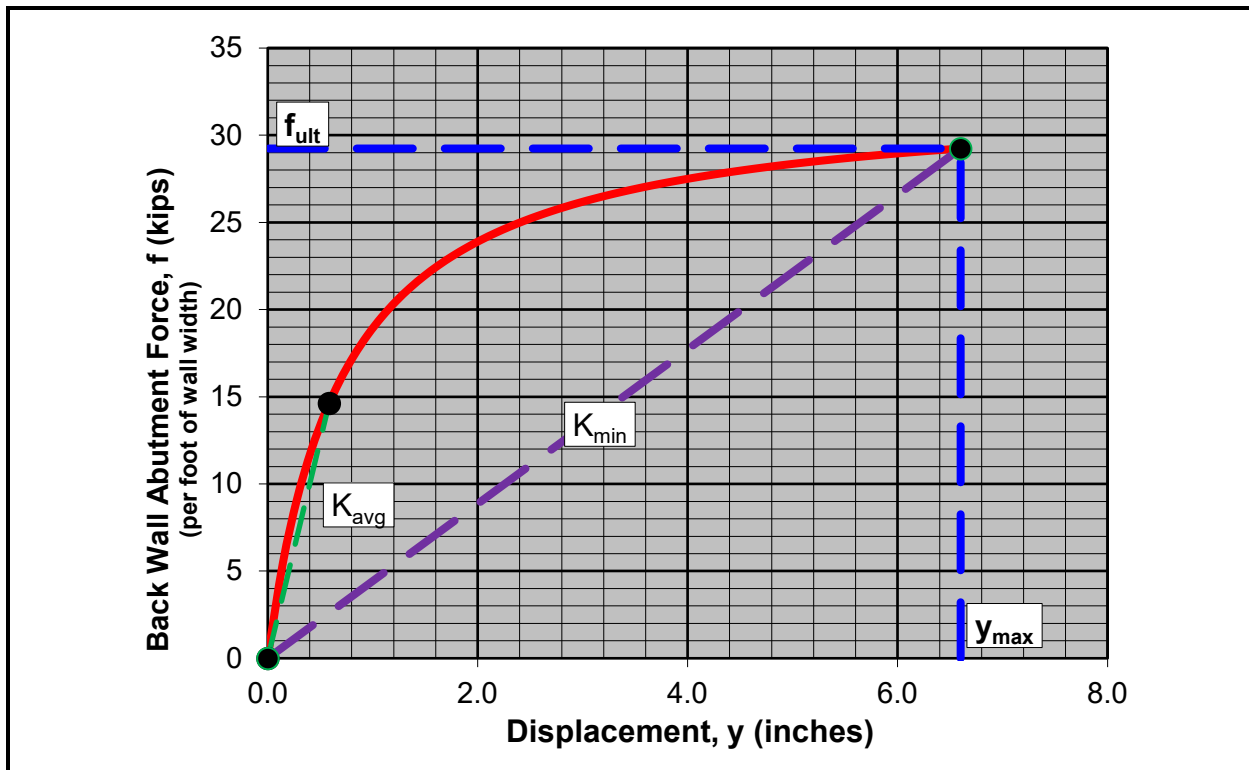
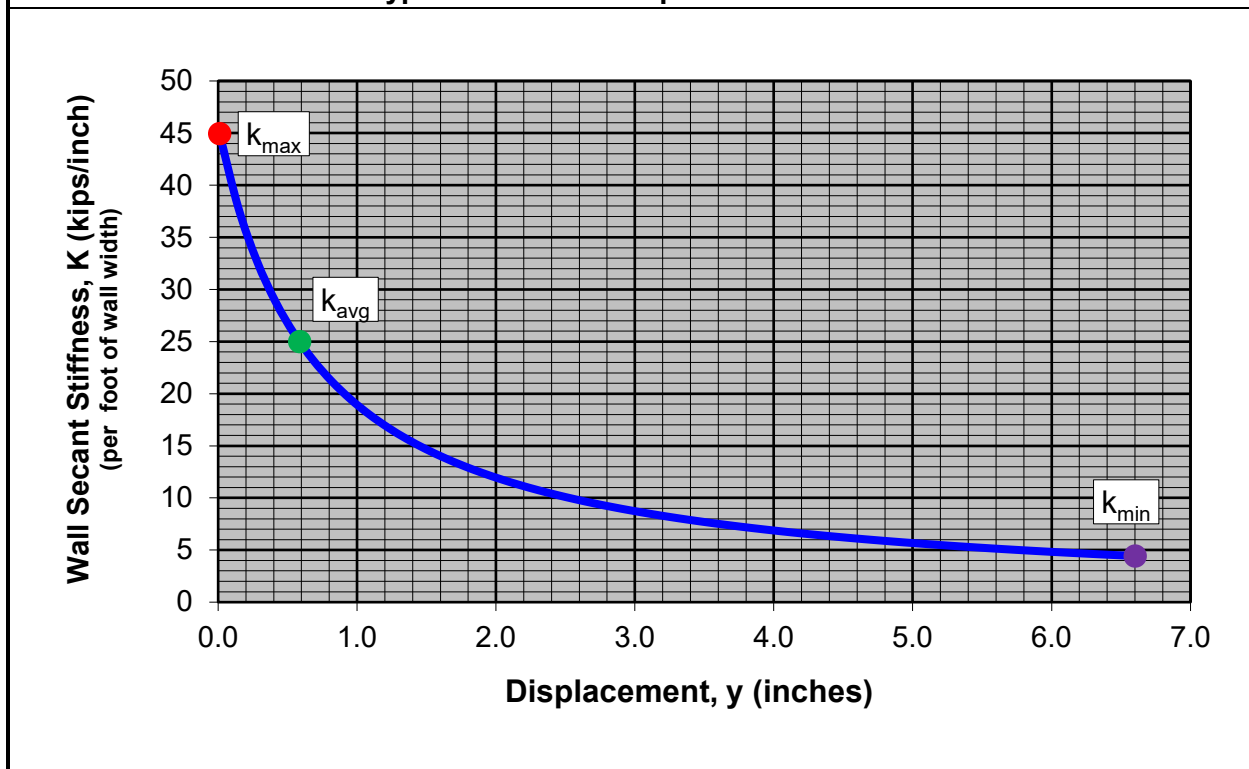


Figure 14-53, Bridge Abutment Wall Passive Pressure, Sand-Like Backfill Example

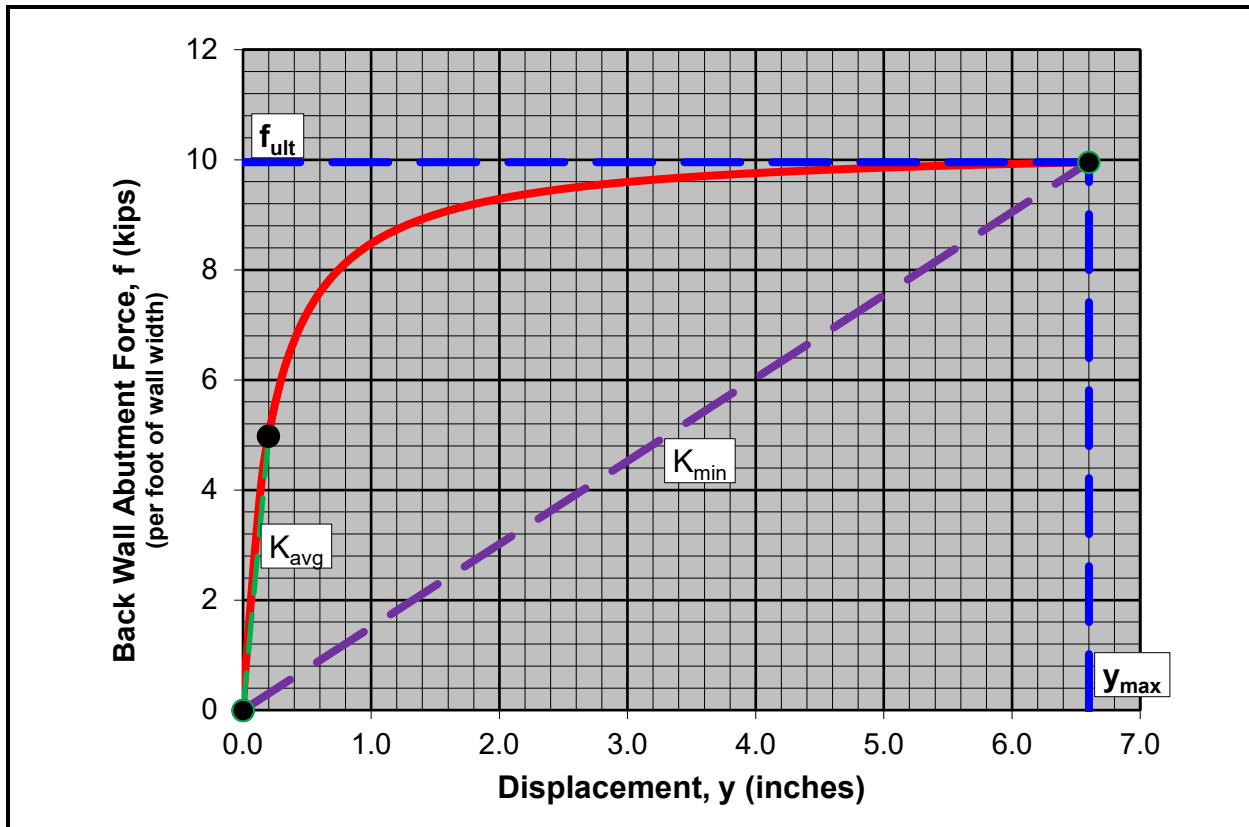


Hyperbolic Force-Displacement Curve

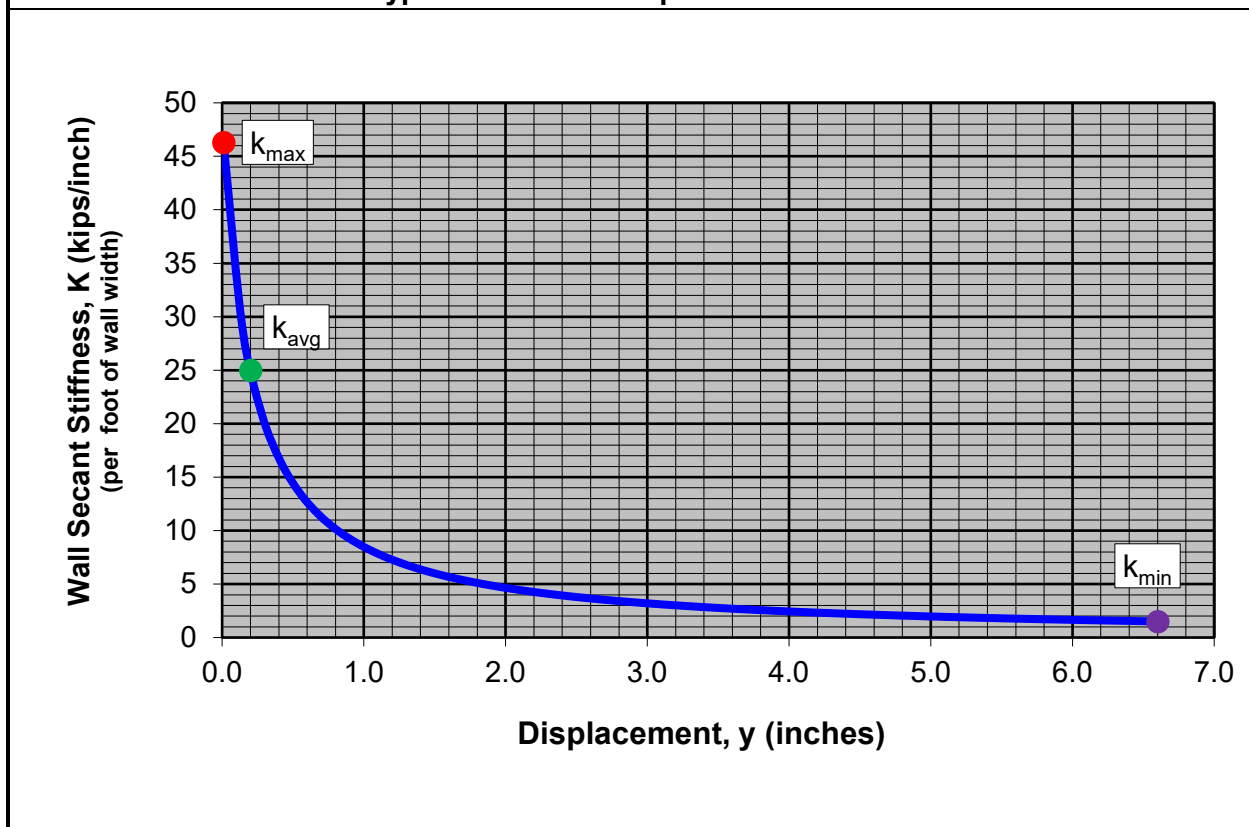


Wall Secant Stiffness-Displacement Curve

Figure 14-54, Bridge Abutment Wall Passive Pressure, Clay-Like Backfill Example



Hyperbolic Force-Displacement Curve



Wall Secant Stiffness-Displacement Curve

Figure 14-55, Bridge Abutment Wall Passive Pressure, c-φ Backfill Example

### 14.9.2 Effective Width of Abutment Wall

The development of the total seismic passive resistance ( $F_{ult}$ ) is dependent on the effective width ( $B_{eff}$ ) of the wall being analyzed (see Figure 14-56). The effective wall width ( $B_{eff}$ ) is equal to the wall width ( $b_{wall}$ ) when the bridge skew angle,  $\alpha$ , is zero degrees or when the ground surface adjacent to the abutment is level or sloping upward away from the finished grade of the roadway. The effective abutment width,  $B_{eff}$ , is typically less than the wall width ( $b_{wall}$ ) when the bridge skew angle,  $\alpha$ , is greater than zero degrees and when the ground surface adjacent to the abutment is sloping downward or is vertical (i.e., MSE wall). For skew angles ( $\alpha$ ) greater than 60 degrees, contact the PC/GDS for additional information.

The effective abutment width,  $B_{eff}$ , is computed based on the distance,  $L_{min}$ , perpendicular to the abutment wall (See Figures 14-56 and 14-57).  $L_{min}$  is the distance required to develop the full seismic passive pressure. The distance,  $L_{min}$ , is the critical distance (longest distance) as determined by evaluating the following 2 passive resistance failure mechanisms:

1. Ground surface projection of the passive failure wedge designated as distance  $\overline{AC}$  (see Figures 14-21 and 14-56). As indicated in Equation 14-33, this distance is approximately 3.25 times the height of the abutment wall,  $h_{wall}$ .
2. Length of the sliding soil wedge (trapezoid CEFHGC – see Figure 14-57) along  $\overline{EH}$  ( $L_{Slide}$ ) located behind the passive failure wedge (log spiral shape ABCEDA) required to allow full development of the maximum abutment passive resistance ( $f_{ult}$ ). The length of the sliding soil wedge along  $\overline{EH}$  ( $L_{Slide}$ ) is computed as presented below.

Limiting mechanism No. 2 is related to the shearing resistance of the soil at the base of the wall and the skew angle ( $\alpha$ ). The sliding resistance ( $f_{Slide}$ ) along the horizontal distance  $\overline{EH}$  ( $L_{Slide}$ ) is equal to the sum of sliding resistances  $f_{Skew}$  along the skew horizontal distance ( $\overline{EF}$ ) plus the sliding resistance  $f_{Slope}$  along the side slope horizontal distance ( $\overline{FH}$ ). In order to develop the maximum abutment passive resistance ( $f_{ult}$ ) determined in accordance with Section 14.9.1, the sliding resistance ( $f_{Slide}$ ) along the horizontal distance  $\overline{EH}$  must be equal to or greater than  $f_{ult}$  as indicated in the following equation:

$$f_{ult} \leq f_{Slide} = f_{Skew} + f_{Slope} \quad \text{Equation 14-38}$$

$$f_{Slide} = \frac{f_{ult}}{\phi_{Slide}} \quad \text{Equation 14-39}$$

Where the resistance factor against sliding soil on soil ( $\phi_{Slide}$ ) shall be equal to 1.0 for the EE I limit state.

The minimum sliding resistance ( $f_{Slide}$ ) required to prevent failure of this soil wedge during full seismic passive loading is computed as follows:

$$f_{Slide} = \frac{f_{ult}}{\phi_{Slide}} = (L_{Skew-ult} * \tau_{Skew}) + (L_{Slope} * \tau_{Slope}) \quad \text{Equation 14-40}$$

$$\tau_{Skew} = c + \gamma * h_{wall} * \tan \phi \quad \text{Equation 14-41}$$

$$\tau_{Slope} = c + 0.5 * \gamma * h_{wall} * \tan \phi \quad \text{Equation 14-42}$$

The soil parameters above the base of the wall at  $\overline{DH}$  may be different from those below this shear plane. Whichever set of soil parameters develops the minimum  $\tau_{Skew}$  and  $\tau_{Slope}$  shall be used in evaluating the minimum horizontal distance  $\overline{EH}$  ( $L_{Slide}$ ).

The distance  $L_{Slope}$  extends from the shoulder break, point G, to where the slope intersects  $\overline{DH}$  and is determined using the following equation.

$$L_{Slope} = (X_1^2 + X_2^2)^{0.5} \quad \text{Equation 14-43}$$

Where,

$$X_1 = h_{wall} * Slope_H \quad \text{Equation 14-44}$$

$Slope_H$  = Slope along  $\overline{FH}$  of horizontal (H) distance to one vertical (V).

$$X_2 = X_1 * \sin \alpha \quad \text{Equation 14-45}$$

As shown in Figure 14-57, distance  $L_{Skew}$  ( $\overline{EF}$ ) extends from where the base of the Rankine passive failure wedge intersects  $\overline{DH}$  and extends to directly below the shoulder break. Equation 14-43 should be rearranged to solve for  $L_{Skew}$  as follows:

$$L_{Skew} = \frac{\left[ \left( \frac{f_{ult}}{\phi_{Slide}} \right) - (L_{Slope} * \tau_{Slope}) \right]}{\tau_{Skew}} \quad \text{Equation 14-46}$$

The minimum length ( $L_{min}$ ) required to mobilize full seismic passive resistance (See Figures 14-56 and 14-57) is the lesser of the following:

$$\overline{AC} = 3.25 * h_{wall} \quad (\text{Failure Mechanism No. 1}) \quad \text{Equation 14-47}$$

or

$$\overline{DE} + L_{Skew} \quad (\text{Failure Mechanism No. 2}) \quad \text{Equation 14-48}$$

Where,

$$\overline{DE} = 0.5 * \overline{AC} \quad \text{Equation 14-49}$$

The effective width ( $B_{eff}$ ) for skewed bridge abutments will typically be less than the width of the abutment wall ( $b_{wall}$ ). The effective abutment width ( $B_{eff}$ ) is determined using the following equation.

$$B_{eff} = b_{wall} - b_x \quad \text{Equation 14-50}$$

Where,

$$b_x = L_{min} * \tan \alpha \quad \text{Equation 14-51}$$

The effective abutment width ( $B_{eff}$ ) will be capable of providing fully mobilized seismic passive resistance and displacements perpendicular to the back of the abutment wall as indicated in Section 14.9.1. The resultant of the seismic demand acting perpendicular to the abutment wall face shall be used to evaluate displacements (perpendicular to the back of the wall) resulting from seismic passive resistance. Similar evaluations as those presented above will be required when evaluating shear walls to resist transverse seismic demand parallel to the bridge abutment wall.

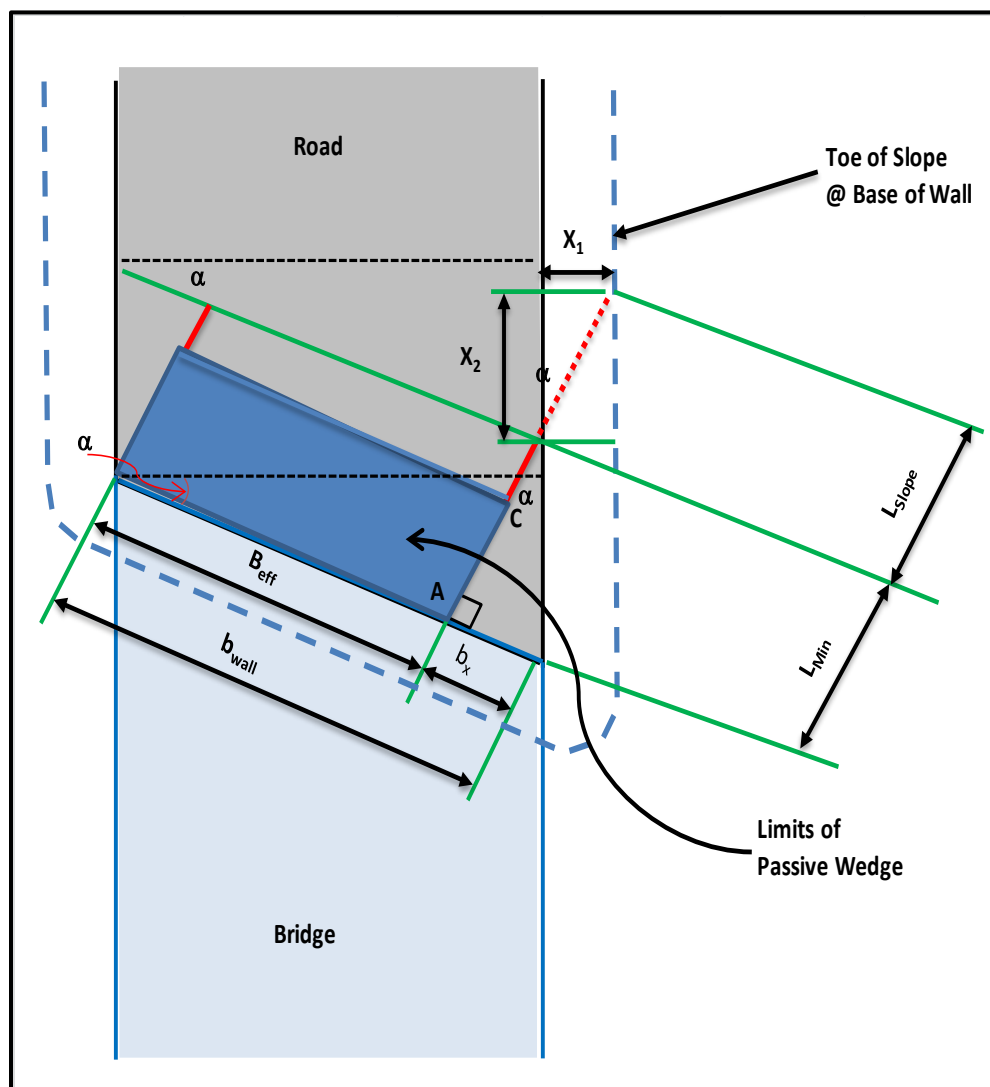


Figure 14-56, Skewed Bridge Abutment Wall Seismic Passive Resistance

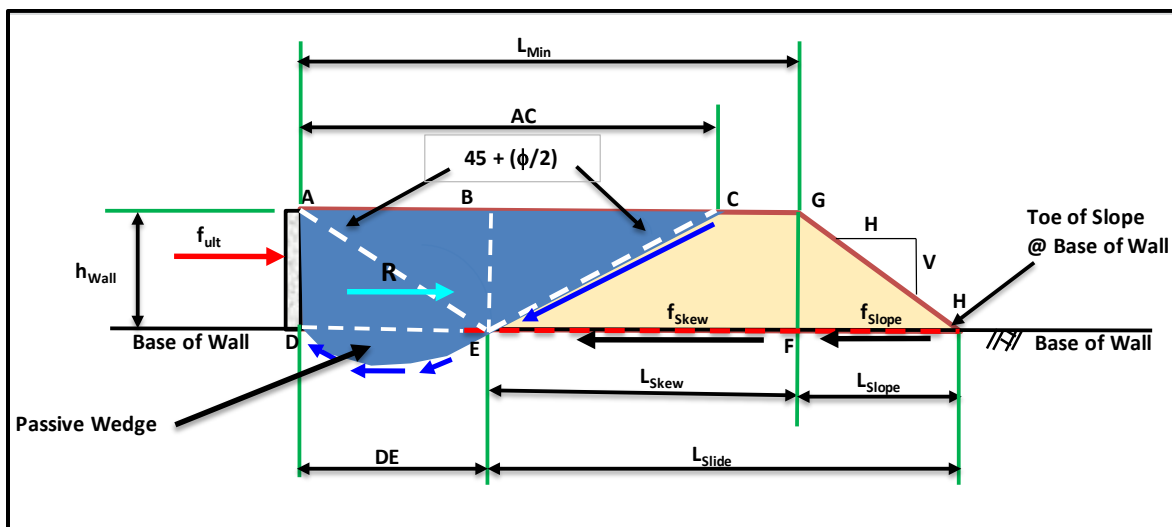


Figure 14-57, Skewed Bridge Abutment Wall Seismic Sliding Resistance

## 14.10 GEOTECHNICAL SEISMIC DESIGN OF EMBANKMENTS

As discussed in Chapter 17, slopes comprise 2 basic categories: natural and man-made (engineered). Typically man-made slopes are comprised of relatively uniform imported soils, thus allowing for more predictable performance and analysis during a seismic event. The design of these slopes becomes problematic when the embankment is placed on soft cohesive soils or loose cohesionless soils that can undergo SSL as described in Chapter 13. Natural slopes present greater difficulties than man-made slopes, because of the potentially wide variation in soil type and shear strength that may be present in these slopes. As indicated in Chapter 17, natural slopes are those slopes that are formed from natural processes. Natural slopes are harder to analyze given the potential variability of not only material type and shear strength, but also thickness as well. Low shear strength layers that are thin may not be indicated in the geotechnical exploration and therefore could have potential consequences in not only seismic design, but also static design. Natural slopes are also hard to investigate because the terrain of most natural slopes is steep (1H:1V) making access extremely difficult. Natural slopes tend to fail during seismic events more frequently than man-made slopes. If the potential for SSL is present beneath the slope, the procedures discussed in Chapter 13 shall be followed.

The seismic design of the embankments shall conform to the procedures discussed in Chapter 13. Settlement induced by the seismic event shall be determined using the procedures discussed in Chapter 13. If seismic instability is determined to occur, all displacements determined shall conform to the performance limits discussed in Chapter 10. For displacements that exceed the limits of Chapter 10, see Section 14.15 for mitigation methods.

## 14.11 RIGID GRAVITY EARTH RETAINING STRUCTURE DESIGN

Rigid gravity ERSs are comprised of gravity, semi-gravity and modular gravity ERSs as defined in Chapter 18. Gravity retaining structures use the weight of mass concrete and retained soil to resist the driving forces placed on the structure. A rigid gravity earth wall is analyzed using the pseudo-static method as shown in Figure 14-1. Discussed in the following paragraphs are the requirements for determining the external stability of a rigid gravity ERS during a seismic event

(EE I). The seismic internal stability calculations shall conform to the requirements contained in the AASHTO LRFD Specifications, except all accelerations used shall conform to the requirements of this Manual (i.e.,  $k_{avg}$ ). Additionally, all load and resistance factors shall conform to Chapters 8 and 9 and all displacements shall conform to Chapter 10.

Similarly to embankments as discussed in Chapter 13, there are conditions for which no seismic analysis of rigid gravity ERSs is required. For rigid gravity ERSs located within bridge embankments, no seismic analysis is required when the PGA is less than or equal to 0.4g ( $PGA \leq 0.4g$ ), the wall height ( $H_{wall}$  in Figures 14-58 and 14-59) is less than or equal to 35 feet ( $H_{wall} \leq 35$  feet) and the subsurface soils do not have the potential for SSL. The no seismic analysis may be extended beyond a PGA of 0.4g provided all of the previous criteria are met; PGA ( $k_{max}$ ) is less than or equal to 0.8g ( $PGA \leq 0.8g$ ); the  $k_y$  to  $k_{max}$  (0.8g) ratio is more than 0.5 (i.e.,  $k_y/k_{max} \geq 0.5$ ); and 2.0 inches of displacement can be tolerated. A seismic analysis for a rigid gravity ERS located within a bridge embankment will be required if any of the previous criteria are not met or if the ERS is located within a larger slope (i.e., the ground slopes upward from the top of the ERS or downward from the bottom of the ERS).

Rigid gravity ERSs located within roadway embankments will not require seismic analysis if the PGA is less than or equal to 0.4g ( $PGA \leq 0.4g$ ), the wall height ( $H_{wall}$  in Figures 14-58 and 14-59) is less than or equal to 10 feet ( $H_{wall} \leq 10$  feet) regardless of the potential for the subsurface soils susceptibility for SSL. If the subsurface soils do not have the potential for SSL, then the criteria established for rigid gravity ERSs in bridge embankments may be applied. A seismic analysis for a rigid gravity ERS located within a roadway embankment will be required if any of the previous criteria are not met or if the ERS is located within a larger slope (i.e., the ground slopes upward from the top of the ERS or downward from the bottom of the ERS) or the ERS supports another structure that could be impacted by the instability of the ERS.

The external stability shall be determined using the following procedure:

- Step 1:** The first step in designing a rigid gravity ERS is to establish the initial ERS design using the procedures indicated in Chapter 18. This establishes the dimensions and weights of the rigid gravity ERS.
- Step 2:** Determine the PGA and  $S_{D1}$  using the procedures outlined in Chapter 12 regardless of whether the 3-Point method or a Site-Specific Seismic Response Analysis is performed. All ERSs are required to be designed for both EE I events (FEE and SEE).
- Step 3:** Determine the PGV using the correlation provided in Chapter 12.
- Step 4:** Compute the average seismic horizontal acceleration coefficient ( $k_h = k_{avg}$ ) due to wave scattering as indicated in Chapter 13.
- Step 5:** Determine  $K_{ae}$  in accordance with the procedures described in Section 14.4.
- Step 6:** Compute the seismic active earth pressure force ( $P_{ae}$ ), horizontal inertial force of the structural soil wedge ( $P_{IR}$ ), and the horizontal inertial force of the slope surcharge above the structural soil wedge ( $P_{IS}$ ) if the wall has a sloped backfill. The seismic force diagrams and appropriate variables are shown in Figure 14-58 for the level

backfill surface case and Figure 14-59 for the sloped backfill surface case. For broken back backfill surface case, convert to a sloped backfill surface case using an effective backfill  $\beta$  angle in accordance with AASHTO LRFD Section 11 and then evaluate as shown in Figure 14-59. The width of the structural soil wedge ( $B_{SSW}$ ) is the distance from the back of the wall to the heel of the footing as shown in Figures 14-58 and 14-59. The height ( $H_2$ ) is the height where the seismic earth pressures are exerted on the structural wedge as is computed using the following equations:

Level Backfill Case (Figure 14-58):

$$H_2 = H_{wall} + H_{ftg} \quad \text{Equation 14-52}$$

Sloped Backfill Case (Figure 14-59):

$$H_2 = H_{wall} + H_{ftg} + B_{SSW} * \tan \beta \quad \text{Equation 14-53}$$

Where,

- $H_{wall}$  = Height of wall stem, feet
- $H_{ftg}$  = Height of wall footing, feet

Once the effective wall height ( $H_2$ ) and the width of the structural soil wedge ( $B_{SSW}$ ) have been determined, compute the seismic active earth force ( $P_{ae}$ ) that is distributed as a uniform pressure over a height equal to  $H_2$ , the horizontal inertial force of the structural soil wedge ( $P_{IR}$ ), and the horizontal inertial force of the soil surcharge above the structural soil wedge ( $P_{IS}$ ) assumed to be triangular as shown in Figure 14-52. The horizontal seismic forces are computed as indicated below:

Level Backfill Case (Figure 14-58):

$$P_{ae} = 0.5 * \gamma_P * K_{ae} * \gamma_{Backfill} * (H_2)^2 \quad \text{Equation 14-54}$$

$$P_{IR} = \gamma_P * k_{avg} * \gamma_{Backfill} * B_{SSW} * H_{wall} \quad \text{Equation 14-55}$$

Where,

- $\gamma_P$  = Permanent load factor, use 1.0 for ERS in EEI
- $K_{ae}$  = Seismic active earth pressure coefficient from Section 14.4
- $\gamma_{Backfill}$  = Backfill wet unit weight, pounds per cubic foot
- $H_2$  = Height over which the seismic earth pressures are exerted on the structural wedge from Equation 14-52, feet
- $k_{avg}$  = Average horizontal acceleration that accounts for wave scattering in accordance with Chapter 13, g
- $B_{SSW}$  = Width of the structural soil wedge, feet
- $H_{wall}$  = Height of wall stem, feet

Sloped Backfill Case (Figure 14-59):

$$P_{ae} = 0.5 * \gamma_P * K_{ae} * \gamma_{Backfill} * (H_2)^2 \quad \text{Equation 14-56}$$

$$P_{IR} = \gamma_P * k_{avg} * \gamma_{Backfill} * B_{ssw} * H_{wall} \quad \text{Equation 14-57}$$

$$P_{IS} = 0.5 * \gamma_P * k_{avg} * \gamma_{Backfill} * \tan \beta * (B_{ssw})^2 \quad \text{Equation 14-58}$$

Where,

- $\gamma_P$  = Permanent load factor, use 1.0 for ERS in EE I
- $K_{ae}$  = Seismic active earth pressure coefficient from Section 14.4
- $\gamma_{Backfill}$  = Backfill wet unit weight, pounds per cubic foot
- $H_2$  = Height over which the seismic earth pressures are exerted on the structural wedge from Equation 14-53, feet
- $k_{avg}$  = Average horizontal acceleration that accounts for wave scattering in accordance with Chapter 13, g
- $B_{ssw}$  = Width of the structural soil wedge, feet
- $H_{wall}$  = Height of wall stem, feet
- $\beta$  = Backslope angle, degrees

Compute the horizontal inertial force of the weight of wall stem ( $F_{IW}$ ) and horizontal inertial force of the weight of the wall footing ( $F_{IF}$ ), as indicated by the following equations:

$$F_{IW} = W_{Stem} * k_{avg} \quad \text{Equation 14-59}$$

$$F_{IF} = W_{Ftg} * k_{avg} \quad \text{Equation 14-60}$$

Where,

- $W_{Stem}$  = Weight of wall stem, pounds per foot of wall width
- $W_{Ftg}$  = Weight of wall footing, pounds per foot of wall width
- $k_{avg}$  = Average horizontal acceleration that accounts for wave scattering in accordance with Chapter 13, g

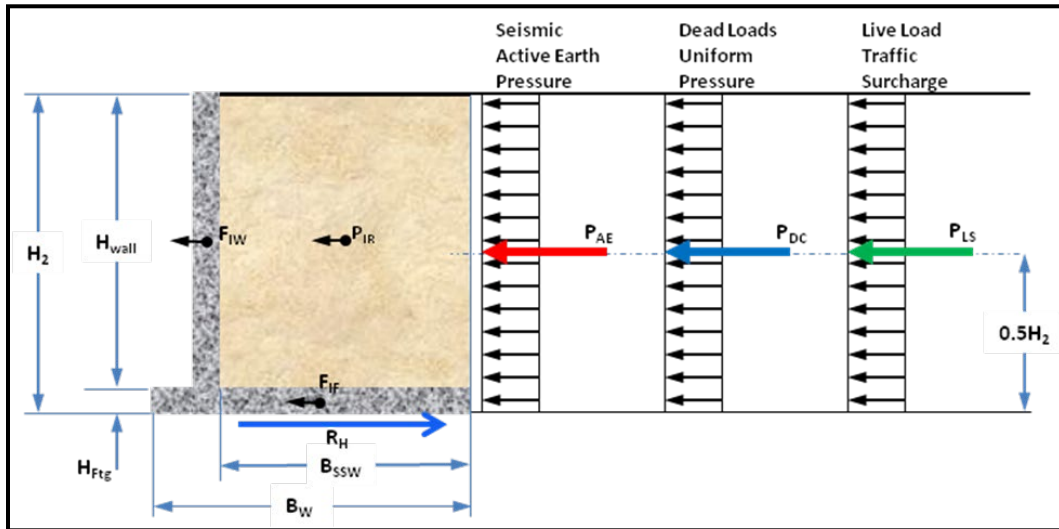


Figure 14-58, Rigid Gravity ERS Seismic Force Diagram – Level Backfill

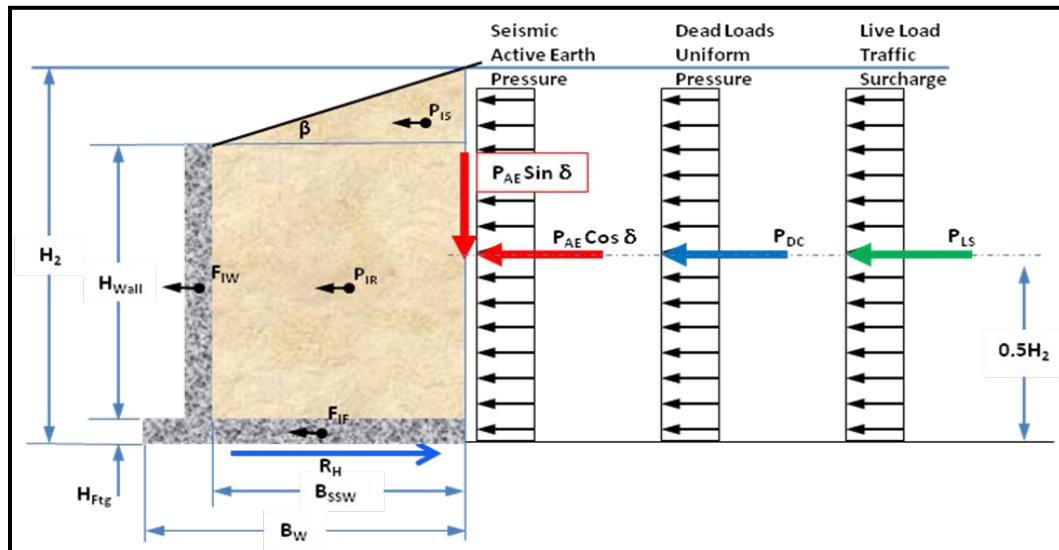


Figure 14-59, Rigid Gravity ERS Seismic Force Diagram – Sloping Backfill

**Step 7:** Compute dead load uniform pressure ( $P_{DC}$ ), and live load traffic surcharge ( $P_{LS}$ ) as indicated below:

$$P_{DC} = \gamma_P * K_{ae} * q_{DC} * H_2 \quad \text{Equation 14-61}$$

$$P_{LS} = \gamma_{EQ} * K_{ae} * q_{LS} * H_2 \quad \text{Equation 14-62}$$

Where,

- $\gamma_P$  = Permanent load factor, use 1.0 for ERS in EE I
- $K_{ae}$  = Seismic active earth pressure coefficient from Section 14.4
- $q_{DC}$  = Dead load uniform pressure, pounds per square foot

- $H_2$  = Height over which the seismic earth pressures are exerted on the structural wedge. For level backfill surface use Equation 14-52 and for sloped backfill surface use Equation 14-53, feet
- $\gamma_{EQ}$  = EE I load factor, See Chapter 8
- $q_{LS}$  = Live load traffic surcharge pressure, pounds per square foot

**Step 8:** Compute the horizontal driving forces ( $F_H$ ). The passive earth pressure force shall only be included for shear keys that are located below the footing (see Section 14.5). The horizontal driving force ( $F_H$ ) is determined by the following equation:

$$F_H = P_{ae} * \cos \beta + P_{IR} + P_{IS} + P_{DC} + P_{LS} + F_{IW} + F_{IF} \quad \text{Equation 14-63}$$

**Step 9:** The frictional resistance of the foundation soils ( $R_{HF}$ ) is computed using the following equations:

$$R_{HF} = \phi * \tau * B_w = \phi * (c * B_w + N * \tan \delta_F) \quad \text{Equation 14-64}$$

Where,

- $\phi$  = Resistance factor, See Chapter 9
- $\tau$  = Foundation soil shear strength, pounds per square foot
- $B_w$  = Base width of the wall footing, feet
- $c$  = Cohesion of foundation soils, pounds per square foot
- $\delta_F$  = Foundation-soil interface friction angle (AASHTO LRFD), degrees
- $\tan(\delta_F)$  = Foundation-soil interface friction coefficient,  $\mu$  (AASHTO LRFD)
- $N$  = Normal force that is the sum of the vertical loads over the base width ( $B_w$ ) of the reinforced soil mass, pounds per foot of wall width. The normal force is computed by the following equation:

**Equation 14-65**

$$N = (B_{ssw} H_{wall} \gamma_{Backfill}) + P_{ae} \sin \beta + 0.5 [B_{ssw} (H_2 - H_{wall} - H_{ftg}) \gamma_{Backfill}] + W_{Stem} + W_{Ftg}$$

Where,

- $B_{ssw}$  = Width of the structural soil wedge, feet
- $H_{wall}$  = Height of wall stem, feet
- $\gamma_{Backfill}$  = Backfill wet unit weight, pounds per cubic foot
- $P_{ae}$  = Seismic active earth force, pounds per foot of wall width
- $\beta$  =  $0^\circ$  - level backfill or  
backslope angle, degrees
- $\gamma_P$  = Permanent load factor, use 1.0 for ERS in EE I
- $K_{ae}$  = Seismic Active Earth Pressure Coefficient from Section 14.4
- $H_2$  = Height over which the seismic earth pressures are exerted on the structural wedge. For level backfill surface use Equation 14-52 and for sloped backfill surface use Equation 14-53, feet
- $k_{avg}$  = Average horizontal acceleration that accounts for wave scattering in accordance with Chapter 13, g
- $B_{ssw}$  = Width of the structural soil wedge, feet
- $\beta$  = Backslope angle, degrees

$$W_{\text{Stem}} = \text{Weight of wall stem, pounds per foot of wall width}$$

$$W_{\text{Ftg}} = \text{Weight of wall footing, pounds per foot of wall width}$$

Evaluate the ERS Wall bearing pressure, limiting eccentricity for overturning, sliding and global stability for the maximum seismic design load in accordance with the appropriate Chapters of the GDM. For determination of bearing capacity, see Chapter 15. If deep foundations are to be used to support rigid gravity ERSs, see Chapter 16 for deep foundation design methodology. It should be noted that all EE I resistance factors ( $\phi$ ) are provided in Chapter 9. If all of the resistance factors are met, the static design is satisfactory and the seismic design is complete. It is reasonable to assume that if the demand/capacity ratio (D/C) for rigid gravity ERS meets the required resistance factors for the SEE design earthquake, the required resistance factors for the FEE design earthquake will be met. If bearing pressure and limiting eccentricity for overturning are not met, then the rigid gravity wall requires redesign to meet these resistances. If the sliding or global stability resistance factor criterion is not met, the ERS is unstable; therefore, continue to Step 10 and evaluate the displacements caused by both the FEE and SEE design earthquakes.

**Step 10:** Determine the yield acceleration ( $k_y$ ) for the global stability of the ERS in accordance with Chapter 13. The  $k_y$  is the acceleration at which the ERS becomes just stable (i.e.,  $\phi = 1.0 = 1/\text{FS} = 1.0$ ). If the ratio of  $k_y$  to  $k_h$  is more than 0.5 ( $k_y/k_h \geq 0.5$ ), then a displacement ( $\Delta L$ ) of 2 inches shall be assumed and reported (Elms and Martin (1979)). As indicated previously, if the failure surface is circular all displacements at the top of the slope shall be considered to be vertical, while all displacements at the top of the slope for a non-circular failure surface shall be considered horizontal.

For evaluating the yield acceleration ( $k_y$ ) for sliding of the ERS, first determine the driving forces ( $F_H$ ) as a function of horizontal acceleration ( $k = k_h$ ) and the resisting forces ( $R_H$ ) as a function of horizontal acceleration ( $k = k_h$ ) as depicted in Figure 14-60. The passive earth pressure force shall only be included for shear keys that are located below the footing (see Section 14.5); otherwise, no passive earth pressure force shall be used to resist lateral seismic forces. The yield acceleration ( $k_y$ ) will be the location where the driving forces ( $F_H$ ) and resisting forces ( $R_H$ ) are equal.

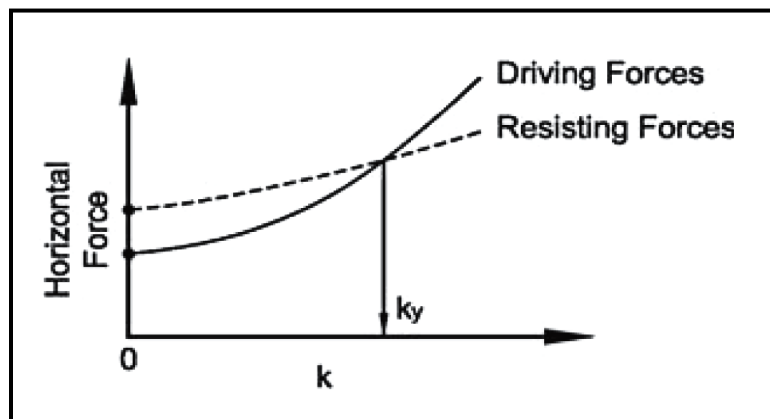


Figure 14-60, Determination of Yield Acceleration ( $k_y$ ) (Anderson, et al. (2008))

After determining  $k_y$ , determine the amount of displacement ( $d$ ) using the procedures in Chapter 13. If the displacement is within the performance limits, as indicated in Chapter 10, then design is complete. If the displacement exceeds the performance limits in Chapter 10, redesign the ERS to achieve acceptable performance limits or determine if the amount of anticipated movement is acceptable to both the design team as well as SCDOT.

## 14.12 FLEXIBLE GRAVITY EARTH RETAINING STRUCTURE DESIGN

Flexible gravity earth retaining systems are comprised of gabion and Mechanically Stabilized Earth (MSE) ERSs as defined in Chapter 18. Flexible gravity retaining structures use the reinforced soil mass for MSE walls and the stone for gabion ERSs, and the foundation soils to resist the driving forces placed on the structure. Discussed in the following paragraphs are the requirements for determining the external stability of a flexible gravity ERS during an EE I event. The seismic internal stability calculations shall conform to the requirements contained in the AASHTO LRFD Specifications (Section 11.10 – Mechanically Stabilized Earth Walls), except all accelerations used shall conform to the requirements of this Manual (i.e.,  $A_s = k_{avg}$  as determined in Chapter 13). Additionally, all load and resistance factors shall conform to Chapters 8 and 9 and all displacements shall conform to Chapter 10.

Similarly to embankments as discussed in Chapter 13, there are conditions for which no seismic analysis of flexible gravity ERSs is required. For flexible gravity ERSs located within bridge embankments, no seismic analysis is required when the PGA is less than or equal to 0.4g ( $PGA \leq 0.4g$ ), the wall height ( $H_{wall}$  in Figures 14-61 and 14-62) is less than or equal to 35 feet ( $H_{wall} \leq 35$  feet) and the subsurface soils do not have the potential for SSL. The no seismic analysis may be extended beyond a PGA of 0.4g provided all of the previous criteria are met; PGA ( $k_{max}$ ) is less than or equal to 0.8g ( $PGA \leq 0.8g$ ); the  $k_y$  to  $k_{max}$  (0.8g) ratio is more than 0.5 (i.e.,  $k_y/k_{max} \geq 0.5$ ); and 2.0 inches of displacement can be tolerated. A seismic analysis for a flexible gravity ERS located within a bridge embankment will be required if any of the previous criteria are not met or if the ERS is located within a larger slope (i.e., the ground slopes upward from the top of the ERS or downward from the bottom of the ERS).

Flexible gravity ERSs located within roadway embankments will not require seismic analysis if the PGA is less than or equal to 0.4g ( $PGA \leq 0.4g$ ), the wall height ( $H_{wall}$  in Figures 14-61 and 14-62) is less than or equal to 10 feet ( $H_{wall} \leq 10$  feet) regardless of potential for the subsurface soils having the susceptibility for SSL. If the subsurface soils do not have the potential for SSL, then the criteria established for flexible gravity ERSs in bridge embankments may be applied. A seismic analysis for a flexible gravity ERS located within a roadway embankment will be required if any of the previous criteria are not met or if the ERS is located within a larger slope (i.e., the ground slopes upward from the top of the ERS or downward from the bottom of the ERS) or the ERS supports another structure that could be impacted by the instability of the ERS.

The external stability shall be determined using the following procedure:

- Step 1:** The first step in designing a flexible gravity ERS is to establish the initial ERS design using the procedures indicated in Chapter 18 and Appendix C (MSE walls). This establishes the dimensions and weights of the flexible gravity ERS.

- Step 2:** Determine the PGA and  $S_{D1}$  using the procedures outlined in Chapter 12 regardless of whether the 3-Point method or a Site-Specific Seismic Response Analysis is performed. All ERSs are required to be designed for both EE I events (FEE and SEE).
- Step 3:** Determine the PGV using the correlation provided in Chapter 12.
- Step 4:** Compute the average seismic horizontal acceleration coefficient ( $k_h = k_{avg}$ ) due to wave scattering as indicated in Chapter 13.
- Step 5:** Determine  $K_{ae}$  in accordance with the procedures described in Section 14.4.
- Step 6:** Compute the seismic active earth pressure force ( $P_{ae}$ ), the horizontal inertial force of the reinforced soil mass ( $P_{IR}$ ) and the horizontal inertial force of the slope surcharge above the reinforced soil mass ( $P_{IS}$ ) if wall has a sloped backfill. The seismic force diagrams and appropriate variables are shown in Figure 14-61 for the level backfill surface case and Figure 14-62 for the sloped backfill surface case. For broken back backfill surface case, convert to sloped backfill surface case using an effective backfill  $\beta$  angle in accordance with AASHTO LRFD Section 11 and then evaluate as shown in Figure 14-62. The height ( $H_2$ ) is the height where the seismic earth pressures and effective inertial wall width ( $B_{Inertial}$ ) are computed as indicated below:

Level Backfill Case (Figure 14-61):

$$H_2 = H_{wall} \quad \text{Equation 14-66}$$

$$B_{Inertial} = \omega * H_2 \quad \text{Equation 14-67}$$

Where,

- $H_{wall}$  = Height of MSE wall facing, feet  
 $\omega$  = Coefficient equal to 0.50

Sloped Backfill Case (Figure 14-62):

$$H_2 = H_{wall} + \left( \frac{\omega * H_{wall} * \tan \beta}{1 - \omega * \tan \beta} \right) \quad \text{Equation 14-68}$$

$$B_{Inertial} = \omega * H_2 \quad \text{Equation 14-69}$$

Where,

- $H_{wall}$  = Height of MSE wall facing, feet  
 $\beta$  = Backslope angle, degrees  
 $\omega$  = Coefficient equal to 0.50 provided that

$$B_w \geq \omega * H_{wall} \quad \text{Equation 14-70}$$

If  $\omega H_{wall} > B_w$  then,

$$\omega = \frac{B_W}{H_{wall}} \quad \text{Equation 14-71}$$

Where  $B_W$  is the base width of the wall as determined in Step 1. For MSE walls with concrete panel facing, the base width of the wall is taken from the back of the wall facing and for MSE walls with concrete block facing, the base width of the wall is taken from the front of the block facing.

Once the effective wall height ( $H_2$ ) and the  $B_{Inertial}$  variables have been determined, compute the seismic active pressures ( $P_{ae}$ ). The seismic active earth pressure is distributed as a uniform pressure over a height equal to  $H_2$ . The horizontal inertial force of the reinforced soil mass ( $P_{IR}$ ) and the horizontal inertial force of soil surcharge above the reinforced soil mass ( $P_{IS}$ ), assumed to be triangular as shown in Figure 14-62, as indicated below:

Level Backfill Case (Figure 14-61):

$$P_{ae} = 0.5\gamma_P K_{ae} \gamma_{Backfill} (H_2)^2 = 0.5\gamma_P K_{ae} \gamma_{Backfill} (H_{wall})^2 \quad \text{Equation 14-72}$$

$$P_{IR} = \gamma_P k_{avg} \gamma_R B_{Inertial} H_2 = \gamma_P k_{avg} \gamma_R B_{Inertial} H_{wall} \quad \text{Equation 14-73}$$

Where,

- $\gamma_P$  = Permanent load factor, use 1.0 for ERS in EE I
- $K_{ae}$  = Seismic active earth pressure coefficient from Section 14.4
- $\gamma_{Backfill}$  = Backfill wet unit weight, pounds per cubic foot
- $\gamma_R$  = Reinforced fill wet unit weight, pounds cubic foot
- $H_2$  = Equal to the wall height,  $H_{Wall}$ , feet
- $k_{avg}$  = Average horizontal acceleration that accounts for wave scattering in accordance with Chapter 13, g
- $B_{Inertial}$  = Effective inertial wall width from Equation 14-69, feet

Sloped Backfill Case (Figure 14-62):

$$P_{ae} = 0.5\gamma_P K_{ae} \gamma_{Backfill} (H_2)^2 \quad \text{Equation 14-74}$$

$$P_{IR} = \gamma_P k_{avg} \gamma_R B_{Inertial} H_2 \quad \text{Equation 14-75}$$

$$P_{IS} = 0.5\gamma_P K_{avg} \gamma_{Backfill} \tan \beta (B_{Inertial})^2 \quad \text{Equation 14-76}$$

Where,

- $\gamma_P$  = Permanent load factor, use 1.0 for ERS in EE I
- $K_{ae}$  = Seismic active earth pressure coefficient from Section 14.4
- $\gamma_{Backfill}$  = Backfill wet unit weight, pounds per cubic foot
- $\gamma_R$  = Reinforced fill wet unit weight, pounds per cubic foot
- $H_2$  = Equal to the wall height,  $H_{Wall}$  from Equation 14-68, feet

- $k_{avg}$  = Average horizontal acceleration that accounts for wave scattering in accordance with Chapter 13, g
- $B_{inertial}$  = Effective inertial wall width from Equation 14-69, feet
- $\beta$  = Backslope angle, degrees

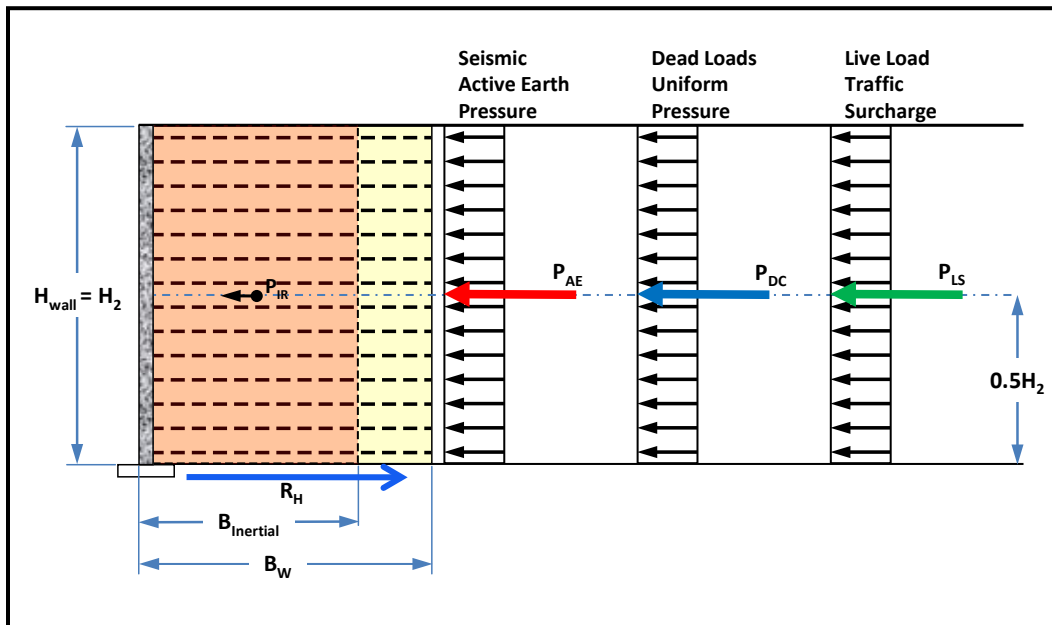


Figure 14-61, Flexible Gravity ERS Seismic Force Diagram – Level Backfill

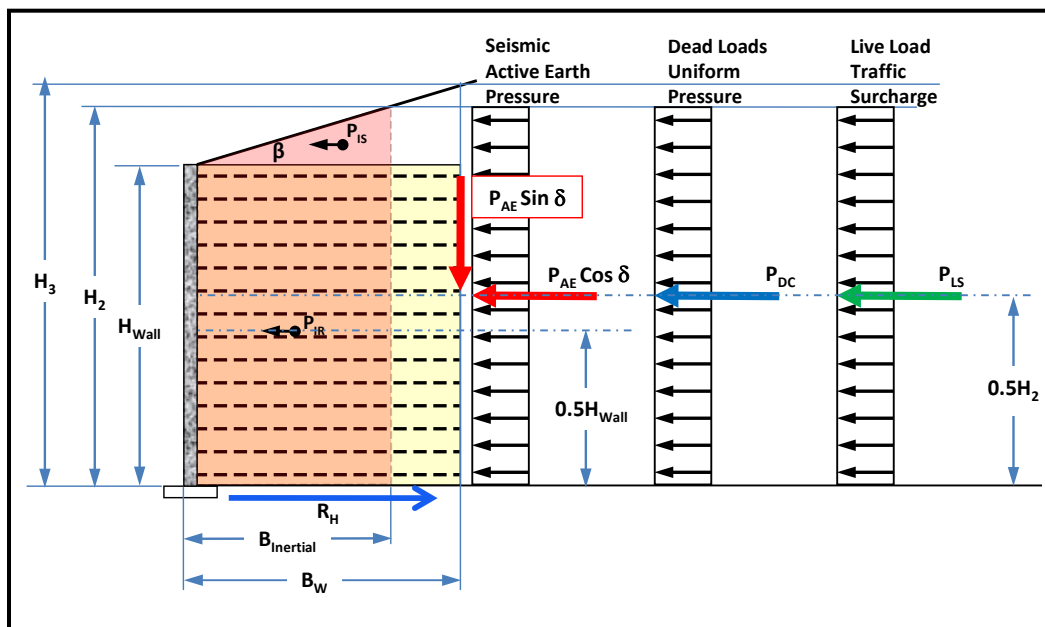


Figure 14-62, Flexible Gravity ERS Seismic Force Diagram – Sloping Backfill

**Step 7:** Compute dead load uniform pressure ( $P_{DC}$ ), and live load traffic surcharge ( $P_{LS}$ ) as indicated below:

$$P_{DC} = \gamma_P K_{ae} q_{DC} H_2 \quad \text{Equation 14-77}$$

$$P_{LS} = \gamma_{EQ} K_{ae} q_{LS} H_2 \quad \text{Equation 14-78}$$

Where,

- $\gamma_P$  = Permanent load factor, use 1.0 for ERS in EE I
- $\gamma_{EQ}$  = EE I load factor, See Chapter 8
- $K_{ae}$  = Seismic active earth pressure coefficient from Section 14.4
- $q_{DC}$  = Dead load uniform pressure, pounds per square foot
- $q_{LS}$  = Live load traffic surcharge pressure, pounds per square foot
- $H_2$  = Equal to the wall height,  $H_{Wall}$ . For level backfill surface use Equation 14-66 and for sloped backfill surface use Equation 14-68, feet
- $K_{avg}$  = Average horizontal acceleration that accounts for wave scattering in accordance with Chapter 13, g

**Step 8:** Compute the horizontal driving forces ( $F_H$ ) and the horizontal resisting forces ( $R_H$ ). No passive earth pressure force shall be used to resist horizontal driving forces on MSE walls. The horizontal driving force ( $F_H$ ) is determined by the following equation:

$$F_H = P_{ae} \cos \beta + P_{IR} + P_{IS} + P_{DC} + P_{LS} \quad \text{Equation 14-79}$$

The resisting force ( $R_H$ ) is determined using the lesser of soil-soil frictional resistance within the reinforced soil mass ( $R_{HSoil-Soil}$ ), soil-reinforcement frictional resistance within the reinforced soil mass ( $R_{HSoil-Reinf}$ ), or the frictional resistance in the foundation soils ( $R_{HF}$ ).

$$R_H = \text{Lesser of } R_{HSoil-Soil} \text{ or } R_{HSoil-Reinf} \text{ or } R_{HF} \quad \text{Equation 14-80}$$

Where the frictional resistance forces are computed using the following equations:

$$R_{HSoil-Soil} = \varphi N \tan \phi_R \quad \text{Equation 14-81}$$

$$R_{HSoil-Reinf} = \varphi N \tan \rho \quad \text{Equation 14-82}$$

$$R_{HF} = \varphi \tau B_w = \varphi (c B_w + N \tan \phi_R) \quad \text{Equation 14-83}$$

Where,

- $\varphi$  = Resistance factor, See Chapter 9.
- $\phi_R$  = Internal friction angle of the reinforced fill
- $\rho$  = Friction angle between the soil reinforcement and the reinforced fill material. For continuous reinforcement (sheet type)  $\rho = 0.67\phi_R$ . For all other non-continuous reinforcement (strip type)  $\rho = \phi_R$ .
- $B_w$  = Base width to the wall as defined in Step 6, feet

$N$  = Normal force that is the sum of the vertical loads over the base width ( $B_w$ ) of the reinforced soil mass, pounds per foot of wall width. The normal force is computed by the following equation:

**Equation 14-84**

$$N = (\gamma_R B_w H_{wall}) + P_{ae} \sin \beta + [0.5 \gamma_{Backfill} B_w (H_3 - H_{wall})]$$

Where,

$H_3$  = The height where the projection of the rear of the reinforced zone intersects the slope, feet

$\beta$  =  $0^\circ$  - level backfill or  
backslope angle, degrees

**Step 9:** Evaluate the MSE Wall bearing pressure, limiting eccentricity for overturning, sliding, and global stability for the maximum seismic design load in accordance with the appropriate Chapters of the GDM and Appendix C. For determination of bearing capacity see Chapter 15. If deep foundations are to be used to support flexible gravity ERSs, please contact the PCS/GDS. It should be noted that all EEI resistance factors ( $\phi$ ) are provided in Chapter 9. If all of the resistance factors are met, the static design is satisfactory and the seismic design is complete. It is reasonable to assume that if the demand/capacity ratio (D/C) for flexible gravity ERS meets the required resistance factors for the SEE design earthquake, the required resistance factors for the FEE design earthquake will be met. If bearing pressure and limiting eccentricity for overturning are not met, then MSE Wall requires redesign to meet these resistances. If the sliding or global stability resistance factor criterion is not met, the ERS is unstable; therefore, continue to Step 10 and evaluate the displacements caused by both the FEE and SEE design earthquakes.

**Step 10:** Determine the yield acceleration ( $k_y$ ) for the global stability of the ERS in accordance with Chapter 13. The  $k_y$  is the acceleration at which the ERS becomes just stable (i.e.,  $\phi = 1.0 = 1/FS = 1.0$ ). If the ratio of  $k_y$  to  $k_h$  is more than 0.5 ( $k_y/k_h \geq 0.5$ ), then a displacement ( $\Delta L$ ) of 2 inches shall be assumed and reported (Elms and Martin (1979)). As indicated previously, if the failure surface is circular all displacements at the top of the slope shall be considered to be vertical, while all displacements at the top of the slope for a non-circular failure surface shall be considered horizontal.

For evaluating the yield acceleration ( $k_y$ ) for sliding of the ERS, first determine the driving forces ( $F_H$ ) as a function of horizontal acceleration ( $k = k_h$ ) and the resisting forces ( $R_H$ ) as a function of horizontal acceleration ( $k = k_h$ ) as depicted in Figure 14-63. No passive earth pressure force shall be used to resist lateral seismic forces. The yield acceleration ( $k_y$ ) will be the location where the driving forces ( $F_H$ ) and resisting forces ( $R_H$ ) are equal.

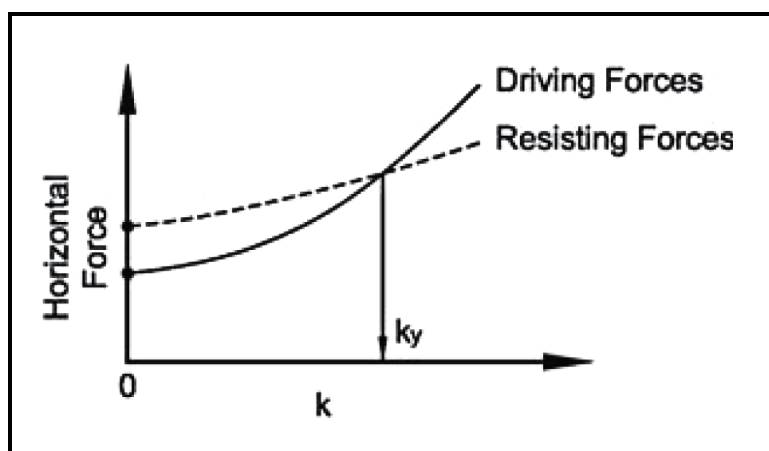


**Figure 14-63, Determination of Yield Acceleration ( $k_y$ ) (Anderson, et al. (2008))**

After determining  $k_y$  determine the amount of displacement ( $d$ ) using the procedures in Chapter 13. If the displacement is within the performance limits as indicated in Chapter 10, then design is complete. If the displacement exceeds the performance limits in Chapter 10, redesign the ERS to achieve acceptable performance limits or determine if the amount of anticipated movement is acceptable to both the design team as well as SCDOT.

## 14.13 CANTILEVER EARTH RETAINING SYSTEM DESIGN

Cantilevered earth retaining systems are comprised of unanchored sheet-pile and soldier pile and lagging and anchored sheet-pile and soldier pile and lagging ERSs as defined in Chapter 18 (see Table 18-1). Unanchored cantilevered walls will be discussed first and then anchored cantilevered walls.

### 14.13.1 Unanchored Cantilever ERSs

Design unanchored cantilever ERSs to establish the initial ERS design using the procedures indicated in Chapter 18. This establishes the dimensions of the cantilever ERS. Typically unanchored cantilevered ERSs are limited to a height of less than 16 feet. It should be noted that it is customary to ignore the inertial loadings of the structure members.

- Step 1:** Determine the PGA and  $S_{D1}$  using the procedures outlined in Chapter 12 of this Manual regardless of whether the 3-Point method or a Site-Specific Seismic Response Analysis is performed. All ERSs are required to be designed for both EEI events (FEE and SEE). It is reasonable to assume that if an unanchored cantilever ERS satisfies the required resistance factors for the SEE, the required resistance factors for the FEE will be met.
- Step 2:** Determine the PGV as described in Chapter 12.
- Step 3:** Compute the average seismic horizontal acceleration coefficient ( $k_h = k_{avg}$ ) due to wave scattering as indicated in Chapter 13.

- Step 4:** Determine  $K_{ae}$  and  $P_{ae}$  in accordance with the procedures described in Section 14.4 of this Chapter. The passive earth pressure coefficient  $K_{pe}$  and the passive earth pressure,  $P_{pe}$ , shall be determined as indicated in Section 14.5.
- Step 5:** Evaluate the structural requirements using either a suitable software package or by hand calculation (i.e., using something similar to the free earth support method). Confirm that the displacements predicted to achieve active earth pressure conform to the performance limits provided in Chapter 10.
- Step 6:** Check the global stability using the procedures outlined in Chapter 17. The acceleration used in the global stability analysis shall be the  $k_{avg}$  as determined in Step 4. If the resistance factor ( $\phi$ ) is greater than 1.0, determine displacements and compare to Chapter 10. If the displacements are within limits, design is complete. If the displacements exceed the limits, redesign the wall and begin again at Step 1.

### 14.13.2 Anchored Cantilever ERSs

Design anchored cantilever ERSs to establish the initial ERS design using the procedures indicated in Chapter 18. This establishes the dimensions of the cantilever ERS. Typically anchored cantilevered ERSs have heights in excess of 15 feet, but typically no more than 70 feet. It should be noted that it is customary to ignore the inertial loadings of the structure members.

- Step 1:** Determine the PGA and  $S_{D1}$  using the procedures outlined in Chapter 12 of this Manual regardless of whether the 3-Point method or a Site-Specific Seismic Response Analysis is performed. All ERSs are required to be designed for both EEI events (FEE and SEE). It is reasonable to assume that if an anchored cantilever ERS satisfies the required resistance factors for the SEE, the required resistance factors for the FEE will be met.
- Step 2:** Determine the PGV as described in Chapter 12.
- Step 3:** Compute the average seismic horizontal acceleration coefficient ( $k_h = k_{avg}$ ) due to wave scattering as indicated in Chapter 13.
- Step 4:** Determine  $K_{ae}$  and  $P_{ae}$  in accordance with the procedures described in Section 14.4 of this Chapter. The passive earth pressure coefficient  $K_{pe}$  and the passive earth pressure,  $P_{pe}$ , shall be determined as indicated in Section 14.5.
- Step 5:** Evaluate the structural requirements using the same pressure distribution from the static analysis. From the resulting loading diagram, check the loads on the tendons and grouted anchors to confirm that seismic loads do not exceed the loads applied during proof testing of each anchor. Confirm that the grouted anchors are located outside of the active seismic pressure failure wedge.
- Step 6:** Check the global stability using the procedures outlined in Chapter 17. The acceleration used in the global stability shall be the  $k_{avg}$  as determined in Step 4. If the resistance factor ( $\phi$ ) is greater than 1.0, determine displacements and compare to Chapter 10. If the displacements are within limits, design is complete. If the displacements exceed the limits, redesign the wall and begin again at Step 1.

## 14.14 IN-SITU REINFORCED RETAINING SYSTEM DESIGN

In-situ reinforced earth retaining systems are comprised of soil nail wall ERSs as defined in Chapter 18 (see Table 18-1).

Design in-situ reinforced ERSs to establish the initial ERS design using the procedures indicated in Chapter 18. This establishes the dimensions of the soil nail ERS. Typically soil nail ERSs have heights in excess of 10 feet but typically no more than 70 feet.

- Step 1:** Determine the PGA and  $S_{D1}$  using the procedures outlined in Chapter 12 of this Manual regardless of whether the 3-Point method or a Site-Specific Seismic Response Analysis is performed. All ERSs are required to be designed for both EEI events (FEE and SEE). It is reasonable to assume that if a soil nail ERS satisfies the required resistance factors for the SEE, the required resistance factors for the FEE will be met.
- Step 2:** Determine the PGV as described in Chapter 12.
- Step 3:** Compute the average seismic horizontal acceleration coefficient ( $k_h = k_{avg}$ ) due to wave scattering as indicated in Chapter 13.
- Step 4:** Use the  $k_{avg}$  determined previously in a pseudo-static analysis of the soil nail ERS, using a commercially available software (i.e., SNAIL<sup>®</sup> or GOLDNAIL<sup>®</sup>). If the resistance factor ( $\phi$ ) is less than 1.0, the design is acceptable. However, if the resistance factor ( $\phi$ ) is greater than 1.0, determine displacements and compare to Chapter 10. First, determine the yield acceleration ( $k_y$ ) corresponding to the point where the horizontal driving and resisting forces are equal (i.e.,  $\phi = 1.0$  or FS = 1.0). After determining  $k_y$ , determine the amount of displacement ( $d$ ) using the procedures in Chapter 13. If the displacement is within the performance limits as indicated in Chapter 10, then design is complete. If the displacement exceeds the performance limits in Chapter 10 either redesign the ERS to achieve acceptable performance limits or determine if the amount of anticipated movement is acceptable to both the design team as well as SCDOT.

## 14.15 SEISMIC HAZARD MITIGATION

If the performance limits established in Chapter 10 are exceeded, then the design team must decide if mitigation is practical or not (i.e., do nothing). “Doing nothing” is a decision that must be made by the entire design team. In some cases, this may be the most viable option. For instance, if flow failure is anticipated, the cost of mitigation would be excessively prohibitive; therefore, it would be less expensive to accept the movement. If mitigation is practical, there are 2 categories, either structural mitigation or geotechnical mitigation.

### 14.15.1 Structural Mitigation

Structural mitigation is where the structure is designed to handle the displacements anticipated during the seismic event. Structural mitigation of displacements should be attempted first before using geotechnical mitigation methods. Typically, structural mitigation efforts are more

economical than geotechnical mitigation methods. The decision to use structural mitigation should be made by the entire design team.

### **14.15.2 Geotechnical Mitigation**

Geotechnical mitigation is where the soil beneath and around the structure is modified to prevent displacements occurring during a seismic event from exceeding the limits contained in Chapter 10. Additional guidance on geotechnical mitigation methods may be found in Idriss and Boulanger (2008). Geotechnical mitigation efforts are limited to those indicated in Chapter 19 or those approved by the PC/GDS on a project specific basis.

### **14.15.3 Selection of Mitigation Method**

The selection of the appropriate mitigation strategy should be based on the cost of the mitigation method, the anticipated results of the mitigation method and the amount of post-seismic displacement that is anticipated to occur. The need for mitigation should be identified as early as possible in the design process to allow for time to consider all mitigation alternatives.

## **14.16 REFERENCES**

American Association of State Highway and Transportation Officials, (2017), AASHTO LRFD Bridge Design Specifications Customary U.S. Units, 8<sup>th</sup> Edition, American Association of State Highway and Transportation Officials, Washington, D.C.

Anderson, D. G., Martin, G. R., Lam, I. and Wang, J. N., (2008), "Seismic Analysis and Design of Retaining Walls, Buried Structures, Slopes and Embankments", NCHRP Report 611, Volumes 1 and 2, Transportation Research Board.

Arduino, P., McGann, C. R., and Ghofrani, A., (2017), "Design Procedure for Bridge Foundations Subjected to Liquefaction-Induced Lateral Spreading", Washington State Department of Transportation, Office of Research & Library Services.

Ashford, S. A., Boulanger, R. W., and Brandenburg, S. J., (2011), "Recommended Design Practice for Pile Foundations in Laterally Spreading Ground", Pacific Engineering Research Center, PEER Report 2011/04.

Boulanger, R. W., Kutter, B. L., Brandenburg, S. J., Singh, P., and Chang, D., (2003), "Pile Foundations in Liquefied and Laterally Spreading Ground During Earthquakes: Centrifuge Experiments & Analyses", College of Engineering, University of California at Davis, 205 pp.

Bowles, J. E., (1982), Foundation Analysis and Design, 3rd ed., McGraw-Hill, New York.

Brandenburg, S.J., Boulanger, R.W., Kutter, B.L., and Chang, D., (2007a), "Liquefaction Induced Softening of Load Transfer Between Pile Groups and Laterally Spreading Crusts", *ASCE Journal of Geotechnical and Geoenvironmental Engineering*, Vol. 133, No. 1, pp. 91 - 103.

Brandenburg, S. J., Boulanger, R. W., Kutter, B. L., and Chang, D., (2007b), "Static Pushover Analyses of Pile Groups in Liquefied and Laterally Spreading Ground in Centrifuge Tests", *ASCE Journal of Geotechnical and Geoenvironmental Engineering*, Vol. 133, No. 9, pp. 1055 - 1066.

Bray, J. D., and Travasarou, T., (2007), "Simplified Procedure for Estimating Earthquake-Induced Deviatoric Slope Displacements", *ASCE Journal of Geotechnical and Geoenvironmental Engineering*, Vol. 133, No. 4, pp. 381 - 392.

Caltrans (2017 A), "Memo to Designers 20-15: Lateral Spreading Analysis Fort New and Existing Bridges", California Department of Transportation (Caltrans) <https://dot.ca.gov/programs/engineering-services/manuals/memo-to-designers> (last visit: 09/17/2021)

Caltrans (2017 B), "Memo to Designers 20-15: Lateral Spreading Analysis Fort New and Existing Bridges, Attachment 1", California Department of Transportation (Caltrans) <https://dot.ca.gov/programs/engineering-services/manuals/memo-to-designers> (last visit: 09/17/2021)

Chugh, A. K. (1995), "A Unified Procedure for Earth Pressure Calculations," Proceedings: Third International Conference on Recent Advances in Geotechnical Earthquake Engineering and Soil Dynamics, Volume III, St. Louis, Missouri.

Clough, G. W. and Duncan, J. M. (1991), "Earth Pressures," Foundation Engineering Handbook, 2nd edition, edited by Hsai-Yang Fang, van Nostrand Reinhold, New York, NY, pp. 223 - 235.

Ebeling, R. M., Chase, A., White, B. C., (2007), "Translational Response of Toe-Restrained Retaining Walls to Earthquake Ground Motions Using  $C_{corps}W_{allSlip}$  (CWSLIP)", Technical Report ERDC/ITL TR-07-01. Vicksburg, Mississippi: Corps of Engineers Waterways Experiment Station, June 2007.

Elms, D. G. and Martin, G. R. (1979), "Factors Involved in the Seismic Design of Bridge Abutments", Proceedings of a Workshop on Earthquake Resistance of Highway Bridges, pp 229-252, Applied Technology Council, Palo Alto, California.

Idriss, I. M. and Boulanger, R. W., (2008), Soil Liquefaction During Earthquakes, Earthquake Engineering Research Institute (EERI), EERI Monograph MNO-12.

Munfakh, G., Kavazanjian, E., Matasović, N., Hadj-Hamou, T. and Wang, J. N., (1998), Geotechnical Earthquake Engineering Reference Manual, (Publication Number FHWA-HI-99-012), US Department of Transportation, Federal Highway Administration, National Highway Institute, Arlington, Virginia.

NCHRP 12-49 (2001), "Comprehensive Specification for the Seismic Design of Bridges – Revised LRFD Design Specifications (Seismic Provisions)," National Cooperative Highway Research Program (NCHRP), Transportation Research Board, Washington, D.C.

Newmark, N.M. (1965), "Effects of Earthquakes on Dams and Embankments", *Geotechnique*, v.5, no.2 London, England.

Norris, G. M. (1992), "Overview of Evaluation of Pile Foundation Stiffness for Seismic Analysis of Highway Bridges", *Transportation Research Record*, No. 1336, pp. 31-42.

Reese, L. C., Wang, S. T., Isenhower, W. M., and Arrellaga, J. A., (2004), "Computer Program L-Pile Plus," Version 5.0, Technical Manual, ENSOFT, Inc., Austin, Texas.

Richards, R. and Elms, D. G., (1979), "Seismic Behavior of Gravity Retaining Walls." *ASCE Journal of the Geotechnical Engineering Division*, Vol. 105, No. GT4, pp. 449 - 464.

Rollins, K. M., Gerber, T. M., Lane, J. D., and Ashford, S., (2005), "Lateral Resistance of a Full-Scale Pile Group in Liquefied Sand." *ASCE Journal of Geotechnical and Geoenvironmental Engineering*, Vol. 131, No. 1, pp. 115 - 125.

Shamsabadi, A. (2006). CT-FLEX – Computer Manual, Office of Earthquake Engineering, California Department of Transportation.

Shamsabadi, A. Rollins, K.M., and M. Kapuskar (2007), "Nonlinear Soil-Abutment-Bridge Structure Interaction for Seismic Performance-Based Design", *ASCE Journal of Geotechnical and Geoenvironmental Engineering*, Vol. 133, No. 6, pp. 707 - 720.

Shamsabadi, A., Khalili-Tehrani, P., Stewart, J. P., and Taciroglu, E. (2010), "Validated Simulation Models for Lateral Response of Bridge Abutments with Typical Backfills", *ASCE Journal of Bridge Engineering*, Vol. 15, No. 3, May 2010, pp. 302 - 311.

Shamsabadi, A., Xu, S.-Y., and Taciroglu, E. (2013a), "A Generalized Log-Spiral-Rankine Limit Equilibrium Model for Seismic Earth Pressure Analysis", *Soil Dynamics and Earthquake Engineering*, Vol. 49, June 2013, pp. 197-209.

Shamsabadi, A., Xu, S.-Y., and Taciroglu, E. (2013b), "Development of Improved Guidelines for Analysis and Design of Earth Retaining Structures", Report UCLA-SGEL Report 2013/02, Structural & Geotechnical Engineering Laboratory, University of California, Los Angeles, California

South Carolina Department of Transportation, (2006), Bridge Design Manual, South Carolina Department of Transportation, [http://www.scdot.org/doing/structural\\_Bridge.aspx](http://www.scdot.org/doing/structural_Bridge.aspx).

South Carolina Department of Transportation, (2008), Seismic Design Specifications for Highway Bridges, South Carolina Department of Transportation, <https://www.scdot.org/business/structural-design.aspx>.

Xu, S.-Y., Shamsabadi, A., and Taciroglu, E. (2015), "Evaluation of Active and Passive Seismic Earth Pressures Considering Internal Friction and Cohesion", *Soil Dynamics and Earthquake Engineering*, Vol. 70, March 2015, pp. 30-47.

Zhang, G., Roberson, P. K., and Brachman, R. W. I. (2004). "Estimating Liquefaction-Induced Lateral Displacements Using the Standard Penetration Test or Cone Penetration Test." *ASCE Journal of Geotechnical and Geoenvironmental Engineering*, v. 130, Issue 8, pp. 861 - 871